THESIS FOR THE DEGREE OF DOCTOR OF PHILOSOPHY

Strategies for Complete Recovery of Carbon in Dual Fluidized Bed Gasifiers

SÉBASTIEN PISSOT

Department of Space, Earth and Environment

CHALMERS UNIVERSITY OF TECHNOLOGY

Göteborg, Sweden 2021

Strategies for Complete Recovery of Carbon in Dual Fluidized Bed Gasifiers
SÉBASTIEN PISSOT
ISBN 978-91-7905-545-5

© SÉBASTIEN PISSOT, 2021

Doktorsavhandlingar vid Chalmers tekniska högskola
Ny serie nr 5012
ISSN 0346-718X

Department of Space, Earth and Environment
Chalmers University of Technology
SE-412 96 Göteborg
Sweden
Telephone + 46 (0)31-772 1000

Printed by Chalmers Reproservice

Göteborg, Sweden 2021

Strategies for Complete Recovery of Carbon in Dual Fluidized Bed Gasifiers
SÉBASTIEN PISSOT
Department of Space, Earth and Environment
Chalmers University of Technology

Abstract

To establish a circular economy and curtail our dependency on fossil resources, technologies are needed to extract carbon from biomass and plastic waste. Dual fluidized bed (DFB) gasification is a carbon-extracting technology that offers flexibility in terms of its inputs, outputs, design, and operational conditions. This thesis investigates the carbon distribution produced by DFB gasification and explores the possibilities to achieve total carbon recovery. The various configurations under which DFB gasification can be designed and operated to facilitate the total recovery of carbon are compared on a theoretical basis. Thus, insights into the carbon distribution and energy demands of each configuration are obtained. A method to increase the catalytic activity of the bed in the DFB gasifier so as to enhance the recovery of valuable forms of carbon is experimentally demonstrated, based on the use of a waste generated from the process. However, it is shown that increasing the catalytic activity is not always beneficial for carbon recovery. The development of oxygen transport along with the catalytic activity, a phenomenon that had been reported but never investigated, is here demonstrated. Taking advantage of the oxygen transport properties of certain bed materials to facilitate the total recovery of carbon is the basis for the chemical-looping gasification (CLG) technology, a DFB gasification configuration. The parameters that affect fuel conversion, an essential aspect of CLG, are investigated for a plastic waste that generates its own oxygen-carrying bed material. Oxygen transport is shown to be the most important parameter for the process. Based on these experiments, the numerous challenges associated with CLG are discussed. Finally, a process through which negative-emissions steel is produced, based on the integration of DFB gasification into a CLG configuration with direct reduction (DR) of iron, is proposed and evaluated. Compared with the traditional steelmaking route and alternative DR routes, the proposed process is found to be the most-competitive for carbon prices >60 €/tCO_2, which corresponds to both the price for CO_2 emissions and the revenue associated with negative emissions. Most of the data used in this work were obtained from experiments conducted at a scale relevant to the industry.

Keywords: dual fluidized bed, gasification, carbon, chemical-looping, waste, circular economy

List of Publications

This thesis is based on the following papers, which are referred to in the text according to their designated Roman numerals:

Paper I

S. Pissot, T. Berdugo Vilches, H. Thunman, M. Seemann,
Effect of ash circulation on the performance of a dual fluidized bed gasification system,
Biomass and Bioenergy. 115 (2018) 45-55.

Paper II

S. Pissot, T. Berdugo Vilches, J. Maric, I. Cañete Vela, H. Thunman, M. Seemann,
Thermochemical Recycling of Automotive Shredder Residue by Chemical-Looping Gasification Using the Generated Ash as Oxygen Carrier
Energy & Fuels. 33 (2019) 11552–11566.

Paper III

S. Pissot, T. Berdugo Vilches, H. Thunman, M. Seemann, Dual Fluidized Bed Gasification Configurations for Carbon Recovery from Biomass
Energy & Fuels. 34 (2020) 16187–16200.

Paper IV

S. Pissot, R. Faust, P. Aonsamang, T. Berdugo Vilches, J. Maric, H. Thunman, P. Knutsson, M. Seemann
Development of Oxygen Transport Properties by Olivine and Feldspar in Industrial-Scale Dual Fluidized Bed Gasification of Woody Biomass
Energy & Fuels. 35 (2021) 9424–9436.

Paper V

S. Pissot, H. Thunman, P. Samuelsson, M. Seemann
Production of Negative-Emissions Steel Using a Reducing Gas Derived from DFB Gasification,
Energies. 14 (2021) 4835.

This thesis is also based on parts of the licentiate thesis published by the author, as part of the evaluation of his doctoral studies:

S. Pissot, Carbon Recovery in a Dual Fluidized Bed Gasifier, 2020.

Contributions report

Paper I

S. Pissot: Experimental investigation, data curation, conceptualization of the manuscript; writing: original draft.
T. Berdugo Vilches: Experimental investigation, data curation, conceptualization of the experiments; writing: review & editing.
H. Thunman: Supervision, funding acquisition; writing: review & editing.
M. Seemann: Conceptualization, supervision, funding acquisition; writing: review & editing.

Paper II

S.Pissot: Conceptualization, experimental investigation, data curation; writing: original draft.
T. Berdugo Vilches: Conceptualization of the experiments, experimental investigation, data curation; writing: review & editing.
J. Maric: Conceptualization of the experiments, experimental investigation, data curation.
I. Cañete Vela: Experimental investigation, data curation.
H. Thunman: Supervision, funding acquisition; writing: review & editing.
M. Seemann: Conceptualization, supervision, funding acquisition; writing: review & editing.

Paper III

S. Pissot: Conceptualization, investigation, data curation; writing: original draft.
T. Berdugo Vilches: Writing: review & editing.
H. Thunman: Supervision, funding acquisition; writing: review & editing.
M. Seemann: Conceptualization, supervision, funding acquisition; writing: review & editing.

Paper IV

S. Pissot: Conceptualization, experimental investigation (large scale), data curation; writing: original draft.
R. Faust: Conceptualization, experimental investigation (laboratory scale), data curation; writing: review & editing.
P. Aonsamang: Experimental investigation (laboratory scale).
T. Berdugo Vilches: Experimental investigation (large scale), writing: review & editing
J. Maric: Experimental investigation (large scale).
P. Knutsson: Conceptualization, supervision; writing: review & editing.
H. Thunman: Supervision, funding acquisition; writing: review & editing.
M. Seemann: Conceptualization, supervision, funding acquisition; writing: review & editing.

Paper V

S. Pissot: Conceptualization, investigation, data curation; writing: original draft.
H. Thunman: Conceptualization, supervision, funding acquisition; writing: review & editing.
P. Samuelsson: Conceptualization; writing: review & editing.
M. Seemann: Supervision, funding acquisition; writing: review & editing.

List of Peer-Reviewed Publications Not Included in This Thesis

H. Thunman, T. Berdugo Vilches, M. Seemann, J. Maric, I.C. Vela, S. Pissot, H.N.T. Nguyen
Circular use of plastics-transformation of existing petrochemical clusters into thermochemical recycling plants with 100% plastics recovery
Sustainable Materials and Technologies. 22 (2019).

J. Maric, T. Berdugo Vilches, S. Pissot, I. Cañete Vela, M. Gyllenhammar, M. Seemann
Emissions of dioxins and furans during steam gasification of Automotive Shredder residue; experiences from the Chalmers 2–4-MW indirect gasifier
Waste Management. 102 (2020) 114-121.

Acknowledgments

Just as it is difficult to put five years of work into this thesis, it is difficult to summarize all the contributions that have helped me throughout the PhD journey. I have had the chance to be surrounded by brilliant and kind people, both at Chalmers and in my personal life.

My gratitude goes first to my main supervisor Martin and my co-supervisor and examiner Henrik. Their guidance and support have been invaluable and have helped me develop into a better researcher and a better human being. I also want to thank Teresa and Jelena for having played the role of unofficial mentors, your help has also greatly contributed to my development. Thank you, Isabel, for your constant engagement and motivating attitude. To the newer members of the gasification group, Chahat, René, Tharun, and Judith, I wish I had had more time to get to know you. I can see clearly that you will continue making this research group exceptional. Being part of the gasification group has also meant spending long and tiring (but exciting!) hours at the power central. I want to thank Jessica, Johannes, and Rustan for their help, without which our scientific results would definitely not have the same quality. Thank you also to the operating staff of the power central for contributing to the research effort.

Beyond the gasification research group, I feel really lucky to have been part of the Energy Technology division. The combination of scientific excellence and friendly atmosphere that the members of the division cultivate have made it so that coming to work was always a pleasure. The number of people at the division who have had a positive impact on me is too great to be listed here, so I would like to address a general “thank you” to everyone at the division for contributing to this atmosphere. Special thanks to Rikard for our lunches and scary-movie sessions, to Mariane for helping me keep a French connection, and last but not least to Max for being an awesome officemate and for helping me through the Swedish integration process when Sweden was making it tough for me.

Finally, I want to thank my family for their unwavering support despite the distance that separates us. I am also grateful to have great friends, here in Sweden, back in France, and scattered across the world. To Alejandra, thank you for having supported me throughout the tough times, and for your constant love.

This work would not have been possible without the financial support of: the Swedish Gasification Center (SFC), the Swedish Energy Agency (Energimyndigheten), Stena Recycling, and Borealis. The operation of the gasifier was made possible by the support of Göteborg Energi, Valmet, Akademiska Hus, and the Swedish Energy Agency.

List of Abbreviations

AAEM: Alkali and alkali-earth metals

AR: Air reactor

ASR: Automotive shredder residue

ASU: Air separation unit

BF: Blast furnace

BOF: Basic oxygen furnace

BTX: Benzene, Toluene and Xylene

CFB: Circulating fluidized bed

CGE: Cold gas efficiency

CLC: Chemical-looping combustion

CLG: Chemical-looping gasification

daf: dry ash-free (in reference to the fuel)

DFB: Dual fluidized bed

DR: Direct reduction

EAF: Electric arc furnace

FGCA: Flue gas coarse ash

GC: Gas chromatograph

HD: Heat demand

HO: Heat output

HTR: High-temperature reactor

LD: Linz-Donawitz (slag)

LS: Liquid steel

OCAC: Oxygen carrier-aided combustion

POP: Persistent organic pollutants

RP: Reduction potential

SPA: Solid-phase adsorption

TGA: Thermogravimetric analysis

TOC: Total organic compounds

WGS: Water-gas shift

Contents

Introduction

In recent years, it has become increasingly evident that the resources of our planet are finite and that human activity is promoting large-scale changes in weather patterns [1], which endanger biodiversity and may threaten the future of mankind. Mitigating these changes and using these limited resources in sustainable ways will require radical changes to our production and consumption systems, as well as to human behaviors. This will prove especially challenging as the worldwide population continues to grow and aspires to achieve a quality of life similar to that of Western populations. The concept of the circular economy as a system to address those challenges is attractive, in that it creates value from the economic, societal, and environmental perspectives [2,3]. One of the cornerstones of this concept is the creation of circular pathways for products that currently end up as waste. Taken to its extreme, this approach means that the very idea of a waste that has to be disposed of must be abolished, as new uses must be found for these materials, for their originally intended purpose or an alternative usage, or transformed into other valuable products.

Mitigating the effects of climate change will require changing the way that we address one type of waste in particular, CO_2, which has been for many decades and still is to a large extent today disposed of into the environment with little concern for its impacts. Radical changes to our industrial and societal practices are necessary. Decarbonization solutions for the electricity, heat, industrial, and transportation sectors must be devised, and the existing strategies must be improved. Actively reversing the trend of increasing atmospheric concentration of CO_2 will require implementing carbon capture and storage or utilization at the global scale. Finally, we must end our dependency on fossil-based carbon sources, which result in the net addition of carbon to the environment.

However, putting an end to this dependency is problematic when considering the carbon-based products upon which our society depends heavily. Indeed, while the energy and transportation sectors can be decarbonized, carbon sources are obviously needed to produce a wide range of everyday products. Carbon sources that are renewable are, nonetheless, limited, consisting of biomass resources, carbon-based anthropogenic waste, and CO_2 from direct air capture. Sourcing carbon from atmospheric CO_2 is challenging due to the high energy cost of separating CO_2. Besides, by producing materials from atmospheric carbon, there is a risk of incentivizing the release of carbon to the atmosphere as part of the carbon cycle rather than encouraging behaviors that limit carbon slippage to the environment. Furthermore, providing the vast amounts of biomass required to supply the global demand for carbon is not realistic, as this would entail a variety of ecological, economic, and societal issues. For instance, a high demand for energy crops could endanger biodiversity or lead to local food supply problems by creating competition with food crops, thereby driving up food prices [4].

The use of carbon-based anthropogenic waste as the primary source of carbon for our materials and chemicals does not entail the same critical issues as atmospheric carbon and biomass resources. Furthermore, it would address many of the issues related to the current lack of recycling of such waste. Chief amongst those issues is the environmental threat posed by plastic waste, which reflects the scale of plastic production, the propensity of plastic to leak into the environment (exacerbated by a single-use, throwaway culture), and the lack of plastic collection and recycling systems in many countries. For instance, Jambeck *et al*. have estimated that, for Year 2010, 99.5 Mt of plastic waste were generated in coastal regions of the world (including populations residing within 50 km of a coast), 31.9 Mt of which was classified as “mismanaged”, and 4.8–12.7 Mt of this waste entered the oceans [5]. Therefore, making plastic waste the main carbon source would ascribe a value to plastic waste collection, which would curtail the leakage of plastic into the environment. In this new circular carbon

system based primarily on plastic waste, biomass would still have an important role to play, despite the aforementioned issues. Biomass waste could, indeed, be used to supply carbon so as to compensate for the inevitable losses from the plastic cycle and to address the increasing demand for carbon. The production of biofuels, for instance for transportation, will also require the use of biomass. Finally, biomass is essential for the creation of negative CO_2 emissions.

Establishing this circular carbon system will require the extraction of carbon from biomass and waste sources. For this, the preferred pathway will employ thermochemical methods. For plastic waste, mechanical recycling can, at first glance, appear to be the more logical approach, given that its aim is to restore the plastic to its original use with limited energy expenditure. However, mechanical recycling is only suitable for highly homogeneous plastic waste streams, and even then, some loss in quality of the newly formed plastic is inevitable. This is not compatible with the fact that the overwhelming majority of plastic waste is expected to be in the form of complex mixtures of polymers. Recycling such mixtures *via* mechanical pathways is challenging, due to differences in melting points, processing temperatures, and the potential immiscibility of the melts formed [6]. Obtaining single-polymer streams for mechanical recycling is also challenging, and the presence of multiple additives [7] makes obtaining a "pure" stream impossible. Even if a stream that is perfect for mechanical recycling can be obtained, its properties will be compromised due to the thermal-mechanical degradations that occur during recycling, which add to those that occur during the lifetime of the product [6]. Thermochemical recycling does not suffer from these issues because it reduces the waste to molecular building blocks, from which a product of virgin quality can be reproduced. Besides, this pathway enables flexibility in the distribution of carbon into the various end-products and renders the circular carbon system adaptable to changes in production and consumption patterns.

However, extracting carbon from waste is more challenging than extracting carbon from the fossil sources that we have relied upon to date. Biomass and plastic wastes are expected to be more heterogeneous, often comprising a mixture of different types of polymers and biogenic materials, with the possibility of both synthetic and natural materials being mixed in the waste, as well as the presence of inorganic waste, such as metals. These wastes often contain elements that can lead to the formation of pollutants during thermochemical reprocessing. Thus, the selection of an optimal operational window will be challenging, as optimal conversion of the various polymers or biomass types may occur at different temperatures. The diversity of inorganics in the waste may lead to operational issues in the thermochemical reactor and within its cooling sections. Therefore, recycling technologies that are sufficiently robust to handle these issues are required.

In this context, Dual Fluidized Bed (DFB) gasification is a strong candidate for the central technology in the future circular carbon system. The DFB gasification technology is analogous to the Fluid Catalytic Cracking technology employed in the petroleum industry to crack gas oil, with the important difference that DFB gasification converts solid fuels. A DFB gasification system consists of two interconnected fluidized bed reactors, as illustrated in Figure 1. One reactor comprises a fluidized bed gasifier in which thermochemical breakdown of the fuel takes place in the presence of steam. The other reactor is a Circulating Fluidized Bed (CFB) combustor, which burns the fraction of the fuel that is not converted in the gasifier, so as to provide the heat required by the gasifier. The heat is transferred from the combustor to the gasifier by a bed material that circulates between the two reactors. The separation of the combustion reaction from the gasification reactions generates a concentrated product gas, without the need to produce pure oxygen, as is the case for direct gasification technologies.

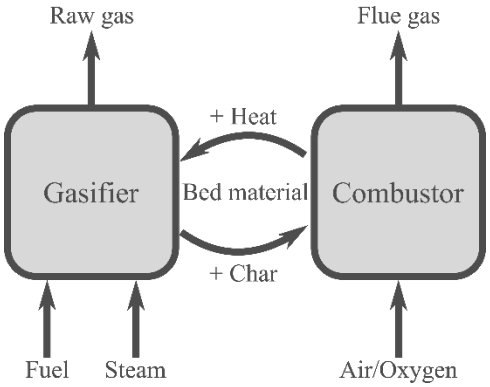

Figure 1. Dual fluidized bed gasification setup.

The DFB gasification technology is particularly well suited to the conversion of waste streams. Fluidized beds ensure high heating and mass transfer rates, enabling high throughput. This also means that little fuel preparation is required beyond drying, which makes the technology flexible with respect to the carbon source. In fluidized bed reactors, the temperature profiles are rather homogeneous, which prevents the formation of hotspots and facilitates operational control of the reactions. The conversion of a waste in a DFB gasifier is also likely to produce lower levels of pollutants and toxic compounds, as compared with the incineration of that waste. For instance, the weakly oxidative environment of the gasifier may be conducive to generating lower levels of emissions, e.g., of dioxins and polychlorinated dibenzofurans [8]. The char that is generated in the gasifier and burnt in the combustor is highly reactive and contains few impurities compared with the parent fuel, with the consequence that there are low levels of emissions in the flue gases. In addition, additives can easily be incorporated into the bed, to reduce emissions by acting as sorbents or catalysts. Catalysts can also be employed to adjust the gas composition in the gasifier. These catalysts will be continuously regenerated in the combustor.

The most promising feature of the DFB gasification technology in terms of its contribution to the circular economy probably lies in its extensive flexibility regarding carbon recovery. The carbon distribution into the products of the gasifier can, to a large extent, be tailored to various requirements by adjusting parameters such as the reactor temperature, the residence time of the fuel, and the level of catalytic activity. The distribution of carbon between the two reactors can be adjusted, for instance by supplying part of the heat using electricity, thus enabling a higher fuel conversion in the gasifier. The recovery of carbon in the form of CO_2 in the combustor, where it is diluted with nitrogen in the traditional DFB gasification design, can be facilitated in several ways. One way is to use oxygen-enriched air in the combustor to increase the CO_2 concentration so as to make the sequestration of that carbon viable. Taking this approach to its extreme, i.e., operating the combustor under oxyfuel conditions, produces a flue gas that is rich in CO_2 and that needs little additional processing for sequestration of the carbon. When plastic waste is the main carbon source being converted, the process can be made carbon-negative by adding biomass. In conclusion, DFB gasification offers flexibility in the valorization of the carbon. This will be an essential feature of a carbon-extracting technology in the circular economy, as it will need to be able to adjust rapidly to changes in consumption patterns and regulations.

Despite its promising characteristics, DFB gasification has not yet been implemented at commercial scale. Only a few plants exist at large scale: the 8-MW unit in Güssing, Austria [9], which was the basis for the 16-MW Senden plant in Germany [10] and the 32-MW GoBiGas plant [11] in Gothenburg, Sweden, and the TIGAR gasifier, which converts 15 MW of lignin, designed and operated by the IHI Corporation in Yokohama, Japan [12]. Furthermore, the conversion of plastic waste in DFB

gasifiers at semi-industrial scale [13] or pilot scale [14–16] is also currently limited. In addition, carbon distribution and recovery have not been in focus in those studies. There is, therefore, a need to develop novel ways of exploring DFB gasification and determining its potential as part of the future circular carbon system.

The overarching goal of this thesis is to gain understanding on the carbon distribution of the DFB gasification technology, and to explore the possibilities to steer it and increase carbon recovery. This would strengthen the position of the DFB gasification technology as one of the carbon-extraction solutions to be applied in the future circular economy. In *Chapter 1*, the carbon distribution of the regular DFB gasification process is presented, and the concept of "carbon recovery" is defined. The parameters that influence the carbon distribution in DFB gasifiers are discussed. The various configurations in which the DFB gasification technology can be operated to facilitate complete carbon recovery are introduced and discussed.

Under this overarching goal, there are three main recurring themes in this thesis. The first relates to the operation of the DFB gasification technology. This technology is highly flexible, with many parameters that can be adjusted to tailor the operation and, thereby, the carbon distribution. However, the interconnection of the two reactors and the role of the bed material as carrier of both species and heat mean that changing a parameter can have a multitude of effects. Furthermore, potential downstream upgrading and synthesis steps of the plant of which the DFB gasification unit is a part also influence the final carbon distribution. Therefore, they must be considered in the carbon distribution and recovery analysis. These aspects are discussed in *Chapter* 1, as well as in other chapters of this thesis.

The second recurring theme is that of the circulation of species by the bed material. Besides transporting heat, the bed interacts with and incorporates species from the fuel ash in the DFB system. The accumulation of these species and their exposure to the two different atmospheres of the combustor and gasifier influence the reactions in the gasifier, either through catalytic effects or direct reactions with gas species, both of which have impacts on the carbon distribution. Furthermore, some bed materials can react with and incorporate oxygen in the combustor, which can thereafter react in the gasifier. This phenomenon, which is referred to as "oxygen transport", has a potent impact on the carbon distribution and is, therefore, the subject of much discussion in this thesis. The interactions of the bed with the fuel ash, as well as the oxygen transport phenomenon are presented in greater detail in *Chapter 1*.

The third recurring theme is that regarding the use of waste materials in DFB gasification. As the valorization of waste becomes one of our main societal goals, finding uses for waste materials is of increasing importance. Waste materials can be used in various forms and for various purposes in the DFB gasification process. These are discussed in *Chapter 2*. In this work, the use of waste materials is considered through the lens of their potential to steer the carbon distribution.

Among the DFB configurations described in *Chapter 1*, Chemical-looping gasification (CLG) is one that is extensively discussed in all of the papers of this thesis, with the exception of **Paper I**. This configuration relies on the use of so-called oxygen-carrying bed materials, i.e., bed materials that have the ability to transport oxygen, to inherently separate CO_2 in the DFB system. This configuration is associated with a number of challenges, and these are discussed throughout the thesis.

The results of the five research articles on which this thesis is built are presented and discussed with the focus on conclusions that can be drawn with regard to the carbon distribution of the DFB

gasification process and the possibilities to increase carbon recovery. Furthermore, the five papers deal with some or all of the three abovementioned recurring themes. Following the third chapter, which provides a description of the Chalmers DFB gasifier facility and of the equipment, methods, and materials common to all five articles, a chapter is dedicated to each of the papers. Figure 2 shows schematically how the five articles, and thereby *Chapters 4–8*, fit with the overarching goal and the three recurring themes. The works presented in this thesis span several of the scales involved in the complete analysis of a DFB process: from the behaviors and roles of the particles in the fluidized beds to the optimization of the entire plant beyond the DFB gasification unit (see panel b in Figure 2). Finally, panel c in Figure 2 shows the different types of studies carried out in the papers. **Paper III** gives a theoretical description and performs a comparison of the DFB configurations, **Papers I**, **II** and **IV** are based on experiments carried out in the Chalmers gasification facility, and **Paper V** presents an application of the DFB gasification technology, together with an assessment of its economic performance.

In this thesis, the five articles are not presented in the order of their writing or publication. **Paper III** is the first to be treated, as it deals with a theoretical description of the carbon distribution of the regular DFB gasification and three configurations that (theoretically) allow for complete carbon recovery. The impacts of gasifier temperature and bed catalytic activity on the carbon distribution are also discussed. *Chapter 5* focused on **Paper I**, discussing a case in which a waste from the DFB process itself, the flue gas fly ash, is circulated back to the DFB loop, with the aim of decreasing the tar content. Thus, the goal here is to convert carbon from a non-valuable and problematic form to a valuable form. The general impacts of catalytic activity on the carbon distribution, which are explored theoretically in *Chapter* 4, are further explored experimentally in *Chapter* 5. In **Paper I**, it is shown that, in the process of developing catalytic activity, the bed also started to exhibit oxygen transport properties that it did not initially have. The development of oxygen transport along with catalytic activity in beds that initially lack such properties has been reported previously in the Chalmers gasifier [17–19]. Given that the transport of oxygen between reactors can drastically affect the energy and carbon balances of the DFB system, this issue was investigated in **Paper IV**, which is the subject of *Chapter 6*.

If oxygen transport develops to a significant extent in the bed, then the DFB gasification process will shift to a CLG configuration. In this configuration, two aspects are critical: (1) maximizing the conversion of the fuel in the gasifier to avoid the loss of carbon in the combustor and to maximize carbon recovery; and (2) minimizing the oxidation of the carbon in the raw gas to CO_2. *Chapter 7*, which is based on **Paper II**, investigates the parameters that influence fuel conversion in CLG and discusses the challenges related to the two critical aspects mentioned above. The experiments upon which these discussions are built investigated the conversion of automotive shredder residue (ASR), which is the rest fraction (waste) from car recycling. As a consequence of its very high content of metal, ASR was found to generate its own oxygen-carrying bed material. As a heterogeneous waste that contains many different kinds of plastics and a high and diverse inorganic content, ASR is also representative of the composition of a rest fraction from an intensive plastic waste sorting process.

Finally, *Chapter 8*, which is based on **Paper V**, presents a triple-bed system operated in a CLG-like configuration and that overcomes the main challenges associated with CLG. The aim of the process is to provide a reducing gas for the direct reduction of iron, with associated negative emissions. The off-gas from the direct reduction reactor is rich in H_2 and CO. Part of this off-gas can be used subsequently to reduce the oxygen-carrying bed material in the DFB gasification loop, thereby limiting the transport of oxygen to the gasifier and limiting its oxidation. The oxygen carrier proposed for this process is a waste from the steelmaking industry. In this chapter, the economics of the production of steel using

DFB gasification are compared with those using alternative direct reduction routes, as well as with the traditional coal-based steelmaking route.

The discussions on carbon distribution and carbon recovery in the various chapters are crucially relevant to the conversion of both biomass and plastic waste. It should be kept in mind, however, that the effects of ash components on the bed material will likely differ, as the compositions of the ash fractions in plastic waste and biomass will differ. The results described in **Papers I** and **IV** may, therefore, not be directly applicable to the conversion of plastic waste. Nonetheless, the general effect of catalytic activity on the carbon distribution discussed in **Paper I** remains relevant, and oxygen transport properties may still develop when using a plastic waste, with consequences for the carbon distribution that are similar to those discussed in **Paper IV**.

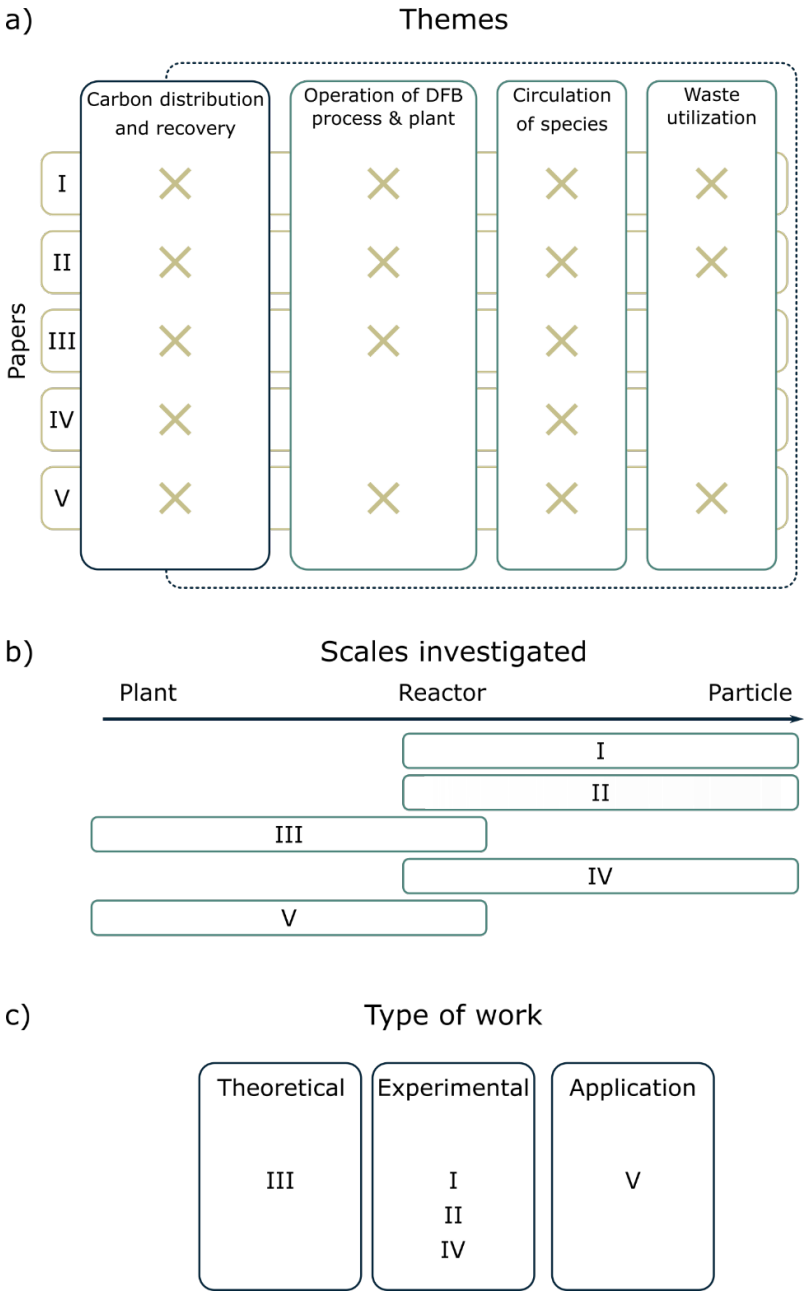

Figure 2. Conceptual representations of: (a) the recurring themes of the thesis and the papers that expand on these themes; (b) the scales investigated in the various papers; and (c) the types of work carried out for each paper.

Chapter 1: Enhancing carbon recovery in DFB processes

1.1. Carbon distribution in a DFB gasification system

Strengthening the status of the DFB gasification technology in the circular economy requires maximizing both its carbon extraction efficiency and its energy efficiency, as well as minimizing its energy demand (Figure 3). While 100% carbon efficiency could be achieved for many processes if unlimited energy was introduced into the system, this is hardly in line with the ethos of the circular economy, in which the parsimonious use of resources, including energy, is paramount. In the DFB gasification technology, the carbon introduced with the fuel fed to the gasification reactor (and, potentially, to the combustor) exits the reactor in two streams. These two streams then undergo a series of separation and upgrading steps, wherein the various species are separated and further reacted to obtain products that meet the requirements of, for instance, a downstream synthesis step.

The carbon efficiency or recovery of the DFB gasification process is reflected in the ratio of the carbon valorized, i.e., recovered as valuable products after upgrading or sequestration, to the carbon fed into the DFB. If carbon is introduced into the separation and upgrading section, for instance in the form of a scrubbing agent to separate a given species, it must be accounted for in the input to the process ($C_{in,2}$ in Figure 3). Similarly, the energy efficiency is the ratio of the energy in the valorized products (as well as any extracted heat from the process) to the energy introduced into the DFB gasifier and into the separation and upgrading section. The former corresponds mainly to the energy content of the fuel introduced ($E_{in,1}$ in Figure 3). Additional energy can be introduced into the DFB or the fuel dryer, for instance in the form of electrical heating, in which case it also must be accounted for in the determination of the energy efficiency ($E_{in,3}$ in Figure 3).

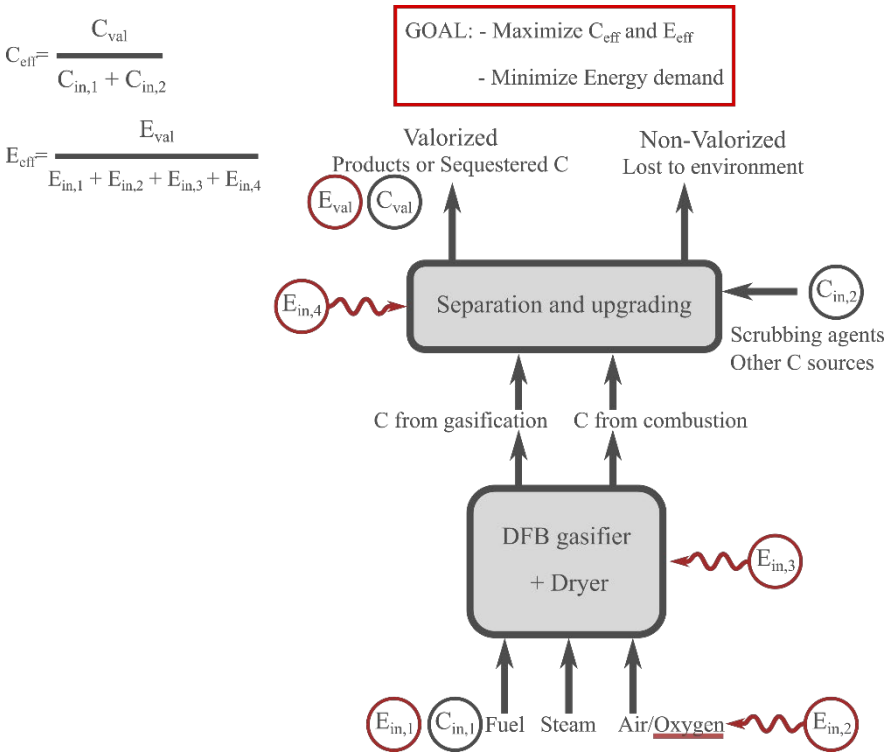

Figure 3. Conceptual description of a DFB process with the emphasis on the carbon (indicated as "C") and energy (referred to as "E") efficiencies.

The carbon in the raw gas produced in the gasification reactor exists as numerous carbon-containing species. The carbon can be divided into two main categories: carbon in the form of products; and carbon in the form of CO_2 (Figure 4). This distinction reflects the fact that within the DFB gasifier, CO_2 constitutes the only carbon form from which no chemical energy, in the sense of heating value, can be extracted. The carbon in the products is in the forms of CO, light hydrocarbons (here defined as those with up to three carbon atoms), and heavier hydrocarbons (including tar). Therefore, three main forms of carbon are produced by the DFB considered in this work: carbon as part of the products; carbon as CO_2 in the raw gas; and carbon as CO_2 in the flue gases. An additional small carbon stream (not depicted in Figure 4) is the solid carbon from unconverted fuel particles that are entrained with the raw gas as fly ash; these are usually recirculated to recover the energy content of the carbon. Therefore, this carbon is recovered in either the combustor's flue gas or in the raw gas.

In the raw gas exiting the gasifier, not all of the carbon contained in the products is equally valuable. Depending on the intended output of the plant and the distribution of the product created by the fuel in the DFB process, some fractions may be valuable whereas others may have little value or may be produced in insufficient quantities to justify being valorized or sold. In general, light hydrocarbons, such as methane, ethylene, and propylene, are considered valuable forms of carbon. That is because they have a high value in themselves and can be extracted as the main outputs of the plant. For instance, ethylene and propylene can be used as monomers for the downstream production of plastics. They can also be readily converted to H_2 and CO, to produce H_2 or other end-products synthetized from syngas. CO_2 will, in most cases, be considered as a non-valuable form of carbon, as it has no energy content, and its conversion to CO or hydrocarbons requires reaction with hydrogen (or electricity if CO_2 electrolysis is used), the production of which entails a high energy demand. If a high value is placed on sequestrating biogenic CO_2, then it could become a valuable species, which, for large-scale processes, could be an additional or the main end-product of the DFB gasification plant.

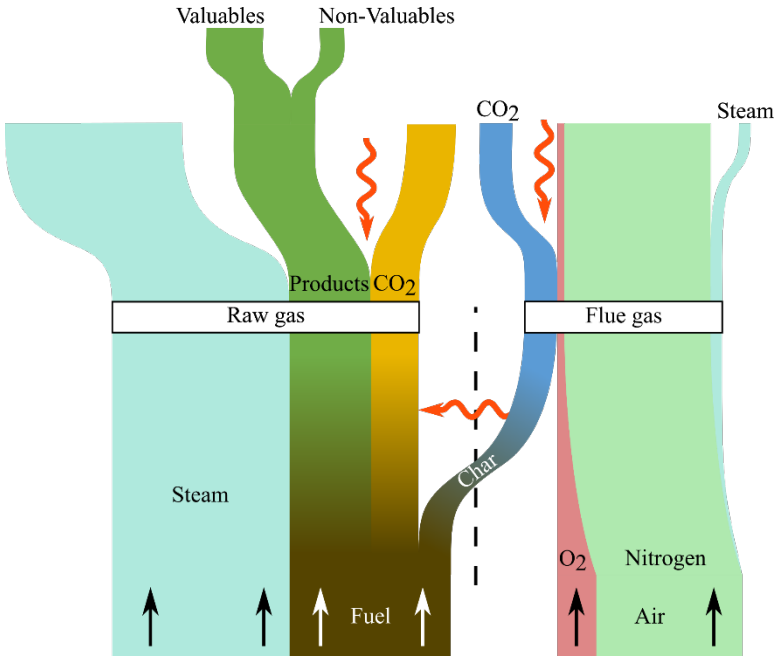

Figure 4. Conceptual representation of the flow of carbon through a DFB gasifier. The carbon flows that result from the fuel are shown in green, gold, and blue. The steam fed into the gasifier and the air fed into the combustor are also shown. The width of each carbon flow represents its approximate relative level in a typical DFB gasifier, and the widths of the steam and nitrogen flows represent their approximate amounts relative to the carbon flows. The red wavy arrows represent the energy or heat inputs, i.e., the energy used for the separation

of CO_2 from the raw gas and flue gas, and the heat transported by the bed material from the combustor to gasifier.

Some other carbon species, such as hydrocarbons with high boiling points, may cause operational problems downstream of the DFB section. These non-valuable carbon-containing species are often disposed of in the combustor, where their energy content contributes to fulfilling the heat demand of the gasifier and can, therefore, enable a higher level of recovery of carbon from the char in the raw gas. For instance, in the GoBiGas plant, tar was removed using a Rapeseed Methyl Ester (RME) scrubber and was fed to the combustor, while BTX (Benzene, Toluene, and Xylenes) was removed by active carbon beds and fed to the post-combustion chamber of the combustor [20].

The carbon content of these non-valuable fractions can also be recovered as CO and light hydrocarbons by further cracking or reforming of the raw gas in a downstream reactor, for instance using chemical-looping reforming [21]. However, the best way to convert the non-valuable carbon into valuable carbon is to manipulate the kinetics and thermodynamics of the reactions within the gasifier itself by adjusting the operating parameters, using catalytic materials, or tuning the residence times of the fuel, gas, and bed material in the reactor [22]. Valuable carbon in the products can be converted to CO_2 in the raw gas by oxidation with oxygen or with steam, *via* the water-gas shift (WGS) reaction.

Depending on the extents of those reactions in the gasifier, a significant fraction of the carbon can be obtained in the form of CO_2. In most cases, regardless of whether the product gas is directly utilized or upgraded and further synthesized, separation of the CO_2 is required, which means that this separation step is inherent to the cleaning sections of existing DFB gasification plants. Carbon from the CO_2 in the raw gas can, therefore, be recovered in a rather pure stream, which then becomes available for sequestration or for synthesis, for instance of hydrocarbons *via* the methanol-to-olefins route [23,24]. Nonetheless, as depicted in Figure 4, the separation of CO_2 from the raw gas entails an energy demand, the magnitude of which depends on the technology used. This increases the energy demand of the process and influences its overall energy efficiency.

Similarly, the separation of CO_2 from the flue gas strongly affects the energy efficiency of the DFB process. The choice regarding whether to separate or emit that CO_2 will, to a large extent, be based on the CO_2 concentration and, thereby, the energy cost of the separation process. In a regular DFB process, the heat demand of the gasifier is fulfilled by burning part of the char with air, resulting in a CO_2 stream that is diluted with nitrogen, at a volumetric concentration of about 15%. At this low concentration, the separation of the CO_2 from the flue gas is energetically demanding. The use of oxyfuel combustion in the combustor resolves this energy penalty, although it introduces a new one in the form of the production of pure oxygen, as illustrated in Figure 3.

In light of this discussion, three main avenues to facilitate complete carbon recovery in a DFB gasification process can be proposed. The first approach (*Section 1.2*) is to increase carbon recovery in the form of valuable products or as CO_2 by converting non-valuable hydrocarbons within the gasifier, so as to avoid the cost associated with converting them to valuable forms or the cost associated with separating the CO_2 that they would produce if they were burnt in the combustor. The second approach is to produce a concentrated CO_2 stream in the combustor, one that is ideally amenable to compression and sequestration, or utilization, after minor purification steps. The third approach is to replace the heat source in the combustor with a carbon-free one, thereby allowing complete conversion of carbon in the gasifier. The second and third approaches imply substantial changes in the operation of the DFB gasification process, requiring the use of bed materials with specific properties, the use of an oxidant other than air in the combustor, or the introduction of electric heating. These changes result

in new DFB gasification configurations, which are described in *Sections 1.3* and *1.4* and which are compared in *Chapter 4* on the basis of their carbon distributions and potentials for carbon recovery.

1.2. Steering the fuel conversion and carbon distribution in the gasifier

As mentioned above, a strength of DFB gasification is its flexibility in adjusting the recovery of carbon in different forms. The carbon that is present in the products as non-valuable species can, to a certain extent, be transformed into valuable species within the gasifier, by adjusting the process parameters and bed material properties. The five main parameters that can be adjusted to direct the distribution of carbon in the gasifier are: (i) the temperature of the gasifier; (ii) the catalytic activity of the bed; (iii) the transport of oxygen; (iv) the extent of the gasification reaction; and (v) the heat demand of the gasifier. These five possibilities are discussed in this section.

1.2.1. Temperature

The temperature in the gasifier influences the product distribution by affecting the reaction rates and the residence times of the gases, as well as the reactions equilibria, although the impact of the latter is limited because the reactions in the gasifier are generally kinetically-constrained. With an increase in temperature, the gasification reaction, as well as the cracking and reforming reactions, intensify. The overall result is the conversion of carbon to CO and light hydrocarbons. The composition of the tar is affected by the gasifier temperature. In the context of the present section, tar is understood to comprise all condensable hydrocarbon species. Biomass tar is mainly oxygenated and monoaromatic forms at low temperatures; it evolves towards non-oxygenated, unsubstituted polyaromatic hydrocarbons and, eventually, becomes soot [25]. The presence of tar is generally not desirable, as the condensation of tar on heat transfer surfaces can cause severe operational problems, and many of the gas end-use applications require minimization of the concentration of tar [25]. With higher temperatures, the yield and concentration of tar decrease at the expense of the gas [26], although the share of large polyaromatic compounds in the tar increases, which, even at low concentrations, can greatly increase the dew-point of the tar [27]. Therefore, although higher temperatures are conducive to lower tar yields, they can also lead to operational issues.

Moreover, a high temperature in the gasifier entails a high heat demand from the gasifier. This means that higher levels of carbon need to be converted in the combustor to fulfill that heat demand, as compared with a lower temperature case. Therefore, a compromise must be found between, on the one hand, a low permanent gas quality and less mature tar (albeit with a lower heat demand and less-troublesome tar) and, on the other hand, a high-quality permanent gas and high gasification rates (albeit with a higher heat demand and increased risk of operational issues). These aspects are discussed further in *Chapter 4*, in which the impact of temperature on the carbon distribution is also investigated.

1.2.2. Catalytic activity

The other main way to affect the carbon distribution in the products within the gasifier is to use a material that exhibits catalytic properties towards the reactions of interest. A recent review of six large-scale DFB gasifiers, including the Chalmers gasifier, conducted by Larsson *et al.* [28] has shown that the availability of active components has a much stronger impact on gas quality, in terms of gas and tar yields and compositions, than parameters related to the thermal severity of the process, such as the bed temperature, gas residence time, and gas concentrations. Controlling the catalytic activity in the gasifier is, therefore, of paramount importance for controlling the carbon distribution.

There are several ways to introduce catalytic activity into the gasifier. A material that has an intrinsic catalytic activity can be either utilized as the bed material for the DFB process or mixed with an inert bed material. In a DFB gasifier that converts ash-containing fuels, an inert bed material can develop catalytic activity with time, due to the interactions of the fuel ash with the bed [29]. Besides, inorganic particles contained in or fed with the fuel can, assuming that they are large enough to remain within the bed, contribute to the catalytic activity of the bed. Ash species that are volatile can also exert a homogeneous catalytic activity. Finally, additives can be used to enhance the catalytic activity. Note that additives that are introduced for other purposes can also contribute to the catalytic activity. For instance, limestone can be used to reduce SO_2 emissions in the combustor [30,31] or to capture chlorine in the gasifier [32,33]. Under the prevailing conditions in DFB gasifiers, limestone is expected to form calcite, which is known to have catalytic properties that enhance tar abatement [34] and the WGS reaction [35]. The WGS reaction is generally desirable in gasification processes, as it increases the production of hydrogen and causes an increase in the H_2/CO ratio, which needs to attain a value that is set according to the envisioned downstream synthesis process.

The main catalysts that have been investigated for gasification are based on alkali and alkali-earth metals (AAEM) or on transition metals such as nickel and iron [36–38]. Olivine, which is an iron-magnesium silicate, has been the bed material of choice for most of the large-scale DFB gasifiers [22,28]. The choice of olivine has been motivated by: (1) low cost and good availability compared to synthetic bed materials; (2) resistance to attrition that is superior to that of dolomites and comparable to that of silica sand [39]; (3) lower propensity to agglomerate compared to silica sand with woody biomass [40]; and (4) catalytic activity that has been extensively studied under laboratory conditions [41–48]. The chromium and nickel contents of olivine, however, make its disposal challenging [29]. This has spurred research into alkali-feldspar as an abundant and non-toxic alternative to olivine for DFB gasification [19].

Concerning the nature of additives used to enhance the catalytic activity, Larsson *et al.* [28] have noted that large-scale steam gasification units have "limited their choice of active specie to the components already present in the biomass ash, mainly potassium (K) and calcium (Ca)". Indeed, alkali species such as K are known to catalyze char gasification [38,49,50], the WGS reaction [51], and tar-abating reactions [36,37]. Similarly, Ca-containing species, such as dolomites and calcites, have been shown to have catalytic activities for tar elimination [36,52] and the WGS reaction [36].

In large-scale DFB gasifiers, the interactions of biomass ash, in particular AAEM, with bed particles have been shown to lead to catalytic activity, and are linked to the formation of ash layers on the particles [29]. The formation of ash layers requires initial interaction of the ash species with the particles, which can occur through condensation or a chemical reaction involving volatile ash species, such as alkali, the attachment of particles through van der Waals forces or the adherence of molten ash particles [53–55]. The layers themselves are composed of several sublayers, which are formed as a result of the differences in diffusion rates of the species within the particle crystalline structure and the replacement of atoms by those migrating ash species. With respect to DFB gasification, such mechanisms have been investigated for silica sand [56–58], olivine [58–62], feldspar [19,58,63–66], and bauxite [18].

The ash layers formed by the interaction of the bed particles with biomass ash confer an improvement in gas quality and a reduction of the tar content of the product gas *via* several mechanisms. Kuba *et al.* have shown that the catalytic activities towards light hydrocarbons (modeled by ethylene) and aromatics (modeled by toluene) are increased when the particles have an ash coating [67]. Moreover,

the same authors have reported that the Ca-rich layers on used olivine increase its catalytic activity towards the reforming of 1H-indene (a stable intermediate in the decomposition of tar), thereby preventing its polymerization into polycyclic aromatics, such as chrysene [68]. In addition, Berdugo Vilches *et al.* have demonstrated that ash-coated olivine promotes the reforming of early tar precursors, thereby preventing their maturation to aromatic hydrocarbons [69]. This result, supported by the abovementioned review of the six large-scale DFB gasifiers by Larsson *et al.*[28], indicates that the role of active olivine is to alter the reaction pathways for tar rather than simply promoting the reactions that occur in the absence of catalytic activity.

While the catalytic activity of the ash layer is likely due to its high content of calcium (Ca), as suggested by Kuba *et al.* [67], the results presented by Berdugo Vilches *et al.* [69] indicate that the interactions of the ash coating with the tar precursors also occur in the gas phase. This is supported by the finding that alkali is released from the bed in the gasifier [59,61] and by the finding that K additions (through fuel impregnation) in entrained flow gasifiers strongly affect the tar yield, which has been attributed in part to a gas-phase catalytic role of the K [70,71]. Furthermore, Berdugo Vilches *et al.* have shown that K from a coated olivine, activated through K and S additions, is transferred to a char particle, mostly likely through the gas phase, which leads to an increase in the char reactivity [72]. The mobility of some ash species such as K could be a reason for the enhanced catalytic activation observed when using coarse flue gas ash circulation (described in *Chapter 5*), as discussed in **Paper I**, and this has also been proposed as one of the reasons behind the development of oxygen transport, as investigated in **Paper IV**. Besides its role in homogeneous catalysis, K can have a catalytic effect in the ash layer. Synergistic interactions between Ca and K in the ash layer have been shown to activate the surface for tar oxidation [73]. Consequently, Ca and K play key roles in the development of catalytic activity through the formation of ash layers.

The buildup of an ash layer and the corresponding increase in catalytic activity of the bed, at least in the case of biomass ash, represent an attractive feature of DFB gasifiers, since even if an inert bed is initially used, a very active bed can be obtained following a period of residence within the system. Through its catalytic activity, the ash layer contributes to converting carbon into the valuable and easy-to-handle forms of CO and light hydrocarbons. However, it is worth considering the impact that this activity has on the WGS reaction. The ash-layered particles have indeed been shown to exhibit a higher catalytic activity towards the WGS reaction, as compared to their non-layered counterparts, in the cases of olivine and silica sand [67,68]. The WGS reaction is important because it is a follow-up to the tar- and light hydrocarbon-reforming reactions, as well as to the gasification reaction, and it converts carbon to its final form (CO_2) in the gasifier. Consequently, as the catalytic activity increases, carbon is transferred from heavy hydrocarbons to light hydrocarbons, and then to CO, eventually ending up as CO_2. Therefore, a balance needs to be achieved in terms of the recovery of carbon in the forms of valuable species and CO_2, which places a limit on the desired activity level. Besides, as mentioned in *Section 1.1* and depicted in Figure 4, as carbon is transferred to CO_2, the heat demand placed on the desorption step in the separation of CO_2 increases. The impacts of the catalytic activity on the carbon distribution are further explored in this thesis, in theoretical terms in *Chapter 4* and experimentally in *Chapter 5*.

1.2.3. Oxygen transport

Another way in which the composition of the bed material can affect the composition of the gas in the gasifier is through its potential capability to transport oxygen. Some materials, which are referred to as oxygen carriers and are often transition metals [74], when in contact with oxygen at high temperature become oxidized, i.e., bind oxygen. This reaction is exothermic and releases an amount

of heat that is comparable to the heat released by the combustion of char (per molecules of O_2 reacted). In the reducing atmosphere of the gasifier, the oxygen carrier can transfer the oxygen to the gas, through reaction of the raw gas species with the bound oxygen. By reacting with hydrocarbons, the transported oxygen shifts the distribution of carbon in the raw gas. Invariably, CO and CO_2 are formed. Reaction of the oxygen with tar compounds to form CO and CO_2 increases the recovery of the valuable and more-manageable forms of carbon. Oxygen carriers used in DFB gasification have been shown to lead to a decrease in total tar yield, although attributing this effect to the oxygen transport rather than the catalytic properties of metals is challenging [75,76]. Some oxygen carriers have also been shown to release oxygen directly to the gas phase, a phenomenon referred to as Chemical-Looping with Oxygen Uncoupling [77]. In this thesis, this effect is not discussed, even though it is possible that some of the results, in particular those described in *Chapters 6* and *7*, were affected by such a phenomenon.

The oxygen transport can also affect the carbon distribution by enhancing the rate of char gasification. Indeed, oxygen carriers have been shown to enhance the rate of the gasification reaction by hindering the inhibitory effects exerted by H_2, CO, and tar species around the converting particles [78–81]. An enhanced gasification rate results in the production of H_2 and CO, thereby increasing the rate of carbon recovery. However, as the inhibitory H_2 and CO are precisely those released by the converting particle, given that they need to be oxidized to enhance the gasification rate, part of the H_2 and CO formed will be immediately converted to H_2O and CO_2.

As stated above, the binding reaction of oxygen in the combustor releases heat, so the heat demand is partly covered by this reaction. The effect is three-fold. First, it results in the effective transfer of CO_2 from the combustor to the gasifier, although not necessarily in a one-to-one manner, depending on which species the transported oxygen reacts with in the gasifier. Second, it leads to a competition for oxygen between the char and oxygen carrier. Third, more char is available to be converted in the gasifier, since less char is required to meet the heat demand.

The overall effect of oxygen transport on the carbon distribution is complex. It depends on the reactivity of the oxygen carrier with the different species in the gasifier and the hydrodynamics of the bed, which influence the gas-oxygen-carrier contact, while the amount of transported oxygen depends on the composition of the material, the temperature levels of both reactors, the circulation rate, and the competition with char for oxygen in the combustor. The impact of oxygen transport on the carbon distribution is a central consideration in this thesis, and it is mainly discussed in the context of the CLG configuration, a DFB configuration that relies on oxygen carriers to inherently separate CO_2. In *Chapter 6*, it will be shown that materials that lack oxygen-carrying properties can acquire such properties by interacting with the fuel ash, thus justifying the importance of studying how the oxygen transport influences the carbon distribution beyond the case of the CLG configuration.

1.2.4. Extent of the gasification reaction

The recovery of carbon in the form of CO can be enhanced by increasing the extent of the gasification reaction in the gasifier. As a consequence, less char is available to cover the heat demand, which requires replacing part of the heat production in the combustor with a process other than char combustion. This can be done, for instance, by the introduction of oxygen-carrying materials, as discussed in the previous section. The simultaneous increase in carbon recovery as CO in the gasifier and destruction of non-valuable species can be achieved by replacing part of the char combustion with the oxidation of these non-valuable species. However, it should be noted that for a given design of the DFB system, enhancing the degree of char gasification in the gasifier requires one or a combination of the following: (1) an increase in the gasifier temperature; (2) an increase in the residence time of the

char; (3) the use of catalysts; and (4) the removal of gasification inhibitors by oxygen transport. However, the endothermic nature of the gasification reaction causes an increase in the heat demand of the gasifier, requiring additional oxidation in the combustor, which may negate the desired effect. Furthermore, the use of a catalyst may result in the enhancement of the conversion reactions for the hydrocarbons that are meant for combustion. The fourth solution, as described in the preceding section, will lead to the formation of CO_2 in the gasifier, which in most cases will not be considered as valuable as the CO produced from gasification. The design of the gasifier can also be optimized for fuel conversion, for instance through the introduction of internals, such as baffles, as suggested by Lundberg [82]. It should, however, be noted that enhancing the gasification reaction does not increase the overall level of carbon recovery if the carbon in the flue gas is recovered.

1.2.5. Tuning the heat demand

Reducing the heat demand in the gasifier increases the amount of carbon that is available for conversion in the gasifier, mainly as char. Various strategies exist to decrease the heat demand that are not related to changing the operating parameters of the DFB loop itself, i.e., affecting neither the temperature of the gasifier nor the circulation rate of the bed. This is particularly important given that the methods used to increase carbon recovery mentioned in the previous sections would likely lead to an increase in the heat demand. The heat demand can be decreased through increased preheating of the input streams to the DFB reactors, increased drying of the fuel, and reducing heat losses through improved insulation and refractory lining of interior surfaces. The extent to which preheating and drying can be carried out depends on the possibilities for heat integration in the plant. Another way to reduce the heat demand is to use oxygen-enriched air in the combustor. If the concentration of nitrogen becomes so low in the combustor that CO_2 separation becomes viable, full carbon recovery can be achieved, which is the basis for the oxyfuel configuration discussed in the next section. This DFB gasification configuration is compared to other configurations in *Chapter 4* on the basis of their carbon distributions.

1.3. Producing a concentrated CO_2 stream in the combustor

To maximize CO_2 separation, the air fed into the combustor can be entirely replaced with oxygen. Thus, a near-pure stream of CO_2 is obtained that is only slightly diluted with oxygen and contains some impurities, such as SO_2 and NO_2. Due to the absence of dilution with nitrogen, the dimensions of the combustor can be reduced and the amount of char required to fulfill the heat demand can be decreased. The temperature in the combustor can be controlled by circulating the flue gases; this also allows for control of the bed circulation independently of the oxygen requirement.

Several technologies exist for the production of pure oxygen, with the most widely applied being the cryogenic separation of oxygen from air in a so-called Air Separation Unit (ASU). Oxygen can also be produced by electrolysis of water, which has the advantage that it also produces H_2. H_2 can be used to adjust the $H_2/(CO+CO_2)$ ratio of the syngas, for instance to obtain the optimal value for the methanolation process. Thus, full recovery of carbon as valuable species, such as syngas and olefins, becomes feasible. It is noteworthy that the electrolysis pathway can also serve as a way to balance the grid during periods of excess power production [23].

1.3.1. Sorption-enhanced DFB gasification

The use of calcium oxide-containing bed materials in a DFB gasifier can lead to carbonation-calcination cycles, whereby CO_2 is captured by the bed in the gasifier and released in the combustor [83], given favorable conditions of temperature and CO_2 partial pressure in both reactors. This may be

of interest when a high yield of H_2 is desired and oxy-combustion is carried out in the combustor. Indeed, the removal of CO_2 by the bed in the gasifier displaces the equilibrium of the WGS reaction, resulting in increased production of H_2 and CO_2. This, in combination with the catalytic activity of calcium oxide species towards the reforming of tar and light hydrocarbons, allows for high yields of H_2. By operating the combustor in oxyfuel mode, the CO_2 in the flue gas can be recovered. This is of interest when negative CO_2 emissions are desired, promoting the use of biomass in combination with carbon capture. The sorption-enhanced DFB gasification configuration is not investigated in this thesis.

1.4. Carbon-free heat production in the combustor

1.4.1. Electrification

In theory, part or all of the heat demand of the gasifier can be covered by electrical heating. This can be achieved by placing electrical coils in a moderately fluidized section prior to the combustor, so as to limit erosion. Although it would be possible to heat the gasifier directly with coils, thereby removing the need for a combustor, the products that are not valorized still need to be combusted. These products include the carbon in the fly ash from the gasifier, which may represent a significant fraction of the total carbon. Furthermore, the combustor is involved in regenerating the catalytic bed material. Consequently, the combustor is needed, and meeting all of the heat demand with electrical heating is not desirable. Electrical heating can also be used in a steam reformer downstream of the gasifier, to convert non-valuable, carbon-containing species into valuable species. Nevertheless, electrical heating is likely to be feasible only if cheap and renewable electricity is available. The DFB configuration based on electrification, referred to as the "Electrical" configuration, is one of the configurations compared in *Chapter 4* in terms of the carbon distribution that it produces and its potential for carbon recovery.

1.4.2. Chemical-Looping Gasification

The CLG concept is based on the use of an oxygen carrier as the bed material in a DFB system [84]. Ideally, the oxygen transported to the gasifier reacts with non-valuable carbon species to convert them to valuable forms. As the oxidation of char is replaced by that of the oxygen carrier, char is no longer needed to fulfill the heat demand of the gasifier. It can and should instead be gasified. This ideal case is depicted in Figure 5. Thus, CLG offers the potential for full recovery of carbon on the gasifier side. Note that the reactor in which the oxidation occurs is usually called the "air reactor" (AR) and the gasifier is termed the "fuel reactor" (FR). These terms will be used in this thesis when discussing CLG, although they represent the same conceptual units as the combustor and the gasifier, respectively.

Despite the attractive features of the CLG process, there are a number of crucial obstacles that must be overcome for the process to attain the ideal scenario described in the preceding paragraph. Many of these issues are related to the oxygen carrier itself. Indeed, long-term operation of a CLG process requires that an oxygen carrier be used that remains stable under the thermal and mechanical stresses, as well as during the repeated reduction-oxidation cycles [85]. The material must also retain its reactivity for a sufficiently long time, such that frequent makeup feeding of fresh oxygen carrier is not required. Obviously, low-cost oxygen carriers are desirable, especially to alleviate the two aforementioned issues. In this context, using a waste or a waste-derived material as the oxygen carrier would confer tremendous advantages. Finally, the heat of oxidation of the oxygen carrier must be sufficient to cover the heat demand of the gasifier under the conditions selected. Moreover, these conditions must be compatible with the thermodynamics of the reduction-oxidation profile of the material.

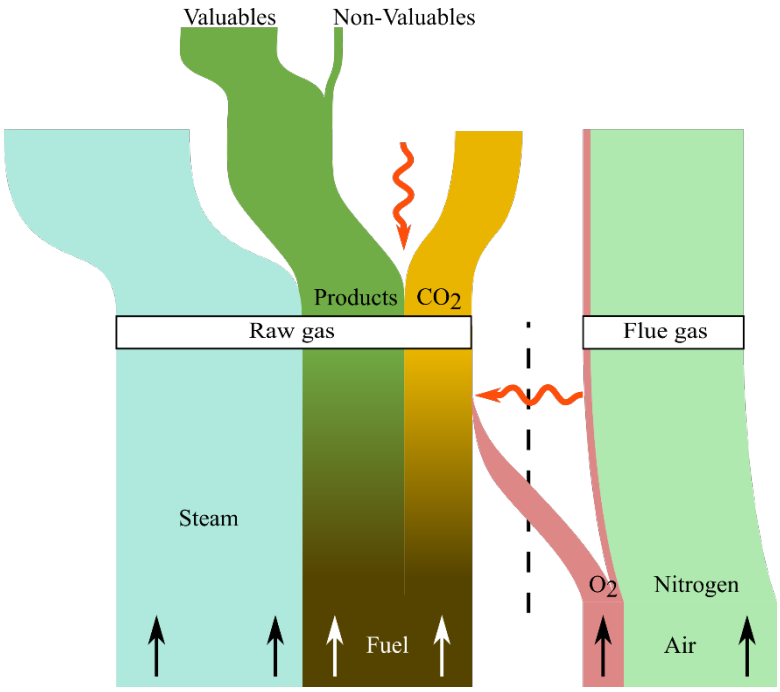

Figure 5. Conceptual representation of the flow of carbon through an idealized CLG unit. The carbon flows that result from the fuel are shown in green and gold. The steam fed into the gasifier and the air fed into the combustor are also shown. The widths of the carbon flows represent their approximate relative amounts for an idealized CLG case, in which the oxygen transport leads to an increase in the levels of valuable products and a decrease in the levels of non-valuable products, whereas the amount of CO_2 is only slightly increased.

Another major challenge is to ensure complete conversion of the fuel in the FR. Obviously, complete conversion is not achievable, given the stochastic nature of the mixing in the fluidized bed of the FR and the entrainment of fine carbon particles. Nonetheless, conversion needs to be maximized, since any carbon lost to the AR is likely to be emitted to the atmosphere, given that the CO_2 concentration will be low, well below that of a regular DFB. One way to prevent char being transported to the AR is to use a so-called "carbon stripper", as described elsewhere [86]. Note that the regeneration of the bed from potential coking also results in the emission of a small amount of carbon in the AR. Whether or not non-valuable species such as tar are still destroyed in the AR will depend on whether the associated loss of carbon to the atmosphere is deemed acceptable.

Even if all these issues can be resolved, there remains the problem as to the form in which carbon is recovered in the FR. Indeed, the oxygen transported to the gasifier is likely to react with the valuable carbon-containing species or with hydrogen, rather than with non-valuable species (generally tar). One reason for this is that the concentration of valuable (excluding CO_2) carbon species is higher than the concentration of non-valuable species. Moreover, devolatilization is more likely to occur on the surface of the fluidized bed, due to the fuel particles being lifted by their own volatiles [87], and this is the position at which the degree of gas-oxygen carrier contact is lowest. Besides, H_2 has been shown to react faster than CO and CH_4 when using common oxygen carriers such as ilmenite or manganese ores [88–90], and this will lead to a lower H_2/CO ratio in the gas. In a situation in which a specific H_2/CO ratio is desired for downstream synthesis, this implies that more CO will likely need to be oxidized to CO_2 *via* the WGS reaction to reach the desired H_2/CO ratio. In light of these factors, a compromise must be found between the recovery of carbon in the FR in a valuable form and the "C-free" fulfillment of the heat demand in the AR.

The issues related to achieving complete conversion in the CLG configuration and the oxidation of valuable species are in focus in *Chapter 7*, in which the parameters that affect the conversion of a plastic waste are investigated and serve as the basis for comprehensive discussions on the issues described in this section and on the potential role of CLG in the future circular economy.

1.5. Carbon recovery exclusively as CO_2: Chemical-Looping Combustion

In a scenario in which the circular use of plastics is well-established and sufficiently efficient to require only a limited input of biomass to compensate for the inevitable losses, and in which removal of CO_2 from the atmosphere is assigned a value by Society, then the thermochemical conversion of biomass might be limited to the production of biofuels and CO_2 for negative emissions. In such a case, the application of oxygen carriers in a DFB system becomes an attractive way of achieving the latter goal. By targeting very high levels of oxygen transport between the reactors, the carbon from the biomass can be fully converted to CO_2 in a pure stream in the gasifier, while heat that exceeds the FR's heat demand is produced in the AR. This process, which is called Chemical-Looping Combustion (CLC), has been extensively investigated [84,85,91].

1.6. Aspects of carbon recovery in DFB processes investigated in this thesis

In this thesis, the various parameters that influence the carbon distribution and its rate of recovery, as well as the various configurations in which the DFB gasification technology can be operated to facilitate complete carbon recovery are discussed. The results chapters (*Chapters 4–8*) discuss one or several of the aspects considered in the present chapter. In *Chapter 4*, the different configurations are compared in terms of the carbon distributions that they produce. In *Chapter 5*, the possibility to increase the value of carbon in the gasifier by converting tar to valuable forms of carbon is investigated, through increasing the catalytic activity of the bed. The more general impacts of the catalytic activity on the carbon distribution are also investigated, theoretically in *Chapter 4* and experimentally in *Chapter 5*. The increase in catalytic activity was also found to increase the oxygen transport, a phenomenon that has been reported previously, which is verified in *Chapter 6*. This phenomenon constitutes a shift from the regular DFB gasification configuration to the CLG configuration (described in *Section 1.4.2*), which can drastically alter the carbon distribution and possibilities for carbon recovery. *Chapter 7* investigates the parameters that influence fuel conversion in CLG, a critical aspect of the configuration, as described in *Section 1.4.2*. The results shown are those from **Paper II**, which deals with the conversion of a metal-rich plastic waste that forms its own oxygen-carrying bed material. Finally, *Chapter 8* presents a case in which the DFB gasification technology, in a CLG-type configuration, is used to provide a reducing gas for the reduction of iron ore. The configuration proposed for the DFB gasification is based on the use of a waste material as oxygen carrier, with the addition of a third reactor to the loop, wherein the oxygen carrier is reduced prior to entering the gasifier. These specificities of the design and operation resolve many of the issues related to the CLG configuration (as discussed in the present chapter and throughout the thesis). Carbon separation and sequestration (in the form of CO_2) of most of the carbon introduced to the process is also a feature of the proposed process.

Chapters 5, *7*, and *8* all discuss the use of waste materials to increase or facilitate carbon recovery. A plastic waste that also acts as the source of the oxygen carrier is converted in *Chapter 7*, a waste stream from the steelmaking industry is used as the oxygen carrier in *Chapter 8*, and flue gas ashes generated

from the DFB gasification process are used as a catalytic additive in *Chapter 5*. These three levels of utilization of waste materials in DFB gasification, i.e., as fuel (or carbon source), as bed material and as additive, are discussed in *Chapter 2*. The specific waste materials used in the three aforementioned chapters are also presented.

Chapter 2: Possibilities for using waste in DFB gasification processes

Besides its role as a carbon-extraction process and its potential as a negative-emissions technology, DFB gasification could contribute to the circular economy by using waste materials. There are three main pathways through which the DFB gasification technology could utilize waste materials efficiently. The first way is to convert in the gasifier a carbon-containing waste rather than a fossil fuel or an energy crop. The second route is to replace the bed material with a waste that fulfills the same purpose (heat transport and thermal flywheel effect) and that has potential catalytic or oxygen-carrying effects. The third pathway employs waste as an additive to the process, so as to improve the process performance or drive the compositions of the products in a desired direction.

In this chapter, these three pathways for DFB gasification to use waste are discussed in terms of the features of the wastes that make them suitable for use in the DFB gasifier and their expected behaviors within the system. For each pathway, the waste that was examined in the work of this thesis is presented and the investigations of its use in DFB gasification or similar applications are discussed. For the first two pathways, the considered waste is sourced external to the process, whereas for the third pathway, the waste is sourced from within the DFB process itself, thereby introducing an additional layer of circularity to the process.

2.1. Conversion of waste

An obvious possibility for waste utilization in DFB processes is the conversion of carbon-containing waste streams. As stated in the *Introduction*, these waste streams are either of biogenic origin, i.e., biomass waste, such as forest and agricultural residues or food waste, or of fossil origin, i.e., plastic waste (which can be contaminated with biogenic residues). Converting these wastes in DFB gasifiers entails several challenges, due to the nature of the wastes and the systems used to collect them. For instance, a waste stream of plastic packaging contains many types of polymers, which are often contaminated with food and other biogenic residues and may contain contaminants from other waste-sorting streams, such as metals, glass, cardboard and paper. Although additional sorting occurs after recycling by the consumer, some of those contaminants inevitably end up in the final plastic packaging waste.

This variability of the compositions of waste streams means that it is challenging to predict both the behavior of the waste in a conversion unit and the compositions of the products, which in turn makes it difficult to fine-tune the process. In addition, given the potential inclusion of inorganic materials in the waste, issues such as agglomeration, clogging, fouling, and corrosion render the operation of the process problematic. When converting biomass waste, the alkali content has to be carefully monitored, given that alkali interactions with the silica in the bed material, dirt, and the mineral inclusions in the biomass itself, can lead to agglomeration [54]. Furthermore, the presence of halogens in plastic waste means that, during conversion, persistent organic pollutants (POP) such as dioxins and polychlorinated dibenzofurans can be formed.

The properties of the selected waste will significantly influence the carbon distribution resulting from its conversion. The critical properties of the waste with regard to the carbon distribution are its: (i) elemental organic composition, especially its C, H, and O contents; (ii) chemical structure; (iii) volatiles and fixed carbon yields; (iv) moisture content; and (v) ash content and the composition thereof. Fuels with a high concentration of oxygen will produce more CO and CO_2 than other fuels.

The chemical structure of the fuel determines the devolatilization step [92], which will affect the amounts and compositions of the permanent gas and tar, as well as the yield of char. The latter also depends upon the process conditions, i.e., heating rate, temperature, and pressure [93]. The carbon content of waste that produces a lot of char will primarily be recovered as either CO (through gasification) or CO_2 (through oxidation in the combustor or *via* the WGS reaction in the gasifier). Conversely, wastes with high levels of volatiles will produce much more tar and generate lighter hydrocarbons from tar decomposition. The fixed carbon level may be too low to be compatible with the regular, self-sustained operation of the DFB. In that situation, heat needs to be provided through an alternative pathway, possibly by combusting non-valorized products and even valuable products if the closure of the heat balance requires it. The combustion of an alternative waste fuel can also be carried out in the combustor.

The moisture content of the waste has a significant impact on the heat demand of the gasifier, since the moisture acts as a heat sink. The increased heat demand leads to a necessary shift of carbon to CO_2 in the flue gases. The steam added to the system increases the degree of dilution of the reactive gases, thereby affecting the reactions. Similarly, the ash content of the fuel can have a strong impact on the rate of carbon conversion and, more generally, on the reactions within the gasifier. Indeed, active species may be present in the ash, acting as a catalyst or activator for the bed material, as discussed in *Section 1.2.2*. Conversely, these species can poison catalytic sites in the catalytic bed or react to form non-catalytic phases. From the energetic standpoint, if the ash content is high it can act as a heat sink. Furthermore, ash that has an oxygen-carrying capacity, if it remains in the bed, facilitates the displacement of carbon from the combustor to the gasifier.

2.1.1. Automotive Shredder Residue

In this thesis, a plastic-containing waste that is rich in metals was used as both the fuel and the source of the oxygen carrier for a CLG process. This waste, automotive shredder residue (ASR), is the remainder fraction of the shredding and sorting process for automobiles, corresponding to about 20%–25% of the original weight of the vehicle [94]. After depollution and dismantling, shredding of the car body is carried out and the metals are separated, which results in a rest fraction that contains plastics, foams, non-ferrous inorganics, and dirt, as well as metals that were not separated. This fraction, which is the ASR, is thus a highly heterogeneous carbon waste that contains high levels of inorganic compounds, notably metals [94–96]. Due to its metal content, ASR can be used to generate its own oxygen-carrying bed material for the CLG process, which is the subject of **Paper II**.

Based on its properties and as a consequence of regulatory pressures, there have been extensive investigations of ASR thermochemical recycling [94–97]. Indeed, EU Directive 2000/53/EC [98] requires the EU Member States to ensure that the reuse and recovery of end-of-life vehicles reach a minimum of 95% (by average weight per vehicle per year), and that reuse and recycling should reach a minimum of 85%. It can be expected that, in the future, more stringent requirements will be set, with energy recovery rates lower than the 10% allowed by the current directive. Owing to the increasing use in car manufacturing of lightweight materials, such as plastics and polymer composites [99], meeting these requirements will place intense pressure on the recycling of ASR.

However, the lack of a standard definition or composition for ASR makes it challenging to find a technology that addresses both the variability of its composition and its heterogeneity. Differences in shredding and separation process technologies and efficiencies, as well as the evolving composition of cars create differences at the local and national levels. Furthermore, cars are rarely the sole input to shredders, which are typically also fed with scrap iron and white goods [95,97,100]. Nevertheless,

ASR is expected to comprise polyolefins, polyurethanes, polyvinyl chloride, polyamides, polystyrene, and various blends of compounds, such as acrylonitrile butadiene styrene and glass fiber-reinforced polymers [96,101]. The metal fraction of ASR comprises iron, aluminum, and copper in large quantities, as well as zinc, lead, chromium, and nickel [96,102]. It is noteworthy that the chlorine content of ASR can be high [95,102], which can lead to the formation of POP during thermochemical conversion [95,103].

The ASR fraction converted in the experiments described in **Paper II** and reported in *Chapter 7* corresponds to the residual fraction obtained after additional sorting of the ASR to meet the aforementioned requirements regarding the rates of reuse, recovery, and recycling. This rest fraction is referred to hereinafter simply as 'ASR'. Investigating the thermochemical recycling of ASR constitutes an interesting case study, as ASR is an example of the rest fraction that emerges from extensive sorting. The circular use of plastics means that homogeneous plastic streams with few impurities must be produced. The refuse from this process will typically consist of inorganics, probably including metals, as well as plastics due to process inefficiencies. As such, thermochemical recycling strategies that work for ASR are likely to be applicable to these wastes.

2.2. Waste-derived bed materials

For a waste material to be usable as a bed material for DFB gasification, the same criteria that apply to standard bed materials must be met. First, the waste must be thermally and mechanically stable under the conditions of temperature and flow prevailing in the DFB loop. Second, materials with too-high attrition rates cannot be used, as the rate of makeup feeding of new bed material would be detrimental and the production of fines would be overwhelming. Third, the melting point of the material must be well above the operating temperatures. Finally, if no further application exists for the exhausted bed material, i.e., when it is extracted as bottom ash or fly ash, its disposal must meet the environmental regulations in force.

The interactions of the bed with ash components released by the fuel in the gasifier must also be carefully considered. Particular attention must be paid to the risk of agglomeration, which is a prevailing problem with alkali from biomass ash. Nonetheless, the waste material can develop a beneficial catalytic activity by interacting with the ash components. Conversely, the material can develop catalytic activity towards undesirable reactions or it can develop an oxygen-carrying propensity, as explored in *Chapter 6*, which could be beneficial or detrimental depending on the aim of the process.

Waste-derived bed materials can be introduced into the DFB gasifier in the form of a waste fuel ash, provided that the ash content of that fuel and the sizes of the ash particles are sufficient to remain in the bed material loop and gradually replace the starting bed material. This type of intrinsic bed material is highly advantageous in terms of the cost-competitiveness of the process, since the cost associated with makeup feeding of bed material is avoided. ASR is one example of a type of waste fuel that provides its own bed material. In the Chalmers gasifier, the high metal content of the ASR ash was shown to generate an oxygen-carrying bed, which was then used to investigate the parameters that influence fuel conversion in CLG (**Paper II** and *Chapter 7*). A crucial issue linked to bed materials derived from ash-rich waste fuel is that, if the ash forms a bed with undesirable properties, then the cost associated with maintaining a bed with the desired properties becomes high.

2.2.1. LD slag: a metallurgic waste

In *Chapter 8*, a waste from the steelmaking industry, steel slag, is used as the oxygen-carrying bed material for the CLG configuration that provides the reducing gas to the process involving the direct reduction of iron. Most of the steelmaking slag produced globally comes from the basic oxygen furnace (BOF), which is the main route for steelmaking, rather than from the direct reduction route, i.e., from the electric arc furnace (EAF). Nevertheless, and although the slag composition depends on the steelmaking process and fluxing agents used, the bulk compositions of EAF and BOF slags are similar; notably, they have a relatively high iron content, which is 20%–30% (in mass) for EAF slag [104]. The properties and typical fate of the slag are, therefore, discussed for the BOF slag, with the understanding that a similar profile can be expected for the EAF slag. BOF slag is also known as LD slag, and is referred to as such hereinafter. In general, LD slag is produced in large quantities, at 85–165 kg for every tonne of steel produced [105]. The elemental composition of LD slag (on an oxides basis) is dominated by CaO (30%–60%), FeO (5%–38%), and SiO_2 (8%–26%), while it can contain significant amounts of MgO, MnO, Al_2O_3, TiO_2, P_2O_5, and V_2O_3 [105–108].

LD slag is not a hazardous waste and is suitable for use in a wide range of applications. For instance, it can be used as a soil stabilizer and conditioner, as fertilizer, for road-making, or for CO_2 capture and flue gas desulfurization [108,109]. Nevertheless, despite efforts to identify applications for this material, large quantities of LD slag are still landfilled or stored for later applications [110]. Given its iron content, LD slag shows potential for use in chemical-looping applications, such as CLC and CLG, as well as in chemical-looping reforming, which is a technology that upgrades a raw gasification gas by converting tar. The potential of LD slag in these applications has mostly been investigated at the laboratory scale. Its ability to convert hydrocarbons, modeled by CH_4 and C_2H_4, is poor [111,112], especially with respect to CH_4, although it displays reactivity and CO_2 yields comparable to those of ilmenite when converting syngas [113].

LD slag has also recently been investigated as an oxygen carrier for Oxygen-Carrier-Aided Combustion (OCAC), which is a CFB combustion process that exploits the properties of oxygen carriers to improve the performance of the process and reduce emissions [114], notably of CO. In a semi-industrial-scale unit, Rydén *et al.* have shown that, when mixed with silica sand, LD slag generates lower CO emissions, although it did not perform as well as other oxygen carriers, such as ilmenite, when investigated in the same CFB [110].

As pointed out by Hildor *et al.*, LD slag has a relatively weak oxygen-carrying capability, which may make it more suitable for OCAC and CLG processes than for CLC [115]. Furthermore, the limited absorption of alkali by the material, which may be problematic in CLC and OCAC, is not as disadvantageous in CLG and may actually be beneficial, as it can result in an increased partial pressure of alkali and, thereby, increase homogeneous catalysis. Hildor *et al.* have further studied the potential of LD slag for CLG at the laboratory scale, focusing on its impact on char gasification, its interactions with various gaseous species, and its catalytic effects [116]. They reported that higher gasification rates could be achieved with LD slag than with olivine or sand as the bed material. In addition, they showed that the LD slag is catalytic towards the WGS reaction and can be partly re-oxidized by water in the gasification environment, resulting in the formation of H_2. These two effects were found to lead to a high H_2/CO ratio at 800°C.

LD slag has also been investigated as an oxygen carrier for CLG at the semi-industrial scale, in the Chalmers gasifier. The results have been presented in a conference article by the author of the present thesis [117]. LD slag, partly mixed with silica sand, was compared with ilmenite and manganese ore,

two extensively investigated natural oxygen carriers. A higher degree of char gasification was observed for LD slag than for olivine and sand as the bed material, in concordance with the findings of Hildor *et al.* [116]. Higher H_2 yields were obtained with LD slag that with the other oxygen carriers, and this was attributed to the catalysis of the WGS reaction. Two measures to control the oxygen transport were also investigated for the different oxygen carriers discussed in the conference paper. The results from this paper are briefly discussed in *Chapter 7*, in relation to the optimal operation of the CLG configuration, and in *Chapter 8*, to show that steelmaking slag can generate the oxygen transport levels required to operate the CLG configuration. Based on the properties discussed in this section, LD slag appears to be a suitable oxygen carrier for CLG, which provides justification for using it (or its EAF slag counterpart) as the oxygen carrier in the CLG process proposed in *Chapter 8* (and **Paper V**) for the reduction of iron ore.

2.3. Waste as additive

The use of additives in DFB gasification can serve multiple purposes. Additives frequently act as sorbents for the removal of pollutants in DFB gasifiers. For instance, limestone is used for desulfurization and chlorine removal, as mentioned in *Section 1.2.2*. Catalytic particles can be added to the bed material to increase its activity. Additives can also be added to enhance the properties of the bed material. Waste that is sourced external to the process may be used as an additive if it has the desired sorbent, catalytic, or activity-inducing properties, and provided that its use does not introduce harmful components. In this thesis, a waste produced by the process itself, namely the fly ash, is considered as an additive in DFB gasification.

2.3.1. Waste inherent to the DFB process: fly ash circulation

The main wastes produced by the DFB process are the bottom ash, which is extracted from the bottom of the combustor bed, and the fly ash, which is derived from the gasifier raw gas and the combustor flue gas. The former stream contains mainly larger bed material particles, agglomerates, and impurities present in the fuel, such as sand or nails. The latter stream comprises mainly attrition-derived bed particles, small fuel ash particles, and aerosols that are formed from condensing ash components and heavy tar molecules.

The bottom ashes of DFB gasifiers are expected to resemble those obtained from CFB combustion of the same fuel. Therefore, it is to be expected that they can be used in similar applications, typically in cement and concrete production [118]. The routes available for the utilization of gasification fly ash are fewer, due mainly to its high carbon content, the presence of polyaromatic hydrocarbons, and, in the case of waste gasification, potentially high concentrations of chlorine and heavy metals [118–121]. A few options exist for direct utilization: as an alternative fuel, for instance in cement kilns; as a filler in asphalt and asphalt-like products; and as a component of lightweight aggregates. Different types of pretreatments of the fly ash expand the range of options, in particular washing to remove chlorine and alkali, heat treatment to decrease the carbon content, and leaching of heavy metals. After treatment, gasification fly ashes can be used in construction, as fillers in concrete mortar, as road base materials, and as fertilizer or soil stabilizer, among other options [118–121].

Although finding uses for the ashes generated from DFB gasification is important, the possibilities to take advantage of these ashes within the DFB system should be investigated, in particular if they offer ways to improve the recovery of carbon. In the GoBiGas DFB plant, the product gas ash from the gasifier, containing 10–15wt% carbon, was circulated back to the combustor for carbon and energy recovery [11], while the coarse flue gas ash was circulated back to the gasifier, mainly to increase bed material retention in the loop. However, this external material loop (in addition to the internal loop

involved in bed material circulation) reintroduced ash components and potential additives to the system, with impacts on the performance and operation of the process.

These ash loops are associated with certain negative consequences, as discussed by Kirnbauer *et al.*, who studied the balance of inorganics in the DFB system of the Güssing plant [9]. These authors reported that the ash loops caused significant accumulations of low-melting-point substances in the system. The accumulation of K was identified as being particularly critical, due to its roles in fouling, slagging, and bed agglomeration. Kirnbauer and colleagues recommended that the recirculation of fine fly ash from the combustor should be avoided. However, the potential beneficial effects of the accumulation of such active species as K were not investigated.

At the intersection of the use of waste as a bed material and its use as an additive, Kuba *et al*. have investigated the impact of replacing part of the fresh material, in that case olivine, with ash-layered olivine recovered from the bottom ash of the combustor [10]. This replacement was carried out as part of the optimization of the organic flows in the HGA Senden DFB gasifier, wherein the fuel is logging residues that contain large quantities of foreign mineral matter, mostly quartz. The bottom ash was sieved to remove the large quartz particles, and the active, layered olivine particles were collected and fed back into the DFB loop. This new ash loop replaced the circulation of coarse flue gas ash, which was instead discharged. The authors reported improved performance of the gasification process as the hydrogen concentration increased, whereas the level of methane decreased, as did the concentrations of tar components, most significantly naphthalene and acenaphthylene.

The circulation of flue gas fly ash, and more precisely the circulation of its coarse fraction, led to the enhanced activation of the bed material in **Paper I**, resulting in reduced tar yields. This effect of the coarse ash circulation on the tar yield is reported in *Chapter 5*, where the focus is on the impacts of this enhanced catalytic activity on the carbon distribution. Notably, the question of whether catalytic activity increases the recovery of valuable forms of carbon is addressed for a wide range of experiments extending beyond the results reported in **Paper I**.

Chapter 3: The Chalmers Dual Fluidized Bed Gasifier

This chapter describes the Chalmers gasifier and its associated gas sampling and measurement system, as well as the methods for establishing the carbon balance and the energy balance of the system. The results shown in *Chapters 5*, *6*, and *7* are based on experiments carried out in this facility, using the methods described in this chapter. The work described in *Chapters 6* and *7* also relied upon laboratory- and batch-scale experiments, the setups of which are not discussed in this chapter, but can be found in **Paper IV** and **Paper II**, respectively. Finally, the compositions of the bed materials and fuels used in the various experiments that constitute this thesis are reported. *Chapters 4* and *8* do not discuss experimental results but are based on the mass and energy balances derived from the gas compositions obtained in experiments conducted in the Chalmers gasifier.

3.1. Description of the unit

The Chalmers DFB gasifier consists of a 12-MWth circulating fluidized bed boiler, to which a 2–4-MWth bubbling bed gasifier has been retrofitted. The boiler is fed wood chips and wood pellets. The boiler is designed to provide heat to the Chalmers University campus during wintertime. As a consequence, it is over-dimensioned when one considers a combustor that would operate with the 2–4-MWth gasifier if the DFB was operated as a standalone unit. Being a research facility, the Chalmers DFB gasifier is not equipped with a raw gas cleaning or upgrading section. Instead, the raw gas is fed to the boiler. Note that this means that one half of the external material loop described in *Section 2.3.1*, namely the circulation of gasification fly ash, is permanently implemented in the Chalmers gasifier. Hereinafter, the CFB boiler is referred to as the ‘combustor’.

A schematic of the Chalmers DFB gasification unit is shown in Figure 6. The CFB combustor is comprised of the combustor itself (#1 in the figure) and the primary cyclone (#2), which when the unit is operated in CFB mode only, recirculates the bed to the combustor *via* the particle distributor (#3). Located between the particle distributor and the return leg of the combustor is a particle cooler (#10), the purpose of which is to extract additional heat, if needed. Heat from the flue gases exiting the combustor is recovered in the convection path (#7), and the particles contained in the flue gas ashes are collected in a secondary cyclone (#8). Finer particles that are not captured by the secondary cyclone are trapped in a bag house filter (#9). When the unit is operated in DFB mode, the bed material circulates from the particle distributor to the gasifier (#5) *via* the first loop seal (#4). The bed material returns to the combustor through a second loop seal (#6), which is connected to the return leg of the combustor. This connection is represented by the two red symbols in the figure. The positions of the fuel feed-points to both the combustor and gasifier are indicated by blue arrows. The combustor is fluidized with air, whereas the gasifier is fluidized with steam, although it can be fluidized with flue gases when not being fed with fuel. For an extensive description of the unit, the reader is directed to the work of Larsson *et al.* [122].

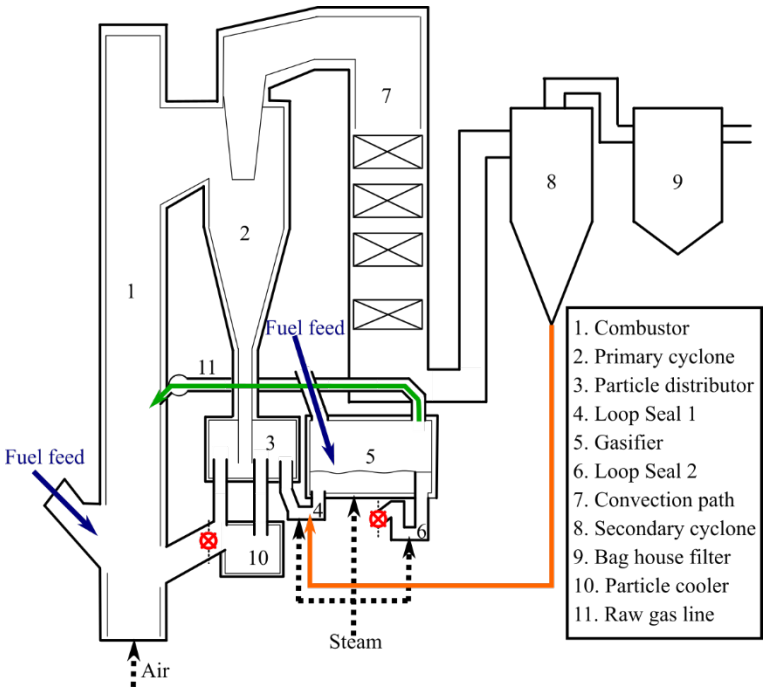

Figure 6. Schematic of the Chalmers DFB gasifier. The blue arrows represent the positions of the fuel-feeding to the combustor and the gasifier, respectively. The green arrow represents the raw gas line, underlining the fact that it is fed to the combustor. The orange arrow represents the circulation of the coarse flue gas ash, which is collected from the secondary cyclone (#8), to the gasifier via the first loop seal (#4). This was part of the investigation carried out in **Paper I**, some of the results of which are reported in *Chapter 5*. The red symbols in the figure are in reality physical connections, whereby loop seal 2 (#6) feeds into the return leg to the combustor.

As mentioned above, the raw gas line (#11) feeds directly into the combustor, as indicated in Figure 6 by a green arrow. This arrow also represents the circulation of the gasifier fly ash. The second half of the external material loop, in this case the circulation of coarse flue gas ash, is represented by an orange arrow. The coarse flue gas ash collected from the secondary cyclone can be fed to loop seal 1 (#4 in Figure 6), thereby completing the external material loop. The circulation of coarse flue gas ash is not carried out during regular operation of the Chalmers gasifier. The consequences of the coarse flue gas ash circulation for the gasification process were investigated in **Paper I** and will be discussed in *Chapter 5*.

It must be emphasized that gasification measurements are only possible when sufficient manpower is available for both the CFB side and the gasifier side. The CFB is operated continuously but is manned for only two six-hours shifts per day. During the remainder of the time, fuel is not fed into the gasifier, which is then fluidized with flue gases. This means that on the CFB side, the fuel input is constant, and is about an order of magnitude higher (in terms of mass flow) than the fuel input to the gasifier, which is intermittent. This has a significant impact when one considers the roles of ash flows and ash accumulation. When feeding biomass to the gasifier it should be borne in mind that the ash input is in that instance dominated by the CFB side. When feeding ash-rich waste, such as the ASR described in *Section 2.1.1*, one must consider that the biomass ash input from the CFB side is not negligible.

3.2. Raw gas sampling and analysis

The raw gas produced by the gasifier is characterized by extracting a slipstream from the raw gas line and then cleansing it of particulate matter in a high-temperature filter. From there, the slipstream is separated into two sub-streams for further analysis. The first sub-stream is used to sample the tar and

determine the dry gas composition, while the second sub-stream is passed through a high-temperature reactor (HTR), to determine the total carbon content of the raw gas.

From the analyses of the two sub-streams, only the concentrations of the permanent gas species and solid-phase adsorption (SPA)-tar become known. To determine the yields and establish the carbon balance of the system, helium (He) gas is introduced as a tracer into the gasifier with the fluidizing steam at a known volumetric flow. The He balance across the system can then be used to convert the concentrations into product yields, expressing their quantities in moles or mass of product per unit mass of dry, ash-free fuel fed (designated as 'daf').

The first sub-stream is quenched with cold isopropanol, to remove condensable hydrocarbons and steam. Once dry, the stream is fed into a micro-gas chromatograph (GC) Varian CP4900 equipped with a PoraPLOT Q column and an MS 5Å column, using He and Ar as carrier gases. The GC measures the concentrations of H_2, He, N_2, CO, O_2, CO_2, CH_4, C_2H_2, C_2H_4, C_2H_6, C_3H_6, C_3H_8, and H_2S. Thus, the permanent gas composition is determined. Prior to quenching, a port allows sampling of the tar by the SPA method. In this method, the gas is passed through an adsorbent column that contains a first layer of 500 mg of aminopropyl-bonded silica, and a second layer that contains 500 mg of activated carbon, the purpose of which is to capture benzene, toluene, and xylene (BTX), which are not adequately absorbed by the first layer. The adsorbed tars are eluted from the columns and are thereafter analyzed in a BRUKER-430 GC equipped with a flame ionization detector. Heavy hydrocarbons with boiling points ranging from those of benzene to chrysene are thus quantified. The hydrocarbons that have boiling points within this range are defined as 'tar' in this thesis. The SPA method and its application for measuring the tar from the Chalmers gasifier have been described previously by Israelsson *et al.* [123].

The second sub-stream is reacted at 1700°C in the HTR, thereby cracking the hydrocarbons and gasifying the soot to form exclusively H_2, CO, CO_2, and H_2O. The gas is filtered to remove any remaining soot particles, then the steam is condensed, and the dry gas is led to a second micro-GC (of the same model as that used for the first slipstream line), equipped with PoraPLOT U and MS 5Å columns, and using He and Ar, respectively, as the carrier gas. The HTR and its use in determining the total carbon from the raw gas have been described by Israelsson *et al.* [124].

The measurements reported in this work correspond to periods of more than 20 minutes, during which the temperature, fuel feeding rate, steam flow, and circulation rate can be considered as stable. Chromatograms are captured every 3 minutes, and the gas concentration for the measurement point is taken as the average of the results from those chromatograms. Similarly, the tar concentration is the average of the concentrations obtained from the SPA samples, which, in general, are collected in the number of at least four.

3.3. Carbon balance

The total carbon determined in the HTR is used to assess the carbon distributions for the various outputs of the gasifier. The degree of conversion or, alternatively, the amount of carbon in the unconverted fuel leaving the gasifier is assessed by comparing the total carbon from the HTR to the carbon content of the fuel. Note that this includes the char and non-devolatilized fractions of the fuel that circulate to the combustor with the bed, coking onto the bed particles, as well as the small carbon particles and soot that leave with the fly ash. The amount of carbon contained in all the hydrocarbons with at least four carbon atoms, referred to as *total organic compounds* (TOC) in this work, is assessed by comparing the total carbon from the HTR to the amount of carbon in the permanent gas. Among

the TOC, those species that are outside the SPA measurement range, referred to as *undetected condensable species*, are assessed by comparing the total carbon to the sum of the permanent gas carbon and SPA-tar carbon.

The oxygen transported into the gasifier by the bed material is also determined using the HTR, by establishing the oxygen balance over the gasifier, as described by Israelsson *et al.* [124]. Equation 1 shows the calculation of the oxygen transport, where n_i refers to the yield of C, H, and O, the subscript *fuel* indicates the yield of CHO in the fuel, *HTR* indicates the yield of CHO measured in the gas downstream of the HTR, *unc* refers to the unconverted fuel, and *tr* refers to the transported oxygen.

$$n_{O,tr}=\left(n_{O,HTR}-n_{O,fuel}\right)-\left(n_{C,HTR}-n_{C,fuel}\right)\cdot\left[\frac{O}{C}\right]_{unc}-\left(n_{H,HTR}-n_{H,fuel}-\left(n_{C,HTR}-n_{C,fuel}\right)\cdot\left[\frac{H}{C}\right]_{unc}\right)\cdot\left[\frac{O}{H}\right]_{H_2O} \quad (1)$$

The oxygen transport is calculated as the difference between the oxygen measured in the HTR and the oxygen contained in the fuel, i.e., the first term of the equation. The oxygen contained in the fuel leaving the gasifier in unconverted form must be removed from this difference, which corresponds to the second term of the equation. However, oxygen addition also occurs in both the gasifier and the HTR through reactions of the gases and the fuel particles with steam, *via* the gasification reactions, the steam reforming reactions, and the WGS reaction. As every mole of oxygen reacted from the steam corresponds to two moles of hydrogen added to the gas, it is possible to remove that contribution to the oxygen balance. This corresponds to the third term of the equation. In the latter term, the hydrogen leaving the gasifier as unconverted fuel is also removed from the difference in hydrogen content between the HTR and the fuel.

There are several possible ways to express the oxygen transport to the gasifier. In all the chapters except for *Chapter 6*, the oxygen transport is expressed as the ratio of the moles of oxygen transported to the moles of oxygen required for stoichiometric combustion of the fuel fed to the gasifier. In *Chapter 6*, the goal is to describe the development of the capability of bed materials to transport oxygen. Therefore, the oxygen transport is expressed in terms of moles of oxygen transported per unit mass of bed circulated. To determine the oxygen transport in this way, the circulation rate of the bed material is required. In the Chalmers DFB system, the circulation rate of the bed material is assessed by interrupting the fluidization in the second loop seal (see Figure 6). This prevents bed material from entering the combustor, which translates into a decrease in the pressure drop across the combustor, which is then linked to the rate of solids circulation. This method has been described previously by Larsson *et al.* [122].

3.4. Energy balance

The energy balances of DFB gasifiers are established in some of the chapters of this thesis with different purposes. In *Chapter 4*, the mass and energy balances of the various DFB configurations are established and compared on an equal footing. In *Chapter 8*, the energy balance is determined as part of establishing the mass and energy balances of a process for the direct reduction of iron based on the production of reducing gas from DFB gasification. For both of these chapters, the mass and energy balances of the DFB gasifier are established from the ground up, built upon gas concentrations obtained from experiments carried out in the Chalmers gasifier. This means that the various contributions to the heat demand are calculated. These contributions include, for the gasifier: the various heat of reactions, which are overall endothermic; the drying and heating of the fuel; and the heating of the steam. For the combustor, the heat demands include the heating of the air and various solid (or liquid) streams to the temperature of the combustor. The heat release in the combustor is calculated as the heat of combustion of the char and other combustible species introduced to the combustor, as well as the heat

of oxidation of the bed material. Based on the balance of the heat release and heat demands, the degree of char gasification that can be achieved, or alternatively the oxygen transport level that sustains the autothermal operation for the operation of the CLG configuration, is determined. Establishing the mass and energy balances of a DFB gasifier in this way relies upon numerous assumptions, which are described in **Papers III** and **V**, for *Chapters 4* and *8*, respectively.

In *Chapter 7*, the aim of the energy balance is not to establish the operation of a theoretical DFB gasification system, but rather to determine the heat demand of the Chalmers gasifier, and the heat output of a combustor that would be connected to the Chalmers gasifier. This theoretical combustor would oxidize an amount of unconverted fuel determined from the measurement in the Chalmers gasifier, and would oxidize the bed material to the extent fixed by the level of oxygen transport measured in the gasifier. The goal here is to compare the heat demand of the Chalmers gasifier and the heat output of the theoretical combustor, to investigate whether a gasifier operating under the conditions of the Chalmers gasifier and producing the same output could be operated without additional energy input to the combustor. This energy balance is then used to extrapolate the results from the Chalmers gasifier to establish the energy balance in a case where complete fuel conversion is achieved, and the DFB is operated, therefore, in the CLG configuration.

In contrast to the method applied to the energy balance used in **Papers III** and **V**, the heat demand of the gasifier is not determined as the sum of the sensible heat and heat of reaction terms within the reactor but rather as the difference in energy content between the outgoing and ingoing streams. This approach is similar to that used by Alamia *et al.* to establish the heat balance of the GoBiGas plant [20,125]. The main assumptions on which the heat balance is based are described in **Paper II** and associated *Supporting Information*.

When oxygen carriers or bed materials that develop an oxygen-carrying capacity are used in the DFB system, the heat of oxidation of the bed material is often of the same magnitude as the heat of combustion of the unconverted fuel from the gasifier. It is, therefore, crucial to be able to derive a reasonable range for this heat of oxidation. In the case of a bed material that is formed from a complex mixture of metals, this may prove to be challenging. The bed material in **Paper II** exemplifies this case, as not only is the ASR-ash itself a complex mixture of metals, but also the bed still contains a large fraction of olivine, which may itself have developed an oxygen-carrying capacity during the formation of an ash layer. Indeed, the ash layer of olivine, formed through interactions with biomass ash, is rich in Ca, which could lead to Ca sulfides-sulfates cycles between the two reactors, resulting in the transport of oxygen from the combustor to the gasifier. The rationale used to estimate the value of the heat of oxidation of that complex mixture is explained in **Paper II**.

For the slag bed material considered in *Chapter 8*, it was assumed that the heat of oxidation is that of the Fe_2O_3/Fe_3O_4 couple, i.e., -476 kJ/mol O_2, based on the high iron content of the slag. This is in contradiction with the results of Hildor *et al.*, as mentioned in *Section 2.2.1*, who showed that the couple involved in oxygen transport in LD slag is Fe_3O_4/FeO, whose heat of oxidation is -627 kJ/mol O_2 [115]. However, the magnetite and wüstite phases detected by Hildor *et al.* included dopants such as Mg and Mn. It could be expected, then, that the presence of these dopants affects the heat of oxidation. A heat of oxidation of -627 kJ/mol O_2 is high relative to the usual heat of oxidation for oxygen carriers proposed for CLC (see Table 11 in [91]). The slag also contains large amounts of Ca, which could react with S from the biomass, and lead to $CaSO_4$-CaS cycles, resulting in oxygen transport. The $CaSO_4$/CaS couple has a heat of oxidation of -482 kJ/mol O_2, comparable to that of the Fe_2O_3/Fe_3O_4 couple. For these reasons, the heat of oxidation of the Fe_2O_3/Fe_3O_4 couple was used as

the assumed heat of oxidation of the slag bed material, to represent a conservative value for the oxygen transport level required for autothermal operation of the CLG configuration.

3.5. Materials

3.5.1. Bed materials

Various bed materials have been used in the studies presented in this thesis. With time spent in the DFB system, these materials evolved by interacting with ash components. This evolution entailed structural changes caused by a succession of reductive-oxidative cycles and high temperatures, and changes brought about by thermal and mechanical stresses. Furthermore, in *Chapters 5* and *6*, general trends combining the results from many different experiments across several experimental campaigns are presented. It is, therefore, unreasonable to detail the composition of each and every bed material at every stage of its evolution. Consequently, the compositions of only seven bed materials, six of them in their virgin state, are described in this section.

The compositions of the bed materials are given in Table 1. Silica sand is typically considered to be inert in DFB gasification, and is used in *Chapter 4* as the reference for the gas composition obtained with an inert bed material. Olivine is the bed material that: is activated by the circulation of flue gas ash in *Chapter 5*; is one of the materials shown to develop oxygen transport properties in *Chapter 6*; and acts as the starting bed material used in the conversion of ASR in *Chapter 7*. It is also the reference bed material for the catalytically active cases discussed in *Chapter 4*. Feldspar is investigated as another bed material that develops oxygen transport properties in *Chapter 6*. The results with olivine and feldspar shown in this thesis were obtained from several experimental campaigns using different batches of bed materials. However, the compositions of the different olivine and feldspar batches (in their virgin states) were similar, so only the composition of a single batch is listed in Table 1. The compositions of ilmenite and manganese ore, two natural oxygen carriers used as references for assessing the development of oxygen transport capabilities for olivine and feldspar in *Chapter 6*, are also shown in Table 1. In **Paper II**, as will be discussed in *Chapter 7*, it is shown that the prolonged use of ASR as fuel leads to accumulation of its ash in the bed. The composition of the resulting bed is referred to as “ASR-ash bed” in Table 1. Finally, the composition of an LD slag sample is shown in Table 1. As discussed in *Section 2.2.1*, it is expected that the slag species from the EAF in the direct reduction steelmaking route will have similar compositions and properties.

Table 1. Elemental compositions of the main bed materials investigated in this work. Values are shown in wt%. The remainder is mainly oxygen.

	Silica sand	Olivine	Feldspar	Ilmenite	Manganese	ASR-ash bed	LD slag
Al	0.09	0.14	9.95	0.19	3.40	1.60	0.64
Si	46.36	19.00	31.55	0.19	3.72	18.00	5.56
Fe	0.04	4.90	0.08	24.48	5.15	7.70	18.61
Ti			0.01	30.57	0.23	0.35	0.78
Mn		0.34		0.82	37.73	0.46	2.09
Mg		29.00	0.02	0.60	0.25	18.00	5.49
Ca		4.50	0.86	0.01	1.88	7.10	28.44
Ba						0.30	
Na		0.23	3.19			0.59	
K		1.50	6.97		0.99	1.70	
P		0.30				0.72	
Cl							
Br							
S		0.13				0.18	
Cr		0.03				0.07	
Ni		0.22				0.16	
Zn		0.07				1.40	

3.5.2. Fuels

The situation regarding the fuels used in the studies of this thesis is similar to that for the bed materials. Many different batches of wood pellets were fed to the gasifier and wood chips were fed to the boiler across all the experiments reported in this work. Nonetheless, little variability was observed in the compositions of these fuels, aside from the moisture level, which displayed the greatest variability for the wood chips and did not affect the operation of the gasifier. For this reason, the proximate compositions of the wood chips and wood pellets used in the Chalmers gasifier that are reported in Table 2 are assumed to be representative of all cases in which wood pellets were used in the gasifier. The proximate analyses of the two batches of ASR used in **Paper II** are shown in Table 2. Note that these batches are numbered 2 and 3 because a first ASR batch was used in the first days of the experimental campaign, prior to the measurements of interest.

The fixed carbon and volatiles contents of the fuels used in this work are not reported in Table 2. For the ASR batches, the reason for this is that the fixed carbon produced during devolatilization was measured in a bench-scale fluidized bed reactor, to obtain a value representative of the conditions in the Chalmers gasifier. Concerning the wood fuels, their fixed carbon contents were determined through thermogravimetric analysis (TGA) and showed some slight differences across the experimental campaigns. However, the heating rate in TGA is very low compared to that in a fluidized bed. Therefore, in the fluidized bed environment, the high heating rates will not produce the same amount of char, and there is no telling that the differences emerging from the TGA tests would emerge in similar fashion, if at all, from a fluidized bed. For this reason, the char yield of the wood pellets in the Chalmers gasifier was set to 16% on a dry, ash-free mass basis, based on pyrolysis experiments in batch-scale fluidized bed reactors with dried wood pellets [122,126].

The compositions of the ashes obtained from the combustion of wood chips, wood pellets, and ASR are shown in Table 3. These values are mainly of interest for the biomass used in **Paper I**, in which the accumulation of certain ash species in the bed material was assessed. While the composition of the ash from ASR was not used in **Paper II**, it is nonetheless of interest to relate the bed composition (given in Table 1) to the accumulation of ASR ash. It should also be noted that, as expected based on its origin, the ASR ash is rich in metals such as Fe, Zn, and Cu.

Table 2. Proximate analysis of the fuels used in this thesis.

	Wood Chips	Wood Pellets	ASR Batch 2	ASR Batch 3
Moisture (wt% as-received)	Typically 40	8.1	1.6	1.4
Ash (wt% dry-basis)	0.5	0.4	37	32
Cl (wt% dry-basis)			0.63	0.64
S (wt% dry-basis)			0.24	0.19
C (wt% dry-basis)	50.2	50.5	42.0	47.0
H (wt% dry-basis)	6.0	6.1	5.0	5.4
N (wt% dry-basis)	0.12	0.07	1.5	1.6
O (wt% dry-basis, by difference)	43.0	43.0	13	13
LHV (MJ/kg, dry-basis)	18.4	18.8	18.0	20.1

Table 3. Elemental compositions of the ashes derived from combustion of the biomass and ASR fuels used in this thesis.

	Wood chips	Wood pellets	ASR Batch 2	ASR Batch 3
Element	Concentration (mg/kg, dry-basis)		Mass percent, dry-basis	
Al	20	50	1.6	1.5
Si	80	150	4.8	4.2
Fe	20	30	8.3	6.8
Ti	<10	<10	0.45	0.43
Mn	70	13	0.10	0.08
Mg	230	210	0.51	0.48
Ca	1200	950	2.3	2.1
Ba	20	10	0.34	0.31
Na	40	30	0.59	0.49
K	670	460	0.34	0.33
P	80	70	0.28	0.29
Br			0.30	0.42
			Concentration (mg/kg, dry-basis)	
As			9	14
Cd			10	9
Co			750	37
Cr			1,400	400
Cu			5,800	5,500
Mo			110	37
Ni			730	260
Pb			660	600
V			32	25
Zn			15,500	13,800

Chapter 4: Comparison of the DFB gasification configurations

In this chapter, which is based on **Paper III**, the various DFB gasification configurations presented in *Chapter 1* and the carbon distributions that they produce are compared on a theoretical basis. Their potentials for complete carbon recovery are compared and discussed by investigating their energy demands for the separation of CO_2 from the syngas and flue gas. The influences on the carbon distribution of the gasifier temperature and the bed catalytic activity level are also assessed, so as to determine how these parameters can be adjusted to optimize carbon recovery. The importance of the downstream gas processing units for the carbon distribution of the plant is also highlighted, and a specific downstream setup common to all DFB configurations (see *Section 4.1*) is used in the analysis for the sake of comparability of the configurations. As certain choices had to be made to ensure comparability, the aim of this chapter is not to propose a specific configuration as the optimal with respect to carbon recovery, but rather to highlight the respective strengths and weaknesses of the configurations, so as to inform the choice of DFB gasification configuration for a given application.

4.1. Method

In this chapter, the usual form of DFB gasification, i.e., the DFB gasification configuration that relies on the oxidation of char with air in the combustor to provide heat to the DFB gasification loop, is compared with three other DFB configurations that theoretically enable complete recovery of the carbon. The regular DFB gasification configuration is referred to as the 'Air' configuration in this chapter. The configurations with which it is compared are: the 'Oxyfuel' configuration, which relies on the oxidation of char with pure oxygen, as described in *Section 1.3*; the 'Electrical' configuration, wherein electrical heating is introduced in the DFB loop, as described in *Section 1.4.1*; and the *CLG* configuration, which is dependent upon the use of oxygen carriers to separate inherently the CO_2 from the flue gas and concentrate all the carbon in the FR, as described in *Section 1.4.2*. Note that sorption-enhanced reforming (SER) and its oxy-combustion iteration (OxySER) are not investigated in this work.

The four configurations were compared on the basis of their potentials for carbon recovery and the possibilities to steer the carbon balance. When considering the carbon distribution produced by a DFB gasification plant, it is important to include the potential downstream upgrading and synthesis processes that convert the raw gas into various end-products. The natures of the downstream processing units and the conditions under which they are operated depend on too many factors to allow for an exhaustive comparison. For the sake of comparability, a specific plant layout was selected. This layout (Figure 7) assumes that, after cleaning, the gas from the gasifier is steam-reformed to produce only H_2, CO, and CO_2, and that the H_2/CO ratio of the gas is subsequently adjusted in a WGS reactor. After a CO_2 separation step, the syngas is converted to a range of end-products in a synthesis section, which is represented by a black box in Figure 7. Note that this theoretical case is not entirely removed from reality, as this type of configuration is likely to be chosen when the goal is to produce biofuel or chemicals from biomass.

This chapter considers the carbon distribution between the end-product (or range of end-products), the CO_2 separated from the syngas, and the CO_2 that is potentially separated from the flue gas. These three end-streams are underlined in Figure 7. The results shown in this chapter are for an end-product with a C/H ratio of 0.25, corresponding to methane as the end-product. This choice is made to simplify the

presentation of the results. As described in **Paper III**, all the trends presented are similar regardless of the C/H ratio.

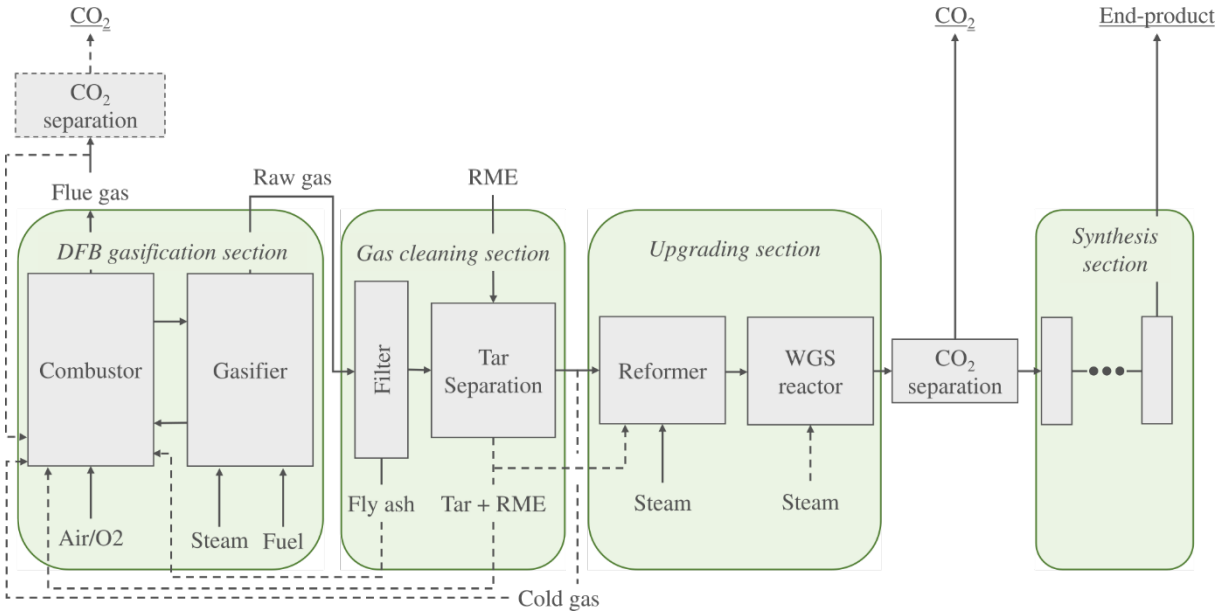

Figure 7. Schematic of the layout of the DFB gasification plant considered in this work. The dashed arrows represent optional pathways. The dashed box for CO_2 separation (upper left-hand corner) signifies that this separation step is optional. The underlined text items indicate the final outputs (end-streams) from the plant. RME refers to rapeseed methyl ester, which is used in the calculation to represent a scrubbing agent for the removal of tar.

To achieve complete carbon recovery, all the CO_2 produced must be separated into a pure stream. Depending on the CO_2 concentration and pressure level, different separation technologies may be preferred. For comparing the DFB configurations, CO_2 separation, whether from the flue gas or syngas, was assumed to be carried out using a state-of-the-art scrubbing process based on methyl ethanolamine (MEA). The heat duty of the reboiler to evaporate the CO_2 from the aqueous amine solution was assumed to be 4 MJ/kg CO_2, which represents a conservative value based on the typical minimum range of 3.6–4.0 MJ/kg CO_2 for 90% CO_2 removal from combustion flue gases [127]. The actual value for the separation of CO_2 from the syngas will likely be lower, since the CO_2 concentration is expected to be higher than in the flue gas. Furthermore, the downstream synthesis process is likely to be operated at higher pressures, and the compression of the cold gas is likely to be performed prior to its reforming to minimize the compression duty. Both these factors decrease the reboiler duty. For reference, the specific reboiler duty for a syngas with 40 %vol CO_2 at 20 bar is estimated to be 1.9 MJ/kg CO_2, based on the model developed by Garðarsdóttir *et al.* [128]. As the pressure and CO_2 concentration in the syngas increase, separation technologies other than amine absorption may be preferred, although this choice will be the same for all the configurations.

The cases that were compared in this work are described in Table 4. For all the DFB configurations, the mass and energy balances of the DFB gasification section were solved based on gas compositions that were obtained experimentally in the Chalmers DFB gasifier. The *Air inert* case was based on experiments performed at 805°C with silica sand as inert bed material. The *Active* cases were based on an experiment conducted at 816°C with a highly active olivine bed. The CLG low-temperature (*CLG Low-T*) case was based on an experiment carried out at 827°C, with ilmenite as the oxygen-carrying bed material. The use of a different gas composition for the CLG configuration is designed to

reflect the different types of catalytic effects (excluding oxygen transport) that ilmenite and olivine can produce. The reference gas compositions are listed in **Paper III**.

In addition to comparing the four DFB configurations, the respective influences of the temperature and of the catalytic activity of the bed materials on the carbon distribution, accounting for the downstream processing units, were investigated. The influence of the catalytic activity was investigated by comparing the *Air Inert* and *Air Active* cases. To investigate the influence of temperatures higher than those that can be achieved in the Chalmers gasifier, extreme cases at 950°C were considered, in which the gas was assumed to be entirely reformed. For the Air and Oxyfuel configurations, these cases are referred to as *Full reforming* cases. For the CLG configuration, the case is referred to as the *CLG High-T* case, which represents the operating conditions under which complete fuel conversion is more likely than it is in the *CLG Low-T* case. Thus, a realistic CLG case will lie between the *CLG Low-T* case based on the Chalmers gasifier experiments and the theoretical *CLG High-T* case. The procedure and assumptions used to establish the mass and heat balances of the cases described in Table 4 are described in greater detail in **Paper III**. A noteworthy assumption that is made for the CLG and Electrical configurations concerns the complete conversion of the fuel in the gasifier, although 10% of the carbon in the char is assumed to be elutriated and escape the reactor unconverted. This carbon is assumed to be oxidized to CO_2 in the combustor.

Table 4. Descriptions of the cases investigated in this work. In the second column, the tag by which each case is referred to in the text and figures is indicated.

Configuration	Case tag	Description
Air	Air Inert	Air as oxidant in the combustor. Inert bed material (silica sand).
	Air Active	Air as oxidant in the combustor. Active bed material (aged olivine).
	Air Full Reforming	Air as oxidant in the combustor. Gas assumed to be fully reformed to syngas.
Oxyfuel	Oxy Active	Pure oxygen as oxidant in the combustor. Active bed material (aged olivine).
	Oxy Full Reforming	Pure oxygen as oxidant in the combustor. Gas assumed to be fully reformed to syngas.
CLG	CLG Low-T	Chemical-looping gasification with ilmenite at 827°C. The gas composition is that derived from experiments conducted in the Chalmers gasifier.
	CLG High-T	Chemical-looping gasification with ilmenite at 950°C. Gas assumed to be fully reformed to syngas.
Electrical	El Active	Electrically heated DFB gasifier. Active bed material (aged olivine).

4.2. Results

4.2.1. Carbon distribution

The carbon distributions obtained for the various DFB configurations are shown in Figure 8. The breakdown of the total heat demands for the cases presented in Figure 8 is shown in Figure 9. The heat demand is divided into the heat demand for reactions in the gasifier, corresponding to the demand for

the gasification reaction itself and for the reactions of the volatiles, and into the sensible and latent heat demands of the gasifier and combustor. The carbon intensity, representing the CO_2 produced in both the flue gas and raw gas from the heat production method, is also shown in Figure 9. For the Air and Oxyfuel configurations, this corresponds to the CO_2 formed in the flue gas during the combustion of char or circulated cold gas, whereas for the CLG configuration, it corresponds to the oxidation of carbon-containing species to CO_2 by the transported oxygen.

Figure 8 shows that there is little difference in the recovery of carbon as end-product between the configurations, with the exception of the Electrical and CLG *High-T* configurations. The Electrical configuration gives the highest recovery of carbon as end-product, as it does not suffer from the loss associated with the need to oxidize part of this carbon to cover the heat demand. The Electrical configuration approaches the theoretical maximum carbon recovery as end-product that can be achieved *via* gasification. The only deviation from the theoretical case is that due to the oxidation of elutriated char, as mentioned in the previous section. The CLG *High-T* configuration has the lowest carbon recovery as end-product, owing to the higher temperature, which increases the heat demand, as seen in Figure 9. The requirement for complete fuel conversion also means that the CLG *Low-T* configuration has the second-highest heat demand, and that the Electrical configuration has a heat demand comparable to that of the Air configuration, despite having a lower flue gas flow. A key result shown in Figure 9 is that the carbon intensity of CLG is comparable with or higher than the carbon intensity of the Air configuration. This means that the CLG configuration does not lead to a decrease in CO_2 production but instead displaces its production to the fuel reactor. This is a consequence of the assumption that the transported oxygen reacts only with H_2 and CO, which is reasonable considering that these are the most-abundant reactive species in the gasifier, as well as the species that are most likely to be in contact with the oxygen carrier, as discussed in *Section 1.4.2*. The Oxyfuel configuration leads to the lowest heat demand and the second highest generation of end-product.

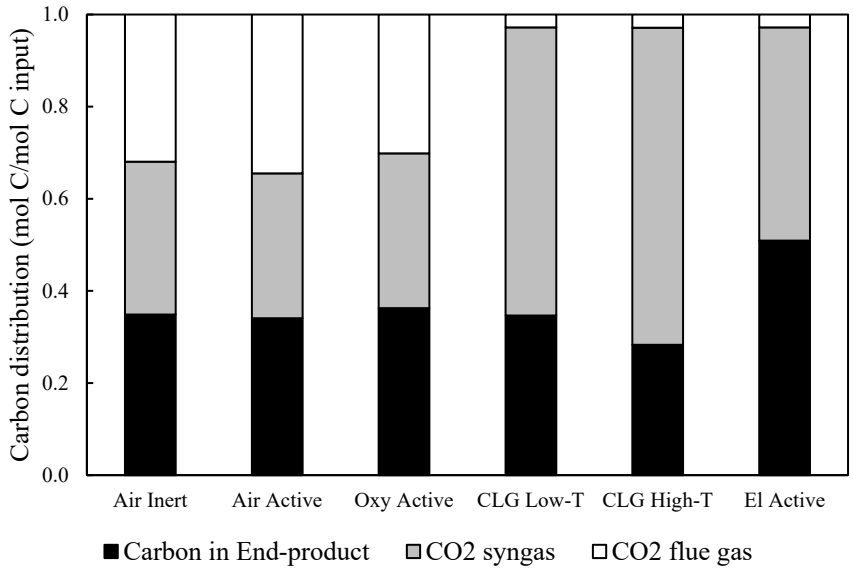

Figure 8. Carbon distributions for the various DFB configurations.

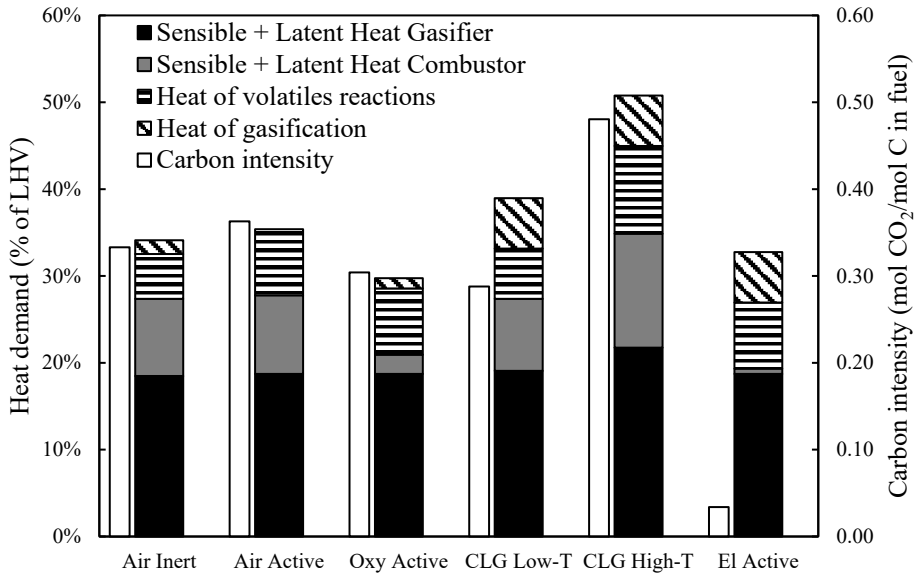

Figure 9. Contributions to the total heat demands in the various cases, and the carbon intensities of the heat production methods (i.e., the amounts of CO_2 produced in both the flue and raw gases due to the production of heat). The carbon intensities are represented by white bars placed next to the stacked bars and their corresponding values are indicated on the right-hand vertical axis.

4.2.2. CO_2 separation

Even though, as shown in Figure 8, the absolute amount of carbon in the form of CO_2 is comparable for the various cases (with the exception of the El Active case), the energy demand and investment cost for separation reflect how this CO_2 is distributed between the flue gas and syngas. Furthermore, it is essential to account for the potential for heat recovery to cover the heat demand, since, in the case of MEA scrubbing, the energy required is heat at a low (typically 120°C) temperature. These aspects are considered in Figure 10. The electrical energy demands for O_2 production for the Oxyfuel configuration and for direct heating for the Electrical configuration are also shown, as these correspond to the energy demands related to avoiding the need for CO_2 separation. In Figure 10, the reboiler duty associated with the CO_2 in the syngas is represented as a range, with a specific duty of 4 MJ/kg CO_2 as the maximum, and a reference value of 1.9 MJ/kg CO_2, corresponding to a syngas with 40% CO_2 and at elevated pressure (20 bar), as described in *Section 4.1*. For a similar pressure level, a higher CO_2 concentration will entail a lower reboiler duty. For this reason, the concentration of the CO_2 in the syngas is shown in Figure 11, along with the concentration of CO_2 in the flue gas for comparison.

Figure 10 shows that the total energy demand for separation of CO_2 for the CLG configuration cases is comparable to but lower than that of the Air configuration. The reboiler duty is expected to be closer to the reference value given, as the CO_2 concentration in the syngas approaches 40%, whereas it is around 20% for the Air configuration. The CLG configuration is also the configuration that has the greatest potential for heat integration, which means that it is likely that the reboiler duty can be covered by heat integration. Conversely, for the Air configuration, there may not be enough heat to cover the heat demand of the reboiler. While a complete analysis of the available heats and their temperature levels is required to answer these questions, Figure 10 gives a first-order estimation of the potential for heat integration. Besides the lower energy demand for CO_2 separation, the associated investment cost will be lower for CLG, as only one CO_2 scrubbing unit is needed, whereas two units are required for the Air configuration if the ambition is to recover all the carbon.

The Oxyfuel configuration represents the most-advantageous case for CO_2 separation, as it has the lowest reboiler duty for separation from the syngas and produces a near-pure CO_2 flue gas stream that is ready for conditioning, while the electrical energy demand for O_2 separation is low. In contrast, the Electrical configuration has a high electrical energy demand. It must be noted that in the case of the Electrical configuration, while the CO_2 concentration in the flue gas is comparable to that of the Air configuration, the absolute amount of carbon in that stream is low. This means that investment in a CO_2 separation unit for the flue gas is likely not economically justifiable. Similarly, in the CLG configuration, the CO_2 in the flue gas is present in low absolute amount and at low concentration, so it will not be recovered.

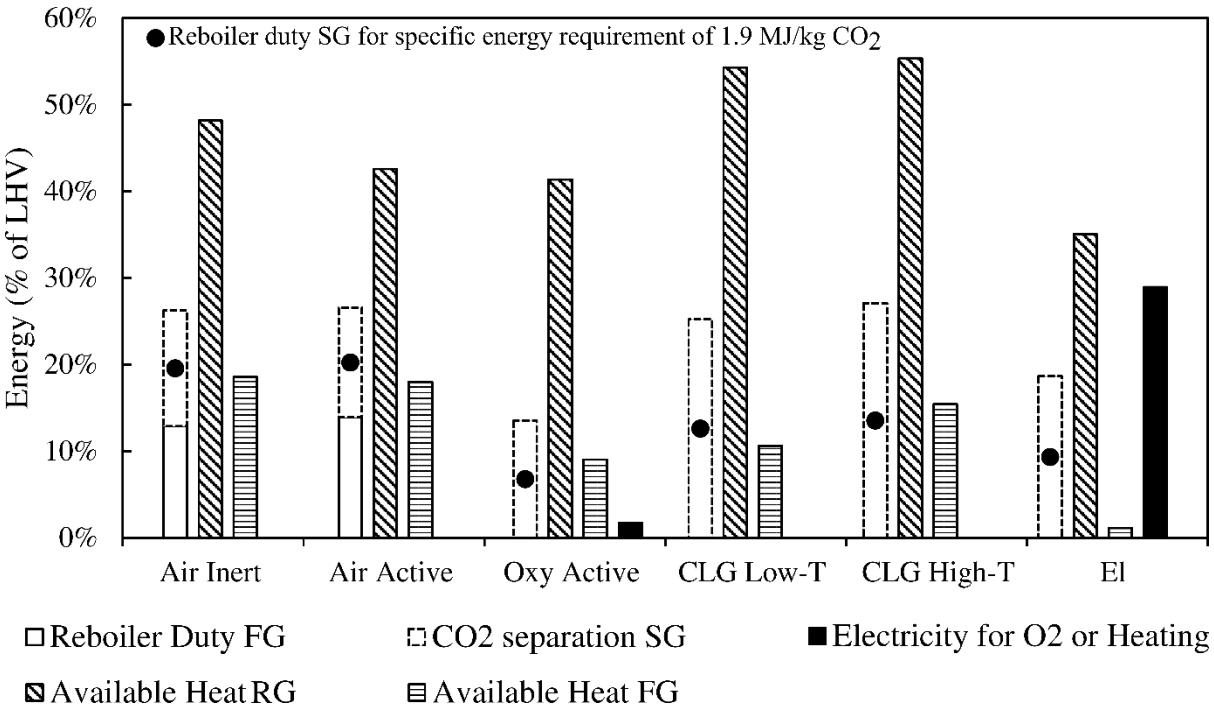

Figure 10. Energy demand for CO_2 separation, as compared with the available heat levels (latent and sensible) from the raw gas (RG) and flue gas (FG), for the various DFB configurations. SG refers to the syngas. The electricity demands for the production of pure O_2 (Oxyfuel configuration) and for direct heating (Electrical configuration) are also shown. The reboiler duties for the separation of the CO_2 from the flue gas are shown in continuous-line boxes, whereas the energy demands for the separation of the CO_2 from the syngas are shown in dashed-line boxes. The black dot represents the energy demand for CO_2 separation from the syngas when MEA absorption is used, for a syngas with 40% CO_2, at 20 bar, corresponding to a specific energy requirement of 1.9 MJ/kg CO_2.

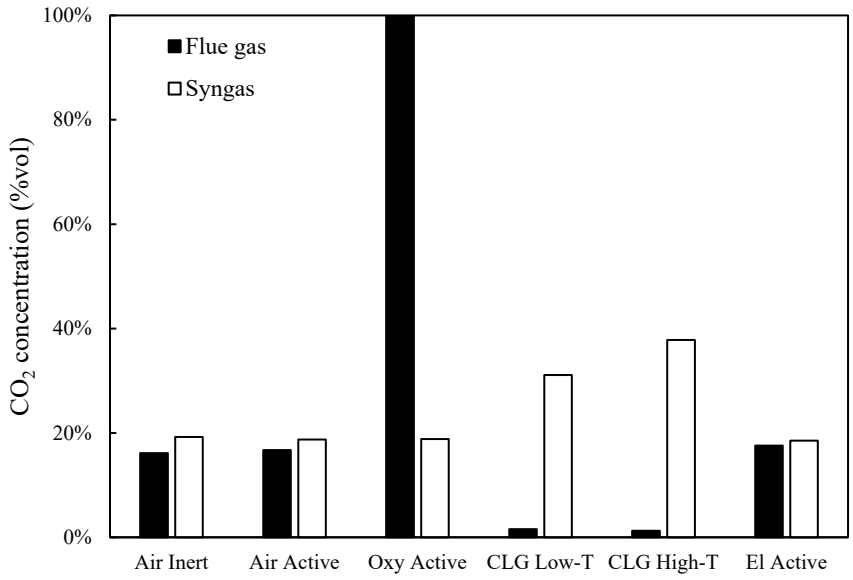

Figure 11. Concentrations of CO_2 in the (dry) flue gas and syngas for the different cases.

4.2.3. Influences of temperature and catalytic activity on the carbon distribution

Although temperature and bed catalytic activity can strongly affect the composition of the raw gas from the gasifier, the results in Figure 8 show that, when considering the carbon distribution of the plant as a whole, these two parameters have limited impacts. This explains the comparable heat demand for CO_2 separation and the comparable potential for heat recovery, as shown in Figure 10 for the *Inert* and *Active* Air cases, and for the CLG *Low-T* and CLG *High-T* cases. The influence of temperature was further investigated for the Air and Oxyfuel configurations by comparing their *Active* cases with their *Full Reforming* cases (as described in *Section 4.1*) in terms of carbon distribution, total reboiler heat duty (including syngas and flue gas separation), and the electrical demand for the Oxyfuel configurations, as shown in Figure 12. The results show clearly that there are no significant differences between the *Active* and *Full Reforming* cases, for both the Air and Oxyfuel configurations, despite a temperature difference of 140°C. The level of carbon in the end-product is slightly decreased in both configurations. The total reboiler duty and electrical demand are unchanged. Given the lack of influence of the temperature, it seems likely that extreme changes in catalytic activity would also not cause any significant changes in the parameters shown in Figure 12. Indeed, as catalytic activity increases, the gas composition will evolve towards that of the *Full Reforming* case, i.e., a gas containing only H_2, CO, and CO_2.

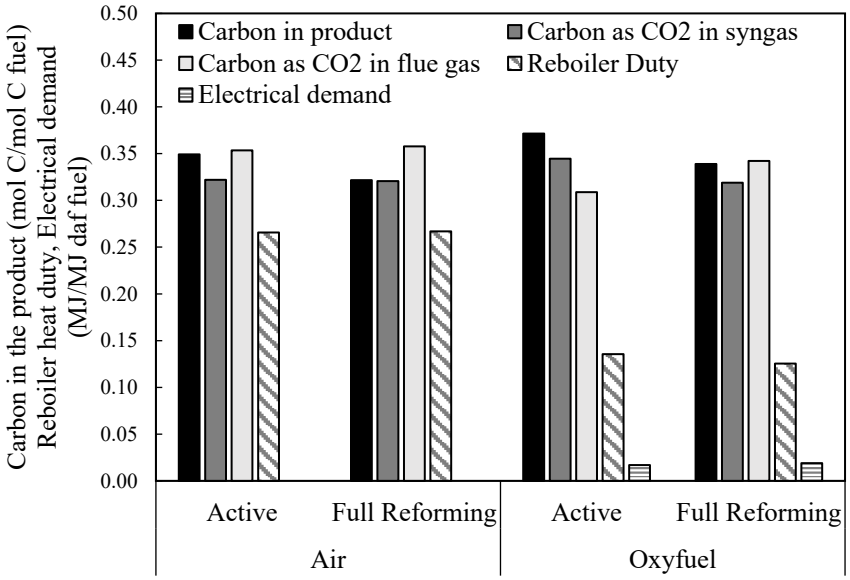

Figure 12. Effects of an increase in operational temperature on the carbon distribution, total reboiler heat duty, and electrical demand for the Air and Oxyfuel configurations. Active refers to the *Air/Oxyfuel Active* case at 810°C. Full Reforming refers to a case in which the gas is fully reformed at 950°C, as described in *Section 4.1*.

The reason for the lack of influences of temperature and catalytic activity is that as these parameters increase, the reforming and cracking reactions of hydrocarbons and the WGS reaction are intensified. As the gas is thereafter fully reformed downstream and shifted to the desired H_2/CO ratio, the roles of temperature and catalytic activity are thus mainly to displace those reactions from the downstream reactors to the gasifier. Based on these results, there is no obvious reasons to increase these parameters. In particular, increasing the temperature of the gasifier causes an increase in heat demand, which in turn necessitates the combustion of more char or part of the cold gas produced. As shown in **Paper III**, but not detailed in this thesis, the combustion of cold gas rather than char is not desirable from the carbon distribution perspective. One reason for increasing the temperature would be to increase char gasification. Thus, unless there is a possibility to cover that heat demand in another way, for instance *via* increased heat integration, there is no point in increasing the temperature. Increasing the catalytic activity level may, however, be desirable to allow operation at a lower temperature, notably in the case where the yield of tar must be limited for operability purposes.

Nevertheless, an important caveat in relation to the present discussion is that the downstream complete reforming of hydrocarbon is here used as a theoretical tool to compare the configurations. While in some cases it will be the actual process used, in other cases the downstream processes will differ, such that the temperature and catalytic activity of the gasifier will play roles beyond those of simply displacing reactions, and will have marked impacts on the overall carbon distribution. Still, when the purpose of the gasification is to produce a syngas precursor for biofuels or the production of chemicals, then the temperature and catalytic activity levels should be seen as tools to minimize the formation of troublesome components (tar) and to facilitate their removal. When the species in the gasification gas are the direct products, which is, for instance, the case when recovering olefins from plastic waste, then the temperature and catalytic activity are key parameters in the recovery of end-products.

4.3. Conclusions of the chapter

This chapter reveals that the downstream upgrading and synthesis steps can mitigate the differences in carbon distribution that exist at the DFB system level, produced from different configurations and

under different operating conditions. Consideration of these downstream steps in the analysis of the carbon distribution and recovery is, therefore, essential. For the extreme case in which the gas is entirely reformed and only H_2 and CO are used in the synthesis section, the DFB configurations show similar levels of carbon recovery as end-products, with the notable exception of the Electrical configuration. When operated at high temperature, the CLG configuration shows a slightly lower recovery of end-product. On the other hand, the CLG configuration will require a lower investment cost for CO_2 separation compared to the Air configuration, and it has greater potential to cover the heat demand of the amine reboiler *via* heat integration than does the Air configuration. Nonetheless, to achieve significant carbon recovery, the CLG and Electrical configurations need to be able to convert fully the fuel in the gasifier. The possibilities and challenges associated with achieving complete fuel conversion in CLG are discussed further in *Chapter 7*.

The results presented in this chapter emphasize that reaching as high a bed catalytic activity as possible should not always be the goal. Careful consideration of its influence, or lack thereof, on the overall carbon distribution is essential in setting the ambition level for the catalytic activity. Nevertheless, a relatively high catalytic activity is desirable in relation to abating troublesome tar species. Besides, rapidly reaching the desired gas composition during plant startup is essential to minimize carbon loss. *Chapter 5* discusses a method for increasing the catalytic activity level and activation rate, using a waste generated form the DFB gasification system itself. The issue of the influence of catalytic activity on carbon distribution is discussed further, based on experimental results obtained from the Chalmers gasifier.

Chapter 5: Enhancing the conversion of non-valuable forms of carbon: circulation of flue gas coarse ash

This chapter is based on **Paper I**, which investigates the recirculation of flue gas coarse ash as a way to reduce the amount of tar in the raw gas by increasing the catalytic activity of the bed. The flue gas coarse ash, hereinafter referred to as *FGCA*, contains potentially-active species such as AAEM, in the form of fragments of the ash layer of the bed material, as well as ash components introduced with the gasifier fly ash. The re-introduction of those species into the internal DFB loop could, therefore, be expected to have an impact on the catalytic activity of the bed. In **Paper I**, the short- and long-term effects of FGCA recirculation on the tar yield and gas composition are investigated, and the roles of the accumulation and mobility of AAEM ash species in the development of catalytic activity are explored. In this chapter, only a brief account of the effect of the FGCA on the tar yield is given. Compared with **Paper I**, the focus here is on investigating whether the positive effects of FGCA circulation on the tar yield, and, thereby, on the operability of the process, translate into increased recovery of valuable carbon products. This chapter also extends the analysis beyond the results of **Paper I**, by looking at the general impact of the catalytic activity level on the carbon distribution for a wide range of experiments conducted in the Chalmers gasifier, thereby expanding upon the theoretical discussion in *Chapter 4*.

5.1. Method

In order to be able to study the effect of flue gas ash circulation on the activities in the Chalmers DFB gasifier, the production of fly ash had to be stimulated. This was achieved by injecting untreated olivine in a fine fraction into loop seal 1 (#4 in Figure 6). Following this injection, the FGCA was collected from the secondary cyclone (#8 in Figure 6). The FGCA was then circulated back to the DFB system, and the new FGCA formed during this circulation was collected. This process was repeated a second time, one day later.

The impact of the circulation of FGCA on the tar level was monitored by comparing the tar yield before and after the injections of olivine fines and FGCA. The long-term effects of the circulation of FGCA on the bed catalytic activity, i.e., effects that remained several days after the circulation of FGCA was performed, were also investigated. To distinguish the potential activation effect of the coarse ash on the bed from the natural activation process (which is known to take place with time through interaction with the fuel ash), the results were compared with tar measurements from an olivine ageing experiment that was previously carried out in the same system, under similar conditions, and with the same type of olivine [61]. In that experiment, replacement of the olivine bed with 800 kg of untreated olivine was performed, corresponding to replacement of about 24% of the inventory. A similar bed replacement step was carried out in the work presented in **Paper I**, although the amount of untreated olivine replaced was double that in the aforementioned reference experiment. Therefore, comparison of the activities of the beds in the two experiments, *via* the tar yields, was used to elucidate whether coarse ash circulation has an impact on the resilience of the bed activity to deactivation through regeneration.

Five measurement cases are referred to in the results section of this chapter. Case I represents a reference measurement establishing the tar yield and carbon distribution before the addition of olivine fines. Case II corresponds to the state after the introduction of the olivine fines into the system, about

400 kg of which were estimated to remain in the bed. Subsequent to Case II, the FGCA generated from the olivine fines injection was circulated. Following this circulation, Case III was established. On the following day (approximately 18 hours later), Case IV was established, after which the FGCA was circulated a second time. More than two days later, during which the aforementioned partial bed replacement was performed, Case V was measured.

The impacts of FGCA circulation on the carbon distribution were also evaluated by comparing the five measurement cases. A generalization of the relationship between catalytic activity of the bed and carbon distribution was also established by representing the carbon distributions obtained through a multitude of experiments against two measures of catalytic activity: the tar yield and the ratio of the quotient of reaction of the WGS to its equilibrium value (K_{WGS}/K_{eq}). The latter parameter increases towards a value of 1 with increasing catalytic activity. These results extend beyond the scope of **Paper I**.

5.2. Results

5.2.1. Impacts of flue gas coarse ash circulation on the tar yield

Figure 13 compares the tar yields obtained when the circulation of FGCA was employed as the activation method with the tar yields obtained from "natural" ageing of the bed material. The ash circulation and the reference experimental campaigns were compared on the basis of fuel ash fed to the system, excluding the coarse ash input. At comparable fuel ash inputs, the tar yield of Case I was similar to that of the reference experiment. The introduction of inactive (compared with the bed material) olivine fines and, more importantly, the retention of a large fraction of these fines in the bed led to a decrease in catalytic activity compared with the reference experiment (see Case II). However, after circulation of the FGCA, the catalytic activity was increased, with the tar yield dropping below that of Case I and that of the reference ageing experiment. These results show that circulation of the coarse ash not only has an immediate effect during its circulation (as shown in **Paper I**, but not reported in this thesis), but also exerts a lasting impact after the circulation is interrupted.

This lasting impact is revealed to persist in the long term by comparing the change in activity towards tar conversion from Case III to Case IV with the change in activity expected as a result of "regular" ageing of the bed. The activity of the reference experiment leveled off at an ash input of approximately 500 kg, at an activity level comparable to that seen in Case III. Conversely, the activity towards tar conversion in the ash-circulation experiments continued to increase, at a rate comparable to the early activity increase, despite there being no additional circulation of coarse ash between Cases III and IV. This shows that the previous coarse ash circulation permanently and profoundly increased the catalytic activity level of the bed material. From Case IV to Case V, following a second round of coarse ash circulation, and more importantly, despite extensive replacement of the bed, the catalytic activity increased further. This is in contrast to the reference case, in which a bed replacement of lower magnitude led to a loss of catalytic activity for the overall bed. In summary, coarse ash circulation affects bed activity by increasing the: 1) activation rate; 2) activation level; and 3) resilience to deactivation.

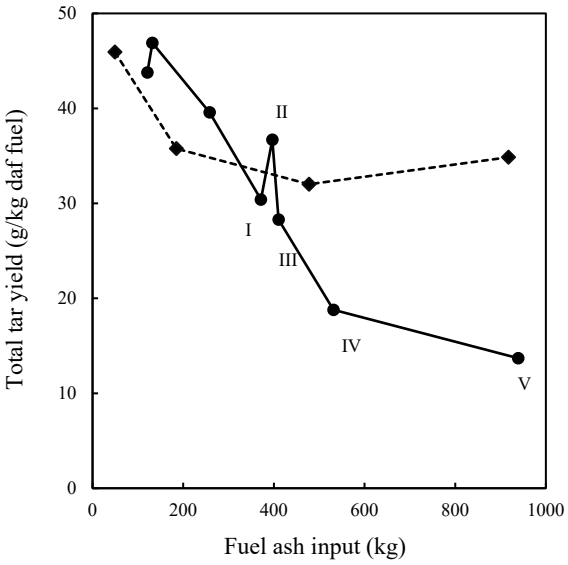

Figure 13. Evolution of the total tar yield (including BTX) with the cumulative fuel ash input (not accounting for coarse ash circulation). The reference aging experiment is indicated by a dashed line. The Roman numerals indicate the five experimental cases.

5.2.2. Contribution of the accumulation and transport of alkali and alkali-earth metals to the development of the catalytic activity

This effect on the activity of the bed material was linked to the accumulation of ash components in the bed, notably active species, such as Ca, K and Na. It was found that the Ca content of the bed increased significantly with time (measured as fuel ash input in Figure 13), following the trend for activity. The amount of leachable K from the bed was found to follow the activity, and it increased substantially after the first round of coarse ash circulation. These results indicate that both Ca and K contribute to the increased activity, most likely due to the former being present in the ash layer and the latter having mobility and being present in the gas phase. This is consistent with results from the literature related to the roles of AAEM in gasification, as discussed in *Section 1.2.2*. Notably, this supports the hypothesis that the ash layer is involved in the catalytic activity *via* gas-phase mechanisms, as suggested by Berdugo Vilches *et al.* [69,72]. Furthermore, the synergetic effects of Ca and K in the ash layer, as proposed by Knutsson *et al.* [73], are consistent with the results shown here.

5.2.3. Impact of enhanced catalytic activity on the carbon distribution of the DFB system

Although a clear improvement in tar abatement may be beneficial in terms of the operability of the process, it is important to consider how the carbon distribution is affected by this change, as discussed in *Chapter 4*. Figure 14 shows the carbon distributions for the five cases investigated. The carbon in the form of CO_2 in the raw gas is divided into that produced from the WGS reaction and that generated from the reaction with transported oxygen. As it is not possible to know in which form the carbon was prior to reaction with the lattice oxygen, the maximal amount of CO_2 from the reaction is shown, i.e., the CO_2 formed from the reaction of CO with the lattice oxygen. It is assumed that half of the transported oxygen reacts in this way with CO, while the other half reacts with H_2. It is reasonable to assume maximal CO_2 formation by oxygen transport, as CO is the carbon-containing gas species that is most likely to react with the lattice oxygen, as discussed in *Section 1.4.2*.

Figure 14 shows that the tar conversion did not lead to increased amounts of carbon in the forms of CO and light hydrocarbons, i.e., in the forms of carbon species that are generally regarded as valuable. Instead, the carbon was transferred to the CO_2 in the raw gas. This transfer of carbon occurred *via* both the WGS reaction and oxygen transport, although the carbon produced from the former follows the activity trend more reliably. Regarding oxygen transport, the circulation rates of the bed material were similar in Cases I, IV and V. This indicates that the increased oxygen transport is imputable to the accumulated ash components' interactions with the bed material. This means that as the ash components interact with and accumulate on the bed particles they induce not only an increase in activity towards tar reforming, but also towards the WGS reaction, as well as an increase in oxygen transport, as verified in *Chapter 6*. This results in a net transfer of carbon to the CO_2 in the raw gas. Note that Figure 14 shows a decrease in the char circulated to the combustor along with the catalytic activity. For an actual DFB gasifier, the higher catalytic activity would drive up the heat demand, thereby requiring an increase in the amount of carbon sent to the combustor (either as char or circulated cold gas). Thus, the increase in activity would result in an even higher level of CO_2 production than that depicted in Figure 14.

As mentioned in *Section 5.1*, the impacts of catalytic activity on the carbon distribution in a DFB gasification system were generalized by investigating a wide range of experiments carried out in the Chalmers gasifier. Here, the carbon distribution produced from the gasifier, i.e., the distribution of carbon into the C in products (CO and hydrocarbons), C in the form of CO_2 in the raw gas, and C sent to the combustor (forming CO_2 in the flue gas), is shown. This was investigated for wood pellet gasification with olivine and feldspar, two materials that are known to develop significant catalytic activity in a DFB gasifier. The carbon distribution is shown in relation to two measures of catalytic activity: the tar yield and the ratio of the quotient of reaction of the WGS to its equilibrium value (K_{WGS}/K_{eq}), as shown, in Figure 15a and Figure 15b, respectively.

The data-points in Figure 15 encompass a wide range of operational conditions that may have a marked effect on the carbon distribution. Nonetheless, the trends evident in Figure 15 are unequivocal: with increasing activity towards tar conversion, a clear transfer of carbon occurs from the products to CO_2. A slight decrease in the amount of carbon circulating to the combustor in the presence of increasing activity is also seen.

These results are consistent with the findings reported in the literature regarding the effect of activation (*via* layer formation) on catalytic activity and the consequent effects on the products of a DFB gasifier, as discussed in *Section 1.2.2*. As the reforming reactions of tar and precursors thereof are intensified, carbon is transferred to CO and light hydrocarbons. Reforming of light hydrocarbons then promotes the transfer of carbon from the light hydrocarbons to CO, and the WGS reaction causes a transfer of carbon from CO to CO_2. The increased activity may also cause a decrease in carbon transfer to the combustor due to increased gasification rates. However, this is limited by the heat balance of the system. Note that, as stated in the *Introduction* and as evidenced in Figure 14, oxygen transport can develop along with the catalytic activity in bed materials operated in the Chalmers gasifier. This phenomenon, which is verified in *Chapter 6*, partly explains some of the transfer of carbon to CO_2 seen in Figure 15.

The results depicted in Figure 14 and Figure 15 expand on those described in Chapter 4, as the impact of the catalytic activity on the carbon distribution of the DFB gasifier, i.e., without including the impact of downstream gas processing, is shown to not necessarily be positive. The implications of these results are significant for the design and operation of the DFB process. First, achieving the highest possible

catalytic activity cannot be the ultimate goal in the optimization of all DFB processes, in the absence of a clear plan, as well as the capacity to recover the CO_2 from the raw gas and valorize its carbon, either chemically or by sequestration. Figure 14 and Figure 15 show that, at high activity levels, there is as much or more carbon in CO_2 as in the products. Thus, the CO_2 stream cannot be considered as simply a side-product. Second, it may be worthwhile to aim for lower activity levels and to apply more robust and sophisticated methods for downstream tar removal. The ambition regarding catalytic activity will also be dependent upon optimization of the downstream processing units. For instance, in the theoretical plant setup discussed in *Chapter 4*, the fact that a high catalytic activity of the bed displaces reactions from the downstream steam reformer and WGS reactor to the gasifier is not necessarily an issue, and may even be a strength, if the optimization of these downstream units is challenging. If the aim of the plant is to generate H_2, then maximizing the catalytic activity of the bed is desirable, since maximizing the production of H_2 entails recovering all the carbon as CO_2.

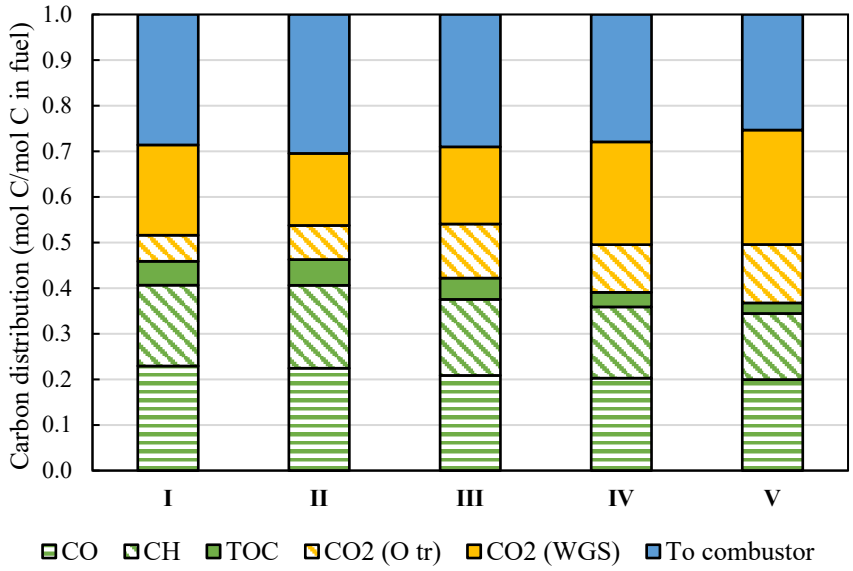

Figure 14. Carbon distributions for the five cases. The blue bars represent the carbon that moves to the combustor as unconverted fuel from the gasifier and ends up as CO_2 in the flue gas. The yellow bars represent carbon in the form of CO_2 in the raw gas, and the green bars represent the carbon in the products. For the carbon in the form of CO_2, a distinction is made between the estimated CO_2 formed from the WGS reaction (filled bar) and that formed from oxygen transport (diagonal hatching). The carbon in the products is divided into: carbon as TOC (filled bar); carbon as light hydrocarbons (diagonal hatching); and carbon as CO (horizontal hatching).

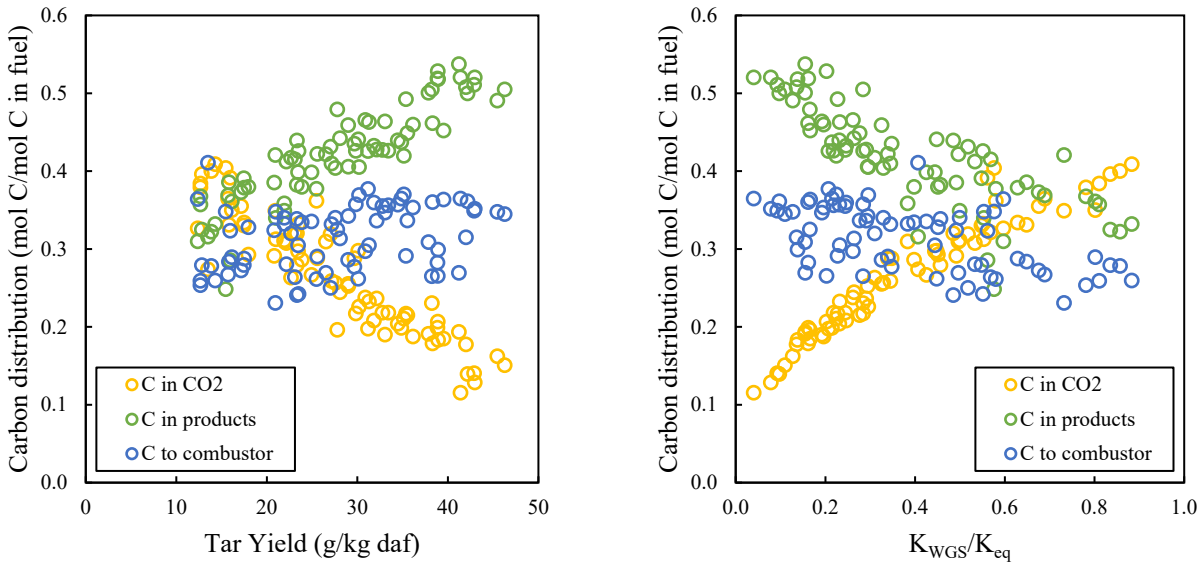

Figure 15. Carbon distribution into CO_2 in the raw gas (yellow), products (green), and CO_2 released in the combustor (blue), plotted against the tar yield (panel a) and the K_{WGS}/K_{eq} ratio of the permanent gas (panel b) for various measurement points obtained from the Chalmers gasifier, with olivine and feldspar used as bed materials.

5.3. Conclusions of the Chapter

This chapter introduces a method for increasing the catalytic activity level and the activation rate of the bed material in DFB gasification, using a waste generated by the process itself. The tar yield is found to be decreased during the circulation of the coarse ash, and this positive effect persists over several days. Moreover, the activity level reached is found to be higher (from the tar yield perspective) than the level reached during aging of the same bed material without ash circulation. The resilience of the bed to de-activation is found to be enhanced. These improvements are made possible by the accumulation of ash components and the increase in mobile ash species that is enabled by the circulation of coarse ash. This highlights the importance of the role of carrier of chemical (ash) species of the bed material for the operation of the DFB gasification system. In light of these results, the circulation of coarse ash is deemed to be an efficient strategy to activate rapidly the bed, which will be especially beneficial during plant startup.

However, the results shown in *Section 5.2.3,* combined with those in *Chapter 4*, indicate that careful assignment of the ambition for the activity level is necessary. *Chapter 4* shows, based on theoretical considerations, that high catalytic activity is not necessarily beneficial for the carbon distribution at the plant level. Similarly, the results of *Section 5.2.3* show, based on experiments performed in the Chalmers gasifier, that this can also be true at the DFB level. Furthermore, additional properties of the bed can emerge together with the catalytic activity through interactions with ash species. For instance, in **Paper I**, oxygen transport is shown to develop, which is consistent with results obtained from previous experiments in the Chalmers gasifier, as reported in the *Introduction*. If a significant oxygen transport capability does develop, then the operation of the DFB process, and indeed of the whole plant, will be shifted and the carbon distribution will be drastically affected. For these reasons, it is crucial to verify and gain further understanding of this phenomenon, which is the topic of *Chapter 6*.

Chapter 6: Development of oxygen transport properties in olivine and feldspar

As mentioned in the *Introduction* and shown in the *Results* section of *Chapter 5*, some bed materials in the Chalmers gasifier develop oxygen transport properties along with catalytic activity as they form ash layers. This phenomenon has been seen for olivine and feldspar, two materials with a limited and no initial oxygen transport capability, respectively. Olivine has been shown, under laboratory conditions and without the extended contact time between bed material and fuel ash components that can be achieved at large scale, to have both catalytic [41–48] and oxygen-carrying [45,48,129] properties. These properties of olivine have been linked to its iron content, and have been shown to be enhanced by an activation process that occurs during repeated oxidation-reduction cycles at high temperature, which leads to the migration of iron to the surface and the formation of iron oxides. However, under industrial conditions and as the bed interacts with the fuel ash, oxygen transport may develop according to a different mechanism than that identified under laboratory conditions. For these reasons, the development of oxygen transport properties by bed materials that form ash layers was investigated in **Paper IV**. In that paper, the linkage between the development of oxygen transport and the development of catalytic activity was established, and the contribution of volatile ash species was explored, in particular the contribution of sulfur-containing species. This chapter focuses on demonstrating that oxygen transport develops alongside catalytic activity in the cases of olivine and feldspar, and discusses the implications for the carbon distribution and carbon recovery.

6.1. Method

The goal of this chapter is to demonstrate that oxygen transport capacity and catalytic activity develop concomitantly in olivine and feldspar used as bed materials in DFB gasifiers. However, it should be borne in mind that "catalytic activity" is not a monolithic term that can be simply measured with a single parameter. Instead, the catalytic activity associated with the formation of ash layers is manifested as the intensification of a number of reactions, including the cracking and reforming reactions of tar and precursors thereof [67–69,130], reforming of light hydrocarbons [67], and the WGS reaction [17,35,67,131], as described in *Section 1.2.2*. Nonetheless, as the activities of all these reactions tend to increase in line with the increases in bed catalytic activity, the latter can be represented with a limited number of variables. Here, as for the previous chapter, the bed catalytic activity is represented by two variables: the tar yield (in g/kg daf fuel); and the K_{WGS}/K_{eq} ratio. To be able to attribute the changes in K_{WGS}/K_{eq} ratio and tar yield to changes in catalytic activity and not to variations in oxygen transport, experiments with two oxygen carriers, ilmenite and manganese, were carried out. These oxygen carriers were used to represent the behaviors of the two measures of bed catalytic activity when oxygen transport is dominant over catalytic activity.

The experimental conditions for the experiments conducted with olivine and feldspar, as well as those with ilmenite and manganese as model oxygen carriers, are described in Table 5. In order to constrain the observed effects to the development of bed catalytic activity and oxygen transport by the particles themselves rather than to varying operational conditions, the experimental points were restricted to narrow ranges of temperature, fuel feeding rate, and steam-fuel ratio. At a constant fuel feeding rate, a constant steam-fuel ratio entails a constant mixing behavior of the bed. Although there are no fundamental differences between the operational ranges of the two sets of olivine and feldspar, these sets are treated separately because, as shown in Figure 16, they generate slightly different results. The reasons for these differences have not been explored.

Table 5. Variations in the bed temperature, fuel feeding rate, and steam-fuel ratio for the six experimental sets. The number of experimental points refers to the number of measurement points in each set, with a "point" corresponding to the averaged gas and tar yields over a period of more than 20 minutes.

Set	Number of experimental points	Bed temperature, range (°C)	Fuel feeding rate, range (kg daf/h)	Steam-fuel ratio, range (kg/kg daf)
Olivine Set 1	9	808–819	264–273	0.83–0.94
Olivine Set 2	6	808–829	265–271	0.83–0.86
Feldspar Set 1	10	809–828	268–271	0.85–0.88
Feldspar Set 2	15	816–824	270–279	0.82–0.86
Ilmenite	6	811–828	244–267	0.74–0.86
Manganese ore	1	809	276	0.79
Complete Set	47	808–829	244–273	0.74–0.94

6.2. Results

Figure 16 plots the levels of oxygen transport against the two measures of catalytic activity (tar yield and K_{WGS}/K_{eq} ratio, respectively) for the two sets of olivine and feldspar (panels a and b) and for the oxygen carriers (panels c and d). In panels c and d, the values for inert olivine and feldspar are shown for reference. Figure 16 a and b show a clear trend towards increasing oxygen transport for olivine and feldspar with decreasing tar yield and increasing K_{WGS}/K_{eq} ratio. Figure 16d shows that the K_{WGS}/K_{eq} ratio does not correlate with the oxygen transport itself when using pure oxygen carriers, and that the value of the K_{WGS}/K_{eq} ratio is similar to those of inert olivine and feldspar. This shows that the increase in K_{WGS}/K_{eq} ratio (Figure 16b) can be attributed entirely to an increase in catalytic activity. The same can, however, not be said for the tar yield. Although Figure 16c shows no correlation between the tar yield and oxygen transport for the oxygen carriers, the tar yield is lower with ilmenite and manganese than it is with inert olivine and feldspar. It is possible that beyond a certain level of oxygen transport, the oxidation of tar is limited by contacts between the oxygen carrier and volatile hydrocarbons.

Nevertheless, Figure 17 shows a near-perfect correlation between the tar yields and K_{WGS}/K_{eq} ratios obtained with olivine and feldspar. Since Figure 16d shows that the oxygen transport does not affect the K_{WGS}/K_{eq} ratio, the observed clear correlation between the tar yield and K_{WGS}/K_{eq} ratio indicates that the oxygen transport does not contribute markedly to the decreased tar yield. Otherwise, no such correlation would be observed. As a consequence, the results shown in Figure 16 c and d, along with those in Figure 17, show that the changes in tar yield and K_{WGS}/K_{eq} ratio in Figure 16 a and b originate predominantly from changes in catalytic activity. These results demonstrate that the development of oxygen transport capability by olivine and feldspar occurs concurrent with the development of catalytic activity.

The development of oxygen transport capacity by the olivine and feldspar bed samples that were obtained from the Chalmers gasifier was verified in a laboratory reactor. Here, inert and active particles sampled from the Chalmers gasifier were oxidized and thereafter subjected to a reducing atmosphere. The reactor system used has been described in detail by Leion *et al.* [132], and the conditions under which it was operated are reported in **Paper IV**. The results, shown in Figure 18, confirm that there are significant increases in the capabilities of active olivine and feldspar to transport oxygen, as compared with their states prior to an extended period of residency in the Chalmers gasifier.

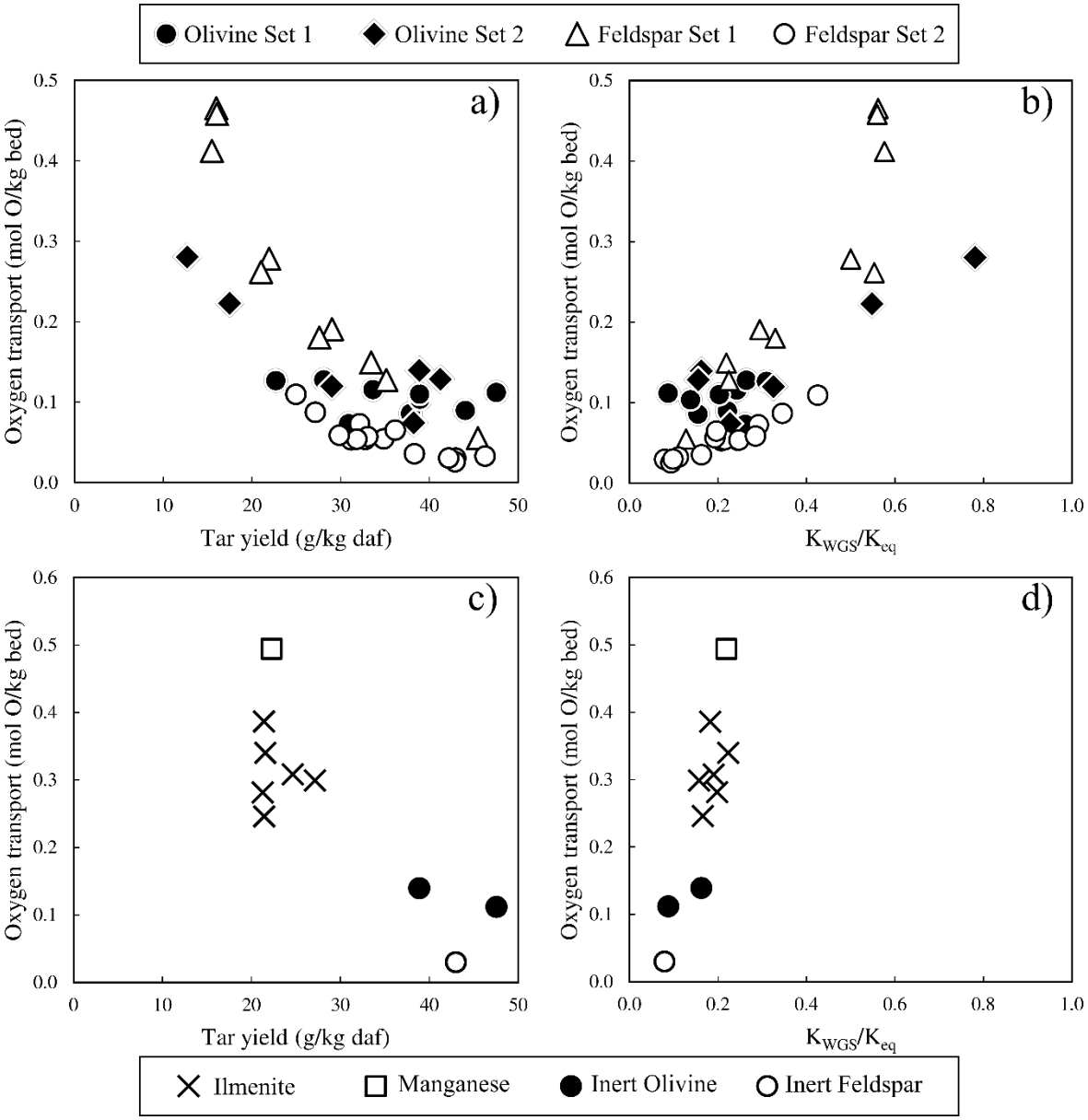

Figure 16. Oxygen transport levels deduced from the elemental balance over the Chalmers gasifier, as a function of the total tar yield (panels **a** and **c**) and the ratio of the reaction quotient of the WGS to its equilibrium value (panels **b** and **d**). Shown are the levels of oxygen transport in relation to these two measures of activity for: the olivine and feldspar sets (panels **a** and **b**); and for the ilmenite and manganese sets (panels **c** and **d**). In panels **c** and **d**, the tar yield and K_{WGS}/K_{eq} values for the inert olivine and feldspar are shown for reference.

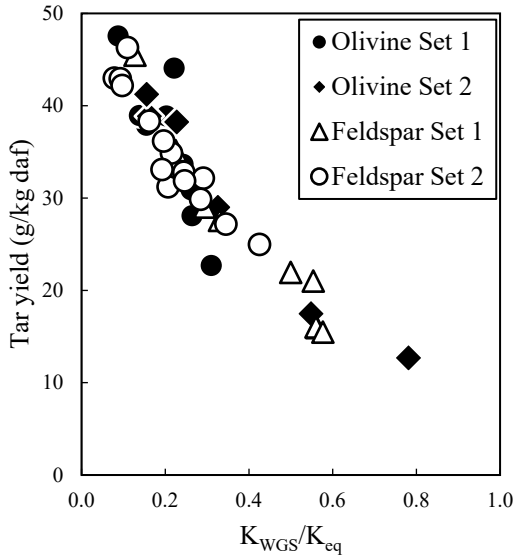

Figure 17. Correlation between the ratio of the quotient of reaction of the WGS to its equilibrium value, i.e., KWGS/Keq, and the tar yield, expressed in g/kg daf, for the different bed material sets.

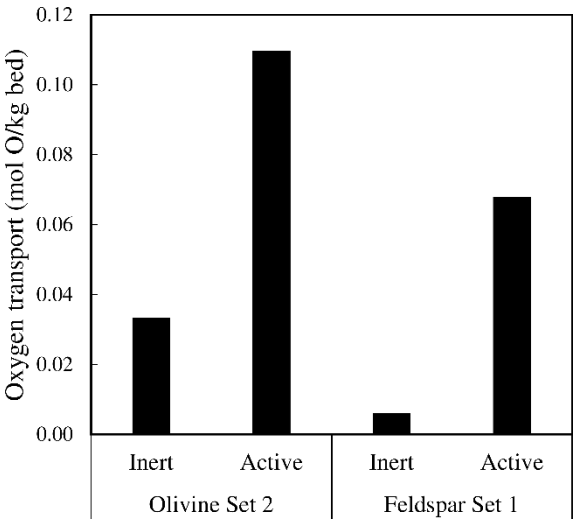

Figure 18. Oxygen-carrying capacities of inert and active olivine and feldspar samples taken from the bed of the Chalmers gasifier, and measured in a laboratory-scale fluidized bed reactor, using CO as the reductant.

6.3. Conclusions of the Chapter

The results outlined in this chapter confirm the previously reported development of oxygen transport capability along with the catalytic activity of the bed, when olivine or feldspar is used as the bed material. **Paper IV** also presents results (not shown in this thesis) that support the contributions to the development of oxygen transport of volatile species, some of which are released from the ash layer in the gasifier. This supports the notion that the ash layer is not only involved in heterogeneous reactions and catalytic effects, but also contributes to the gas-phase reactions by releasing volatile ash species that subsequently exert homogeneous catalytic effects or, in the case of oxygen, react directly with the gas phase. In the context of the recurring theme of the transport of chemical species between reactors, these results highlight how the dual bed configuration, by cycling the bed and fuel ash between two

compartments with distinct atmospheres, promotes drastic changes in the bed material composition, which can have a potent impact on the carbon distribution.

As shown in Figure 16, olivine and, in particular, feldspar attained an oxygen transport capability comparable to that acquired by ilmenite. Even though the oxygen transport level of the latter was likely limited by insufficient gas-bed material mixing, it is, nonetheless, remarkable that olivine and feldspar can transport significant amounts of oxygen. This emergent capability to bind and transport oxygen has a number of important consequences for the operation of the DFB process and the consequent carbon distribution. First, in the combustor, the bed material and the char will compete for the oxygen, which may become problematic in terms of process control. Second, as the oxidation of the bed material releases heat in amounts comparable to that resulting from the combustion of char, and given that the heat demand of the gasifier is left mostly unaffected by the development of oxygen transport capability, more char becomes available for gasification in the gasifier. Note, however, that gasifying more of the char will increase the heat demand. Third, and as noted in *Section 1.4.2*, the transported oxygen in the gasifier will react mainly with H_2 and CO, leading to a decrease in the energy content of the gas and redirection of carbon to the formation of CO_2. This will, in turn, affect the downstream processing and synthesis steps, as well as the energy demand for CO_2 separation. Thus, as oxygen transport develops, the process gradually and effectively shifts towards a hybrid form of the *Air* and *CLG* configurations.

It is important to note that the layout of the Chalmers gasifier enhances the retention of ash relative to the size of the unit, due to the large ash input on the combustor side and the constant circulation of gasification fly ash. Besides this, the availability of oxygen is much greater in the combustor than it would be in a commercial DFB gasification unit, which may lead to higher levels of oxygen transport. Despite these caveats, the overall conclusion of this chapter is that oxygen transport capabilities develop and affect the carbon distribution and the control of the DFB system, warranting careful consideration of this phenomenon.

Regardless of whether the oxygen transport develops to such an extent that the operation of the DFB system shifts completely to a CLG configuration, it is important to consider how the carbon distribution of a CLG configuration can be steered and, most importantly, how to achieve complete fuel conversion in the gasifier. *Chapter 7* focuses on the parameters that affect the rate of fuel conversion and the carbon distribution in the fuel reactor of a DFB operated in the CLG configuration.

Chapter 7: Achieving complete conversion in CLG: parameters that affect the fuel conversion

Maximizing carbon recovery in the CLG configuration requires limiting carbon slippage to the air reactor. This entails either the separation and subsequent valorization of the char or its complete conversion in the fuel reactor, as described in *Section 1.4.2* and touched upon in *Chapter 4*. To address the issue of maximizing fuel conversion, the operational parameters that influence the fuel conversion in CLG are investigated in this chapter. The parameters investigated in this chapter are the circulation rate of the bed material, the fuel feeding rate, the FR temperature, and the level of oxygen transport. These parameters are all, to varying extents, coupled to each other, in particular the oxygen transport and the circulation rate, which makes optimization of the fuel conversion a challenging task. In *Section 7.2*, the issue of decoupling the oxygen transport from the bed circulation is discussed. The chapter concludes with an extensive discussion of the challenges related to the CLG configuration, as well as its potential role in a future circular carbon system.

The influences of the aforementioned parameters on the fuel conversion and the carbon distribution in the FR are discussed based on the results of CLG-like experiments carried out in the Chalmers gasifier. ASR, which is a plastic waste that is rich in metals, was the carbon source that was converted in these experiments. The ASR-ash was found to accumulate in the bed, eventually dominating its composition and leading to the development of oxygen transport capability. The use of such a material, adopting dual roles as both the fuel and the source of bed material, could resolve many of the problems associated with oxygen carriers (see *Section 1.4.2*). Notably, it would represent a cheap source of oxygen carrier material, which is obviously advantageous, particularly if frequent replacements of the bed are needed to compensate for low-level stability.

It is important to note that the fuel and the oxygen carrier investigated in this chapter are not representative of those typically considered in the literature on chemical-looping, and that operation of the Chalmers gasifier with oxygen carriers does not constitute a real (autothermal) CLG configuration. Nonetheless, the results and discussions of this chapter are still valuable for research on chemical-looping processes for the following reasons: (1) CLG or CLG-like experiments at the MW scale are scarce; (2) fuel conversion is a challenge regardless of the nature of the fuel, and the operational parameters that can affect it are, for the most part, independent of the nature of the fuel or oxygen carrier; and (3) to the best of the knowledge of the author of this thesis, **Paper II** is the first example of CLG with a fuel that generates its own oxygen carrier. Furthermore, as mentioned in the *Introduction*, ASR is representative of the rest fraction of an intensive plastic waste-sorting process. Thus, studying its conversion is an essential step towards designing strategies to deal with this type of rest fraction.

7.1. ASR conversion

7.1.1. Method

In **Paper II**, the thermochemical conversion of ASR by CLG was investigated in the Chalmers DFB system, under near-steady-state conditions in terms of the accumulation of ASR-ash in the bed. Although the exact distributions of ASR-ash and olivine (the initial bed material) in the bed are unknown, the ASR-ash can be assumed to be present in significant amounts. From the metal-rich ASR-ash, oxygen-carrying properties evolved in the bed, at a greater magnitude than when the ASR was converted with a bed composed exclusively of olivine. As described in *Chapter 6*, the olivine present in the initial bed may have undergone changes that resulted in the development of oxygen transport

properties, through interactions with the wood ash from the combustor side or the ASR-ash from the gasifier. Nevertheless, given the high ash content of ASR (see Table 2 in *Section 3.5.2*) and the high metal content of the ASR-ash (see Table 1 in *Sections 3.5.1*), it is expected that most of the oxygen transport that emerges can be attributed to the ASR-ash particles themselves.

The aim of **Paper II** was to demonstrate that CLG of ASR, using its own ash as oxygen carrier, is feasible. The issue of achieving complete carbon recovery is tackled here by investigating how the fuel conversion is affected by the following four parameters: the circulation rate of the bed; the temperature of the FR; the fuel feeding rate; and the level of oxygen transport. Only the latter is discussed in depth in this thesis. In addition, the heat balance of the system is established to assess the feasibility of operating the system in an exclusively CLG mode, i.e., without char combustion in the AR.

For **Paper II**, 14 measurement points were used. The operating conditions covered by these measurements are listed in Table 6. In addition, the operating conditions for the three measurement points used to compare the impacts of oxygen transport on ASR conversion are given. Note that the three measurements were not made on the same day. The 14 measurement points were acquired over a period of 5 days, corresponding to Day 9 to Day 13 of an experimental campaign conducted with ASR.

Table 6. Operating conditions for the three measurement points corresponding to various levels of oxygen transport. The operating conditions range is also given for the whole 14-measurement points range.

		Day	Circulation rate (kg/h)	Fuel feeding rate (kg daf/h)	Oxygen transport (mol O/mol O stoichiometric)	Fuel reactor temperature (°C)
Oxygen transport	Point 1	13	18,100	175	0.22	824
	Point 2	11	17,700	174	0.24	826
	Point 3	9	18,000	168	0.29	821
14-measurement points range			14,400–21,200	158–202	0.20–0.29	790–835

7.1.2. ASR conversion in the FR

Given the heterogeneity of ASR, the variability of its composition, and the limited knowledge available regarding its behavior in fluidized bed steam gasification, it was necessary initially to assess its devolatilization time and char formation in a bench-scale fluidized bed reactor. Conversion in the FR was found to be limited, reaching, at best, a level of conversion corresponding to the fixed carbon estimated from the bench reactor. This indicates that the devolatilization of ASR in the FR is incomplete, which is supported by the fact that the estimated devolatilization time is comparable to the expected residence time of the ASR in the FR. Furthermore, a slight increase in the proportion of carbon ending up as TOC was observed when lower circulation rates were used (entailing longer residence times). This can only be attributed to incomplete devolatilization.

7.1.3. Impacts on ASR conversion of circulation rate, fuel reactor temperature, and fuel feeding rate

As mentioned above, the impacts of the other three parameters investigated in **Paper II** (i.e., the circulation rate of the bed, the temperature of the FR, and the fuel feeding rate) are not discussed in detail in this thesis. Nonetheless, a brief account of their effects is pertinent to the topics of this thesis. The circulation rate was found to influence the degree of ASR conversion, most likely by altering the

residence time of the ASR in the FR. The changes in the conversion rate and carbon distribution that occurred following variations of the ASR feeding rate could not be attributed to the feeding rate itself but were most likely the consequences of changes in the rate of oxygen transport. The only change that was attributable to the feeding rate was that in tar maturation, due to the affected residence time of the gas. Finally, changes in the FR temperature had by far the strongest impact on tar maturation, although they had little effect on the distribution of carbon among the various fractions. Variations in the other parameters meant that these changes could not be attributed solely to changes in the FR temperature. The absence of any impact of the temperature on the fuel conversion rate could be a result of the range of temperatures investigated being too low to discern an effect, as well as a result of the incomplete devolatilization of the ASR, as devolatilization is limited by the residence time and not by the temperature of the reactor.

7.1.4. Impact of oxygen transport on ASR conversion

The impacts of oxygen transport on the distribution of carbon into unconverted carbon leaving the FR, permanent gas, and TOC are shown in Figure 19a. The distributions of carbon in the products, in the forms of CO and light hydrocarbons (referred to as "CO plus HC") and as SPA tar, as well as the carbon in the form of CO_2, are shown in Figure 19b. The ratio of carbon in the form of phenol to that in the form of naphthalene (P-N ratio) is also shown, as an indicator of tar maturation.

From Figure 19, it is clear that the oxygen transport increases the level of ASR conversion, and that the carbon is converted exclusively to CO_2. This supports the claim made repeatedly throughout this thesis that, in CLG, the transported oxygen reacts predominantly with H_2 and CO. The TOC fraction is left unchanged, as is the SPA tar maturation. The level of carbon in the SPA tar is only slightly affected, although the last data-point is most likely an outlier, as a change in oxygen transport is not expected to cause changes in the SPA tar fraction.

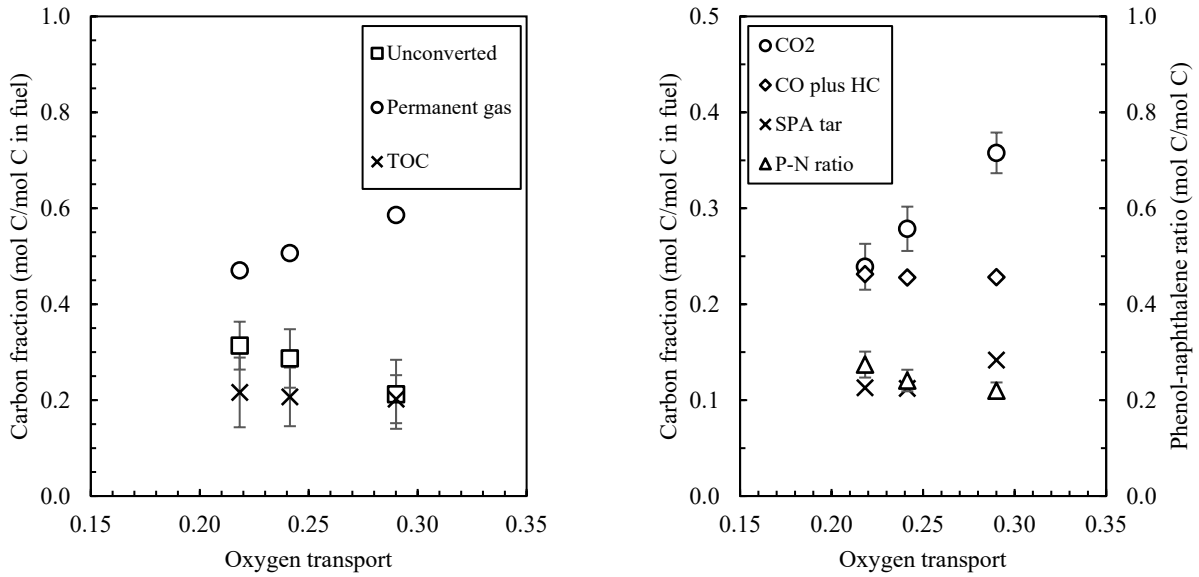

Figure 19. Impacts of oxygen transport on: (a) the distribution of carbon into permanent gas, TOC, and the unconverted fuel leaving the FR; and (b) the distribution of carbon into CO_2, CO plus HC, SPA tar, and the ratio of carbon in the form of phenol to that in the form of naphthalene (P-N ratio). The vertical error bars indicate the standard deviations for the carbon fraction. An explanation of how this standard deviation was estimated is provided in **Paper II**.

7.1.5. Feasibility of operation in CLG configuration

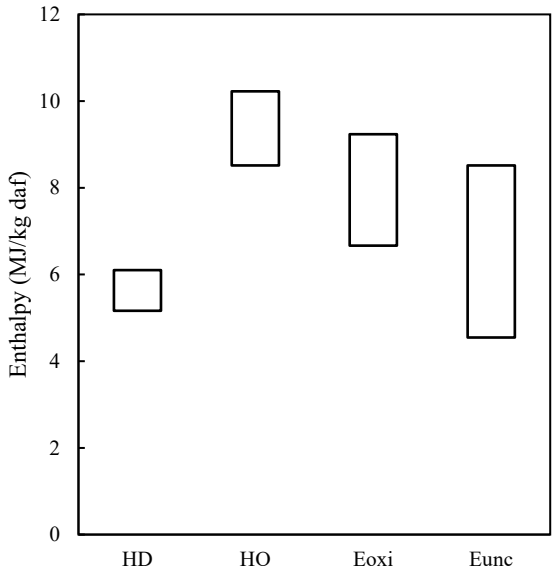

Figure 20. Ranges of values for the heat demand (HD) of the fuel reactor, the heat output (HO) of the combustor, the heat of oxidation of the bed material (E_{oxi}), and the lower heating value of the unconverted fuel leaving the FR and entering the AR (E_{unc}).

The heat balance of the DFB system was determined for the 14 experimental cases. The heat demands of the FR and the heat outputs of the associated AR are shown in Figure 20. The contributions to the heat output of the AR of the two heat production mechanisms, namely the oxidation of the bed material and the combustion of unconverted fuel from the FR, are shown in the figure as E_{oxi} and E_{unc}, respectively.

Figure 20 shows that, for all the cases examined, the heat demand of the FR can be covered by the heat output of the AR. Therefore, the DFB system can be operated under the operating conditions and fuel conversion parameters investigated in this work. The range of values for the heat demand and, to a lesser extent, for the heat output are narrower than the amount of heat released from oxidation of the bed and of the ASR. This indicates that, despite the variability of the conditions covered, the heat balance is rather insensitive to these changes. Moreover, the differences in the heat demand and heat output are such that ASR conversion in the FR can be improved without compromising fulfillment of the heat demand. As the heat produced from oxidation of the bed material is comparable to the heating value of the ASR leaving the FR, this suggests that operation in (autothermal) CLG configuration is feasible, provided that the level of oxygen transport is increased.

It is, therefore, of interest to estimate the oxygen transport levels that would be required to operate the DFB system in the CLG configuration. This, of course, requires that the ASR is fully converted in the FR. As the composition of the raw gas in such a case is not known, it was assumed that the unconverted ASR was exclusively carbon and that its conversion produced only syngas, thus maximizing the energy penalty associated with its conversion. Thus, any incremental amount of oxygen transported (compared with the measurement cases) was assumed to react with the syngas formed from the ASR conversion. From this, two extrapolation cases were derived. In Case I, the level of oxygen transport that satisfied the heat demand of the DFB system was determined. This case, however, only assumes that complete fuel conversion is achieved without concern as to how this might be achieved. Therefore, Case II was established, in which it was assumed that the transport of oxygen is the parameter that

enables complete fuel conversion. An oxygen transport level corresponding to complete oxidation of the gasification products of the ASR was, therefore, determined for Case II. Note that this case results in excess heat production in the AR. As oxygen transport will be a key parameter in ensuring complete fuel conversion, albeit certainly not the only one, the required oxygen transport level will likely lie between those of Cases I and II. These two cases are shown in Figure 21 for the range of oxygen transport levels for all 14 experimental points shown in Table 6.

From Figure 21, it is apparent that levels of oxygen transport higher than those measured in this work are required to convert ASR in the CLG mode. Based on the values obtained for Case II, achieving complete conversion solely by increasing the oxygen transport would require a significant increase in the oxygen transport level. The coupling of the circulation rate, oxygen transport, and residence time of the fuel makes increasing the oxygen transport rate through parameter optimization challenging. Besides, the oxygen-carrying capacity of the bed may be the limiting factor in achieving and maintaining high levels of oxygen transport.

Still, achieving near-complete conversion in the FR is critical for the viability of the CLG configuration. Among the potential strategies, the most promising way to improve significantly the conversion rate of ASR is to reduce further the size of the pellets, given the large ASR pellets used in this work. Increasing the temperature would likely improve the gasification rate, provided that complete devolatilization of ASR could be ensured in the FR. Regardless of the improvements made to ASR conversion in the FR, the use of a carbon stripper would be necessary, as achieving complete conversion without one is unrealistic. Nevertheless, strategies to improve the rate of ASR conversion are needed, to reduce the demand on the carbon stripper and, thereby, improve its efficiency.

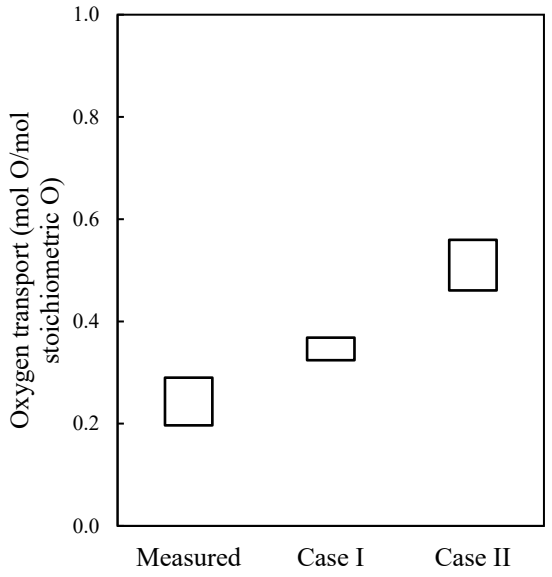

Figure 21. Estimation of the oxygen transport levels required for two extrapolated cases, as compared with the range of measured oxygen transport levels. Case I involves extrapolation to complete carbon conversion in the fuel reactor and increasing the heat of oxidation of the bed *via* oxygen transport until the heat demand of the fuel reactor is equal to the heat output of the air reactor. Case II corresponds to an extrapolation to the level of oxygen transport required to convert fully the fuel, whereby the unconverted carbon becomes CO_2.

7.2. Decoupling bed circulation from oxygen transport

Operation of the CLG configuration is a complex procedure, as it needs to satisfy several conflicting goals. To maximize carbon recovery, the fuel conversion in the FR should be maximized, which requires long residence times. However, the circulation rate of the bed material needs to be sufficiently high to maintain a temperature in the FR that is conducive to high gasification rates. High circulation rates enable high oxygen transport rates, which lead to a decrease in the energy content of the raw gas and a shift in the carbon distribution towards CO_2. At the same time, the oxygen transport is a parameter that greatly affects fuel conversion, as shown in the results of this chapter. The optimization of the process necessitates, therefore, decoupling of the circulation rate from the transport of oxygen and, to some extent, from the residence time of the fuel.

A conference article written by the author of the present thesis (as mentioned in *Section 2.2.1*) describes an effort to increase the cold gas efficiency (CGE) through dilution of the oxygen carriers with an inert bed material, silica sand, which effectively resulted in partial decoupling of the circulation rate from the oxygen transport [117]. This dilution did not, however, lead to improvements in the CGE, although the char conversion rate was negatively affected. Even at 90% dilution, one of the oxygen carrier and silica sand mixtures showed a behavior similar to that of a pure oxygen carrier bed, with low CGE, while the benefits of the oxygen transport in terms of enhanced char conversion were entirely lost. Conversely, the tar yield was markedly decreased compared with that of a pure silica sand bed, even at high levels of dilution. These results suggested that the oxygen-carrier particles were located on top of the bed, whereas the silica sand remained within the deep bed, which is where fuel particles tend to gasify. When the oxygen carrier particles were replaced with sand, the gasifying fuel particles found themselves surrounded by sand, which does not prevent the inhibition of gasification, while the oxygen carrier particles on the top of the bed and projected into the freeboard still oxidized the volatiles and gasification products. These results are consistent with those of Larsson *et al.*, who reported that, even in a bed with only 12% ilmenite (the remainder being silica sand), the CGE was markedly decreased, as was the tar yield. Both of these variables increased with an increase in fluidization velocity [75]. Thus, the hydrodynamics of the FR bubbling bed is an essential consideration if dilution is chosen as a decoupling strategy.

An alternative to dilution, as suggested by Dieringer *et al.*, is to use a bed material that contains a large non-oxygen-carrying fraction [133]. For example, the slag from steelmaking processes could play such a role, as evidenced by its composition (described in *Sections 2.2.1* and *3.5.1*). In the aforementioned conference article, when LD slag was partially diluted with silica sand and used as an oxygen carrier it showed the same trends as the other oxygen carriers, although it led to the highest rate of char conversion and highest CGE [117]. Owing to its high calcium content, it likely also confers catalytic activity, which is beneficial compared with simple dilution with an entirely inert material.

Dieringer *et al.* also investigated the use of sub-stoichiometric conditions in the AR to prevent complete re-oxidation of the bed material, as a means to decouple the heat transport from the oxygen transport [133]. As a large fraction of the bed is in that case inert with respect to oxygen transport, this fulfills the role of dilution without its drawbacks. Furthermore, the reduced metal sites can function as catalytic sites for tar cracking and reforming reactions. An alternative to sub-stoichiometric operation of the AR is reduction of the oxygen carrier in a third reactor placed before the FR, as suggested by Larsson *et al.* [75]. Such a triple-reactor system is used in *Chapter 8*, whereby reducing off-gases from the process are used to reduce the bed material.

7.3. The challenges of CLG and its role in the future system

The oxygen transport governs the CLG process, not only because it confers inherent separation of CO_2, but also because it is a crucial factor in achieving complete conversion in the FR. However, the latter role inevitably entails carbon oxidation to CO_2 in the FR, such that the CO_2 in the raw gas becomes the main carbon stream produced by the system. This makes the goal of operating in CLG mode and recovering most of the carbon in products paradoxical. This is evident in Figure 8, where for the CLG case at high temperature for which complete fuel conversion is more realistic, the level of carbon recovery as end-product is the lowest of all the DFB configurations. Optimizing the carbon distribution will likely prove challenging, due to the complex coupling of the circulation rate, heat transport, oxygen transport, and fuel conversion. As discussed in *Section 7.2*, there are ways to decouple these parameters. Nevertheless, regardless of the optimization of the design of the CLG system or of the conversion process in the FR, CO_2 will still be a major, and most likely the main, output of the process.

This suggests that carbon sequestration to produce negative emissions is a reasonable primary goal for CLG, whereas the production of carbon-containing products should be a secondary goal. Still, it is important to consider the downstream upgrading and synthetic processes. Indeed, for the downstream configuration considered in *Chapter* 4, even though the use of CLG leads to the lowest level of carbon recovery as end-product, it is still comparable to those of the Air and Oxyfuel configurations, for which CO_2 is also the main product of the process. Besides, from the energy demand and investment perspectives, when complete carbon recovery is the goal, CLG is likely to be advantageous compared with the Air configuration, due to a lower total energy demand for CO_2 separation, lower associated investment cost, and greater opportunity for heat integration (see Figure 10 and Figure 11). The competition with the Oxyfuel configuration will depend on the cost comparison of amine scrubbing and subsequent CO_2 desorption on the one hand, and the production of pure oxygen on the other hand. In any case, if significant recovery of valuable carbon or an energy-rich gas is the aim, CLG is probably not the preferred configuration.

While it mainly comes down to a choice of process for the case of DFB gasification of biomass (provided that oxygen transport does not develop to the point of shifting the operation to CLG, as described in *Chapter 6*), CLG is likely the only possibility when considering the gasification of ASR in a DFB. This is because of the cost associated with ensuring sufficient bed replacement to minimize the oxygen-carrying capacity. Similar to ASR, other rest fractions from extensive sorting processes that contain large amounts of metals should be suitable as feedstocks for thermochemical recycling by CLG. Therefore, even if CLG does not find a niche in biomass waste processing, it warrants investigation for its role in ASR-like waste recycling.

If a sufficiently high value is assigned to sequestering biogenic carbon to generate negative emissions, such that the carbon is deemed more valuable when it is in CO_2 than in products, then CLC appears to be a more worthwhile approach than CLG. Indeed, almost all the carbon can then be recovered and sequestered. Furthermore, despite its associated issues, CLC does not suffer from the need to achieve a difficult balance in terms of oxygen transport and quality of products, since oxygen transport can be maximized without any concerns. Both CLG and CLC suffer, however, from the same conversion issue, in that some carbon will inevitably slip from the FR to the AR, in the form of char or coking on the bed material or in the form of non-valuable forms of carbon that become destroyed in the AR.

The challenge linked to achieving full conversion in the FR or, alternatively, of efficiently separating the unconverted fuel before it enters the AR, can be resolved through the use of low-char-forming carbon sources. Thus, plastic-rich waste may be suitable for conversion *via* CLG, as well as *via* the Electrical configuration, which also requires that carbon slippage to the combustor be limited. On the other hand, such carbon sources tend to produce more heavy organic molecules and soot, both of which must be destroyed in the AR. Note also that some plastic waste, such as ASR, may form significant amounts of char, due to their char-forming plastic content. Besides this, metals are known to enhance char formation in polymers [134] and to catalyze graphitization [135]. When considering the conversion of plastic-rich waste by CLG, it is important to take into account that these wastes are predominantly of fossil origin. Therefore, prioritizing the recovery of the CO_2 produced over emitting it is essential.

7.4. Conclusions of the Chapter

The many issues raised in this chapter and in *Chapter 4* highlight the current lack of clarity regarding the precise role and capabilities of CLG as a DFB configuration for carbon recovery. Whether one considers carbon recovery in the form of products or as CO_2 for sequestration, there appear to be other, better-suited options. Optimizing the CLG process remains a challenge, as conflicting aspects must be balanced. Furthermore, preventing slippage of char from the FR to the AR, either *via* complete conversion or separation, is essential in CLG. Otherwise, any intermediary process that oxidizes both char and the oxygen carrier to produce heat in the combustor will lead to decreased carbon recovery with respect to CLG, and will entail a more challenging separation of CO_2 from the flue gas, as compared with the Air configuration. Interestingly, this type of scenario may also be manifested following the development of oxygen transport in bed materials that initially lack such a capability, as described in *Chapter 6*.

Despite the many challenges that face the CLG configuration, there may be niche applications for the CLG configuration. *Chapter 8* presents a case in which a triple-reactor CLG system is used, and this overcomes some of the issues discussed in the present chapter. The CLG process is used to produce a reducing gas that is thereafter used for the direct reduction of iron ore in a shaft reactor. The off-gases from this shaft reactor are partly used in the third reactor introduced in the CLG loop to reduce the bed before it enters the FR, thereby limiting the problematic oxidation of the raw gas. The bed material used in the process is steelmaking slag, which may originate from the electric arc or basic oxygen furnaces. This slag, which is typically a waste byproduct of the steelmaking industry, here acts as an oxygen carrier, thereby greatly reducing the associated cost. The technical and economic feasibilities of this process are described and compared to alternatives in *Chapter 8.*

Chapter 8: A case for CLG: Production of sustainable steel using DFB gasification

This chapter, which is based on **Paper V**, presents a case for the use of DFB gasification in a CLG configuration, so as to produce a reducing gas for the direct reduction of iron ore. The discussion on the topics of the carbon distribution and carbon recovery in the proposed process differs from the previous chapters, as, in this case, the product gas from gasification is not exploited for its carbon content but rather for its reducing power. Most of the carbon in the product gas is converted to CO_2 in the process, and CO_2 is, by far, the main carbon output of the plant. To increase the range of valuable end-products from the plant, the extraction of biochar and valuable tar compounds, e.g., BTX, is also proposed.

This chapter first gives a brief description of the process of direct reduction (DR) of iron, and thereafter presents the three DR routes compared in this work and some of the assumptions used to establish the cases. Results pertaining to the reducing gas composition, operating parameters, and carbon distribution of the proposed route, referred to as the DFB-DR route, are shown. The emissions reduction potentials of the three DR routes, relative to the traditional Blast Furnace – Basic Oxygen Furnace (BF-BOF) route, are compared. Finally, a comparison is made of the costs of the reducing gas produced by the different DR routes, as well as of the total production cost of the liquid steel for the DR routes and for the BF-BOF route.

8.1. Direct reduction of iron ore

The main process for the production of crude steel is the BF-BOF route, which accounts for about 70% of global crude steel production [136]. This process is energy-intensive and relies upon the use of coke as the energy source and reduction agent for the reduction of iron ore. This results in high levels of emissions, typically in the range of 1,600–2,200 $kgCO_2/t$ steel [137], which contributes to making the iron and steel industry one of the largest industrial emitters, accounting for 4%–7% of global CO_2 emissions [138]. Direct reduction (DR) processes have been used since the 1970s, especially in regions with abundant natural gas resources. This iron reduction route accounts today for about 7% of global crude steel production [136]. In DR processes, iron ore in the form of lumps, pellets or fine powder is reduced in the solid state to direct reduced iron (DRI), which is then converted to steel in an electric arc furnace (EAF). The most common DR process, the MIDREX process, relies upon natural gas as the energy source and as the precursor to the reduction agent, conferring a 30%–45% reduction in CO_2 emissions compared with the BF-BOF route [139]. Although this reduction is significant, CO_2 emissions remain high at 1.1–1.2 tCO_2/t steel. The use of scrap significantly reduces the energy consumption of the process, although the input of scrap to the EAF is limited by its availability.

To reduce or eliminate the emissions from steelmaking, carbon capture and storage (CCS) must be employed, or fossil fuels must be replaced by renewable sources. Hydrogen produced from water electrolysis using fossil-free electricity is one proposed alternative to natural gas in the DRI-EAF route, as it can reduce iron ore to metal iron and it can, in combination with electricity, cover the energy demand of the process. The HYBRIT project in Sweden aims to demonstrate the viability of such a process [140]. However, reaching the 1.5°C or 2.0°C targets put forward by the IPCC [1] will likely require negative emissions of CO_2 [141]. This means that the use of biomass coupled with CCS should be considered wherever fossil resources are currently being used, in particular in applications that require a carbon input, given that biomass and directly-captured atmospheric or oceanic CO_2 are the only renewable carbon sources. In steelmaking, biomass can simultaneously act as reduction agent,

carbon source, and energy source. DFB gasification could, therefore, be used to generate the reducing gas required by the DR process, while also producing a CO_2 stream for sequestration, given that CO_2 is one, if not the most abundant, of the carbon forms generated by the process, as demonstrated in the preceding chapters.

As mentioned above, the MIDREX process is the most common DR process. For this reason, it is the process on which the analyses in this work are based. This process is based on DR in a shaft furnace fed with iron ore pellets or lumps, which are reduced by syngas produced from the reforming of natural gas. The heat demand of the DR reactor is entirely covered by the sensible heat content of the reducing gas, which is typically fed to the DR furnace at temperatures in excess of 900°C. The iron ore, introduced at the top of the furnace, is preheated by the top-gases, which exit the furnace at about 350°C. In the reaction zone, most of the ore is reduced to metallic iron, although around 8% of the iron remains as FeO. Subsequently, the reduced iron cools down in a transition zone, where it encounters natural gas that is injected at the bottom of the furnace to increase the carbon content of the DRI *via* the carburization reaction [142]. A carbon content of around 2% is usually considered optimal. The DRI is further cooled by the endothermic carburization reaction with natural gas. To avoid cooling, CO from the reforming of natural gas can be injected instead of natural gas, and this results in exothermic carburization of the DRI [142]. The hot DRI is extracted from the bottom of the reactor. From there, it can be cooled before storage or transportation as DRI. It can also be compacted at high temperature, after which it is referred to as *hot-briquetted iron*, which is then stored or transported. Alternatively, the DRI can be charged hot directly into the EAF to reduce the energy consumption of that step [143].

8.2. Methods

8.2.1. Comparison cases

In this work, the DR of iron using a DFB gasification gas, referred to as DFB-DR, was compared with the MIDREX route that uses natural gas, NG-DR, and with DR using hydrogen produced from the electrolysis of water, H_2-DR. These three routes are schematically described in Figure 22. All three routes were based on a MIDREX DR reactor, as described in the previous section.

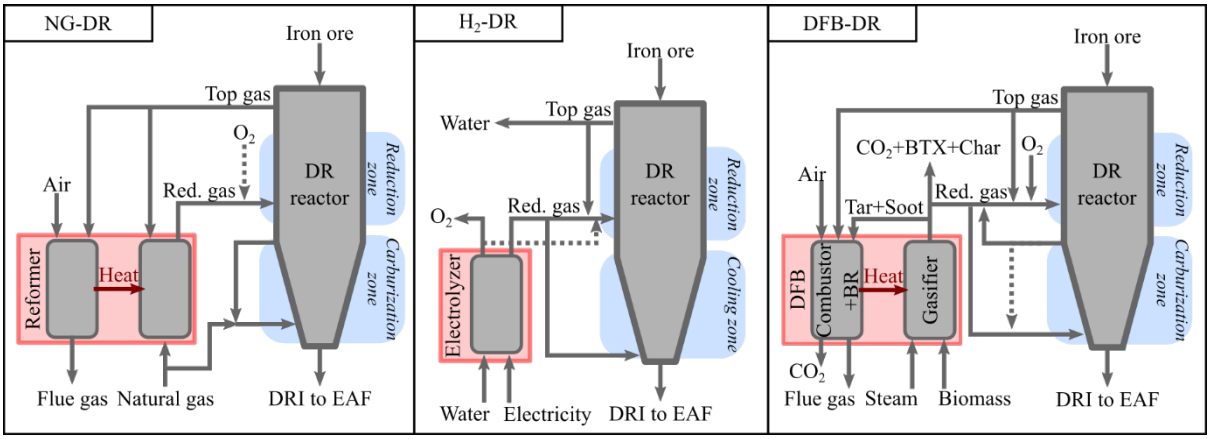

Figure 22. Schematic of the direct reduction routes compared in this work. NG-DR refers to the traditional, natural-gas based direct reduction using the MIDREX technology. H_2-DR refers to direct reduction using hydrogen produced through electrolysis. DFB-DR refers to the direct reduction of iron using gas derived from DFB biomass gasification. Both the H_2-DR and DFB-DR routes are based on a MIDREX DR reactor. Red. gas, reducing gas; BR, bed reducer. The dashed lines represent optional streams.

8.2.1.1. Reference case: NG-DR route

Table 7. Characteristics of the reducing gases and top-gases for the three reference NG-DR plants [144,145].

Plant	H_2 (%vol)	CO (%vol)	H_2O (%vol)	CO_2 (%vol)	H_2/CO	RP
Reducing gas						
Contrecoeur	49.7	32.7	4.3	2.4	1.5	12.3
Gilmore	52.6	30.0	4.7	4.8	1.8	8.7
Siderca	52.9	34.7	5.2	2.5	1.5	11.5
Top gas						
Contrecoeur	40.3	19.6	19.0	17.1	2.1	1.7
Gilmore	46	21	11	16	2.2	2.5

RP, reduction potential

The reference case for the DR of iron was chosen as the MIDREX process using natural gas. The NG-DR route considered was based on that used at the Contrecoeur plant in Montreal, Canada, and the Gilmore plant in Portland, Oregon, using the data from Béchara *et al.* [145], as well as the data from the SIDERCA plant in Campana, Buenos Aires, Argentina [144]. The reducing gas in MIDREX plants is produced through a combination of dry and wet reforming of natural gas.

In the DR shaft furnace, to maintain reducing conditions that facilitate extensive metallization of the iron ore, a certain reduction potential (RP) must be maintained. This means that the gas introduced into the DR reactor must have sufficiently high H_2 and CO partial pressures to ensure reduction of the iron ore, but also that the top-gas leaving the DR reactor should still contain significant amounts of reducing gas. Conversely, the partial pressures of H_2O and CO_2 should be limited. The RP, also referred to as the "gas quality", is typically defined by the $(H_2+CO)/(H_2O+CO_2)$ ratio [145,146]. The compositions and RPs of the reducing gases and top-gases from the Contrecoeur, Gilmore, and Siderca plants are listed in Table 7. These values were used as references for the H_2-DR and DFB-DR routes, in the sense that, to ensure as high degrees of metallization as the NG-DR route, the reducing gas should have an RP value greater or equal to 8.7, and the top-gas should have an RP value greater or equal to 1.7. Note that the RP of the top-gas will, in reality, depend on the heat balance of the DR furnace, and, thereby, on the H_2/CO ratio of the reducing gas. Indeed, the reduction reaction of iron ore with CO is exothermic, whereas with H_2 it is endothermic. Therefore, a lower H_2/CO ratio leads to a less-endothermic reduction, such that more iron ore can be reduced per unit volume of gas fed.

8.2.1.2. H_2-DR route

The H_2-DR route considered was based on H_2, produced from electrolysis of water, being the reductant. The assumptions made to establish this case are detailed in **Paper V**. The compositions of the reducing gas and top-gas produced by the H_2-DR route are shown in Table 8. The reducing gas has an RP of 8.8, which means that it fits the criterion of RP >8.7 defined in *Section 8.2.1.1.* Similarly, the RP of the top-gas is high. These high RPs indicate that high-level metallization of the iron ore will be possible. The high RP value of the top-gas is a consequence of H_2 being the only reducing agent in the gas. As the reduction reaction with H_2 is endothermic (whereas with CO it is exothermic), the heat balance of the DR furnace constrains the amount of iron ore that can be reduced, which explains the high RP of the top-gas.

Table 8. Characteristics of the reducing gas and top-gas in the H_2-DR route.

	H_2 (%vol)	H_2O (%vol)	RP
Reducing gas	89.8	10.2	8.8
Top gas	75.0	25.0	3.0

RP, reduction potential

When interpreting the results in this chapter it is important to recall that the operation of the DR reactor was set to be the same as those for the NG-DR and DFB-DR routes. However, this may not be the optimal operational strategy for the DR when using pure hydrogen. The DRI production efficiencies of the different routes are described in **Paper V**, with the H_2-DR route being found to have the lowest efficiency (results not shown in this thesis). The main efficiency loss was related to the combustion of part of the H_2 produced in order to reach the desired temperature for the inlet to the DR reactor. This loss could be reduced by, for instance, using high-temperature electrolysis.

8.2.1.3. DFB-DR route

The proposed DFB-DR route is better characterized as a triple-reactor system that uses the slag from steelmaking as an oxygen carrier. The process operates, therefore, in the CLG configuration, with the addition of a third reactor to the loop such that part of the top-gas from the DR reactor is used to reduce the slag bed material before it enters the gasifier. This third reactor is referred to as the "bed reducer" (shown in the same box as the combustor in Figure 22). The cold gas from the gasification of biomass is used as both the reducing gas and carburizing gas (split arrows going to the carburization and reduction zones, in the right-hand side panel in Figure 22). The carburizing gas is extracted before the reduction zone, and can be partly recirculated, (as shown by the dashed arrow), while the remainder is mixed with the reducing gas. A detailed schematic of the DFB-DR route is shown in Figure 23. The DFB-DR plant is divided into three main sections: (1) the DFB section, which produces the gasification gas and to which part of the top-gas is returned; (2) the DR reactor, where the reduction of iron ore takes place; and (3) the gas-handling section, where the gasification gas is cleaned and upgraded to generate the reducing gas, and where the separation of CO_2 from the cold gas and top-gas is carried out. In the present section, the most important parts of the DFB-DR route are described. However, for a complete description, the reader is referred to **Paper V**.

With regard to the requirement for the RP of the reducing gas (as stated in *Section 8.2.1.1*), CO_2 and H_2O should be removed from the gasification gas and from the top-gas. Therefore, the separation of CO_2 from these two streams is necessary and will produce the pure CO_2 streams that will be sequestered to create negative emissions. Another pure CO_2 stream is produced by the bed reducer from the oxidation of H_2 and CO. The pure CO_2 streams are mixed and conditioned in preparation for their transport and sequestration.

Prior to the separation of CO_2 from the raw gas, the tar should be removed. The separated tar, as well as the potential spent scrubbing agent used for its separation, are sent to the combustor where they are burnt. Of the species constituting the tar, some have a high value and may be present in sufficient quantities to be separated and sold. Considering the high value of BTX (benzene, toluene and xylenes), and given that it can be difficult to remove them by scrubbing, it is considered in this work that they are separated. BTX could constitute an additional valuable end-product of the plant, increasing its competitiveness relative to the alternatives.

Besides H_2O and CO_2, the presence of hydrocarbons in the reducing gas is also not desirable, as the reaction of Fe_2O_3 with hydrocarbons such as CH_4 is slow [147]. In the reduction zone of the DR reactor, hydrocarbons would act as a dilutant and energy sink (due to their reforming) and, more importantly, in the bed reducer of the DFB loop they would not be converted. The presence of hydrocarbons in the stream leaving the bed reducer would necessitate their oxidation, most likely through the injection of pure oxygen. In the proposed DFB-DR route, light hydrocarbons in the reducing gas are partially oxidized to H_2 and CO using pure oxygen (indicated by the red continuous arrow in Figure 23). Extensive non-catalytic partial oxidation (POX) occurs at very high temperatures, typically in the

range of 1,100–1,400°C [148], with the higher extreme of that range being used in this work. As a consequence, significant amounts of H_2 and CO will be oxidized to reach these temperatures. The pure oxygen needed for POX and to raise the temperature can be produced by air separation or water electrolysis. The latter option has the advantage of producing H_2, which can be mixed with the reducing gas to enable increased production of DRI per unit of biomass fed.

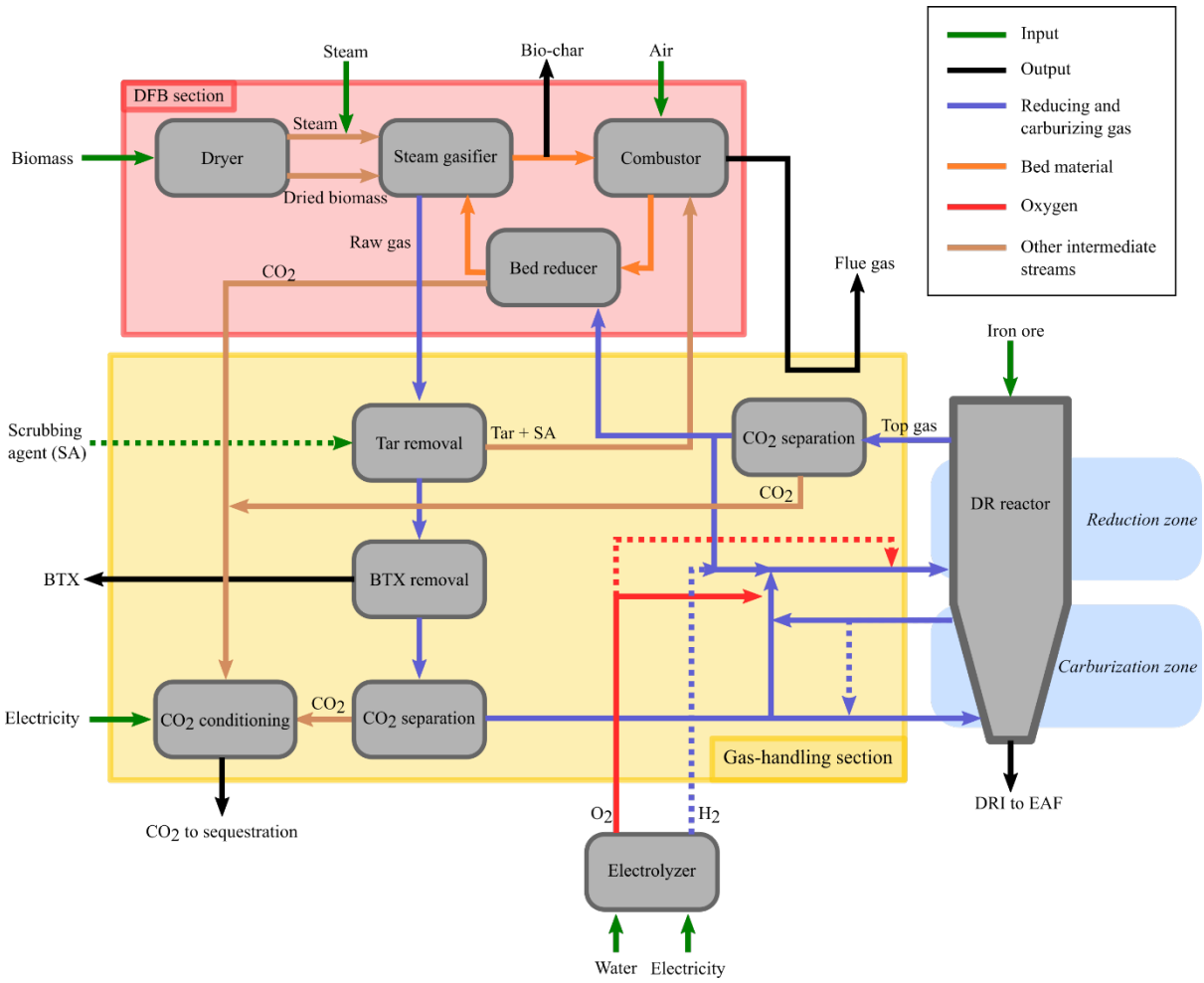

Figure 23. Schematic of the proposed DFB-DR route. The EAF section and downstream steel processing steps are not shown. Dashed lines indicate optional streams. The thicknesses of the arrows are not scaled to the sizes of the respective flows.

Concerning the operation of the DFB section itself, it is characterized by the separation of the biochar formed in the gasifier. The reason for this is that the temperatures required for complete conversion of the char would raise several problems. First, high temperatures entail a high rate of oxygen transport by the slag bed, which means that a large fraction of the top-gas needs to be oxidized in the bed reducer, rather than it being recirculated to the DR reactor, which decreases the amount of DRI produced. Second, while higher temperatures promote reforming of hydrocarbons in the gasifier, which decreases the demand placed on the POX step, they also promote the WGS reaction and lead to a higher H_2/CO ratio. A higher H_2/CO ratio implies more-endothermic reactions in the DR reactor, and therefore a comparatively lower DRI production. Third, a higher temperature increases the risk of operational issues. For these reasons, the gasifier was assumed to be operated at the moderate temperature of about 800°C, and it was arbitrarily assumed that 20% of the char was gasified, with the remainder being separated. Note that the actual operating conditions of the DFB gasification will reflect a trade-off

between the value of the steel and that of the biochar. Regardless of the operational choice made, it is essential that any biochar recovered is valorized. One potential application of the biochar within the steelmaking industry itself is as a replacement for coke in the BF-BOF or in the EAF.

8.2.2. Comparison criteria

The DR routes were compared with respect to: the reducing gases and top-gases that they produced; their potential for emissions reductions compared with the traditional BF-BOF route; and their economic potentials. For the latter, given that the costs for the DR furnace, the EAF, and the downstream steel-processing steps will be comparable for all three routes, the cost of producing the reducing gas was compared. The total production cost of liquid steel for the three routes was also determined and compared with that of the BF-BOF route, while accounting for the cost of emitting CO_2 and the revenue associated with negative emissions.

8.2.2.1. Economics

The reducing gas cost (in €/MWh) is derived from the cost of the units involved in its production and the fuel or electricity prices. The cost of the units includes the annualized investment cost and the operational expenditures. The reducing gas cost is shown versus the electricity price, which is varied from 20 €/MWh to 80 €/MWh. The biomass price is set to 20 €/MWh, corresponding to the cost of forest residues in Sweden. To reduce the cost of the biomass, recovered wood, with a price ranging from 0 €/MWh to 10 €/MWh, will most likely be used. A biomass price of 20 €/MWh represents, therefore, a conservative assumption.

The total production cost is expressed relative to one tonne of liquid steel (LS). This cost includes the (annualized) investment costs and operational expenditures associated with the DR furnace and the EAF, which are assumed to be similar for all three DR routes. The cost for the production of steel from the BF-BOF route was determined based on the investment cost for relining an existing BF-BOF plant, estimated at 190 € per tonne of annual capacity, based on the data from Wörtler *et al* [149]. The cost of emitting fossil-derived CO_2 or, conversely, the revenue associated with creating negative emissions, are also accounted for in the total production cost of the steel. Any revenue earned from negative emissions would cover the costs for the capture of the CO_2, its conditioning, its transport and sequestration, and would allow some profit. The costs for CO_2 capture and conditioning, but not the transport and sequestration costs, are included in the economic calculation of the DFB-DR route. Therefore, the revenue considered in this chapter covers the costs for capture and conditioning, as well as providing a profit margin. This revenue and the cost for positive emissions are varied between 0 €/tCO_2 to 100 €/tCO_2 and are set to be equal. The many assumptions required to establish the reducing gas cost and total steel production cost are not laid out in this thesis, but can be found in **Paper V**. The results for the DFB-DR route presented in this chapter are based on a median cost estimation.

8.3. Results

8.3.1. DFB-DR route: Gas composition, operating parameters, and carbon distribution

The compositions of the gases produced by the DFB-DR route are listed in Table 9. The reducing gas has a high RP, which means that extensive metallization of the iron ore in the DR furnace is possible. The H_2/CO ratio is high compared with that of the NG-DR route (see Table 7), entailing a more-endothermic reduction, which translates into a higher RP of the top-gas. The composition of the carburizing gas suggests that carburization will, to a large extent, occur *via* reactions with CO. The

carburizing gas has a relatively high RP value, which ensures that re-oxidation of the DRI will be limited in the carburization region.

The level of oxygen transport from the combustor to the bed reducer that is required for autothermal operation is 27% (moles of O_2 per moles of O_2 for stoichiometric combustion of the fuel). Note that during the experiments with LD slag reported in the conference paper from the author of this thesis [117] (see *Section 2.2.1*), oxygen transport levels in the range of 30%–45% were achieved, which indicates that the level required here for the DFB-DR route is likely achievable with steelmaking slag as the oxygen carrier. Reduction of the oxygen transport level to 5% requires the oxidation of 17% of the top-gas, with the remainder being recycled to the reducing gas.

The distribution of carbon in the DFB-DR plant, including the EAF section, is shown in Table 10. The total carbon input includes the biomass, the scrubbing agent for tar removal, the carbon in the limestone ($CaCO_3$) used as flux in the EAF, and the graphite that forms the EAF electrodes (for more details, see **Paper V**). The latter two sources constitute the only non-biogenic carbon sources to serve the process, accounting for 32 $kgCO_2$/t LS of the 160 $kgCO_2$/t LS emitted by the process. The amount of carbon recovered as CO_2 and sequestered is significant, accounting for more than two-thirds of the carbon input. This results in net-negative emissions of about 850 $kgCO_2$/t LS. In addition, a large fraction of the carbon (>23%) is recovered as secondary products, in the forms of char and BTX, which highlights the importance of valorizing these products.

Table 9. Compositions of the cold-gas, reducing gas, carburization gas, and top-gas of the DFB-DR route. Species concentrations are given in volume percent. RP refers to the reduction potential, which is defined as the $(H_2 + CO)/(H_2O + CO_2)$ ratio.

	H_2	CO	CO_2	H_2O	CH_4	C_2H_4	C_2H_2	C_2H_6	C_3H_6	H_2/CO	RP
Cold-gas[a]	48.3	22.1	22.4	0.0	5.3	1.4	0.0	0.3	0.2	2.2	3.1
Reducing gas[b]	74.8	18.6	0.8	5.6	0.0	0.0	0.0	0.0	0.0	4.0	14.4
Carburizing gas[c]	65.8	17.6	4.5	6.0	4.2	1.4	0.0	0.3	0.3	3.8	8.0
Top-gas	61.0	11.0	8.4	19.6	0.0	0.0	0.0	0.0	0.0	5.6	2.6

[a] Prior to CO_2 separation.
[b] After mixing with recirculated top-gas and H_2 from electrolysis, and temperature rise to 1,000°C.
[c] Includes the recycled carburization gas.

Table 10. Distribution of the carbon among the outputs of the process, in terms of the fraction of the total carbon input, which accounts for the carbon in the biomass, the scrubbing agent (RME in the calculations), the CO_2 released by the flux agent, which is assumed to be $CaCO_3$ in the calculations (see **Paper V** for more details), and the carbon in the graphite electrodes. The production yields of the various outputs are also shown in kg/t liquid steel (LS).

	Carbon content (% of input)	Production (kg/t LS)
Emitted CO_2	11.6	159
Sequestered CO_2	64.4	879
Char	21.7	90
BTX	1.7	7
Carbon in steel	0.6	2

8.3.2. Reduction in emissions relative to the BF-BOF route

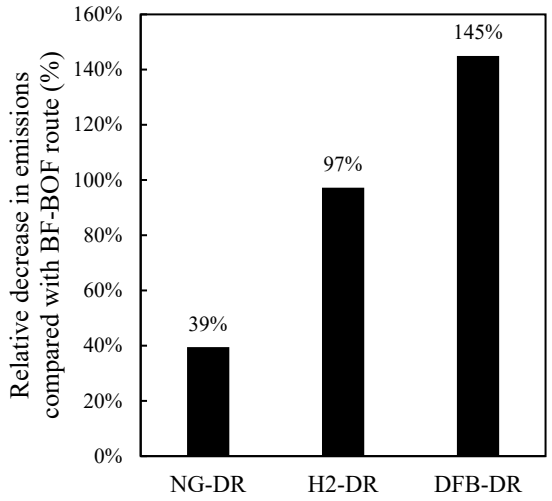

Figure 24. Reductions in CO_2 emissions for the three DR routes, relative to the BF-BOF route.

The decreases in emissions relative to the BF-BOF route for the three DR routes, expressed as percentages, are shown in Figure 24. While the H_2-DR route enables almost total elimination of emissions compared with the BF-BOF route, the DFB-DR route is the only one (of the three discussed in this chapter) that can achieve negative emissions (i.e., a relative decrease in emissions of more than 100%). This means that the production of one tonne of steel by the DFB-DR route offsets the production of half a tonne of steel *via* the BF-BOF route. This can create a significant perceived value for the steel produced by the DFB-DR route, as this steel can be regarded as not only clean in itself, but even as a mode of cleaning the production of previously created steel.

8.3.3. Economics

To produce 1 Mt LS/year, the DFB-DR plant requires a 460-MW gasifier and a 115-MW electrolysis plant. This entails an investment cost of more than 760 million euros (M€), with an upper cost estimation approaching 1,000 M€ (or 1,000 €/t annual capacity). While the lower cost estimation is comparable to the investment cost of the H_2-DR route, which stands at 700 €/t annual capacity, it is higher than that of the NG-DR route, which stands at 570 €/t annual capacity. The upper cost estimation is close to double the investment cost required for the NG-DR route. This is due to the significant costs associated with the DFB and gas-handling sections, which represent 39%–55% of the CAPEX, and to the fact that the proposed DFB-DR route also has an electrolyzer, which accounts for 8%–11% of the investment. In comparison, the NG-DR and H_2-DR routes only have the reformer and electrolyzer, respectively, as additional cost items to their DRI-EAF sections, with the reformer representing about 35% of the investment in the NG-DR route, and the electrolyzer standing for 47% of the investment cost in the H_2-DR route.

Despite having higher investment costs than the H_2-DR route, the DFB-DR route leads to a reducing gas with a lower cost, due to the (generally) lower price of biomass per MWh compared with electricity (see Figure 25). The NG-DR route leads to the lowest cost for reducing gas, and the DFB-DR and H_2-DR routes cannot compete with this level of expense. Note that the case presented for the DFB-DR route in Figure 25 is based on the median cost estimation. For the upper cost estimation (not shown here), the H_2-DR route is competitive up to electricity prices of about 50 €/MWh. Current electricity prices in Sweden are around 40 €/MWh. The cost of the reducing gas for the DFB-DR route, shown

in Figure 25, is comparable to that estimated by Hammerschmid *et al.*, who investigated the production of reducing gas for DR using Oxy-SER (see *Section 1.3.1*), being in the range of 36–54 €/MWh [146].

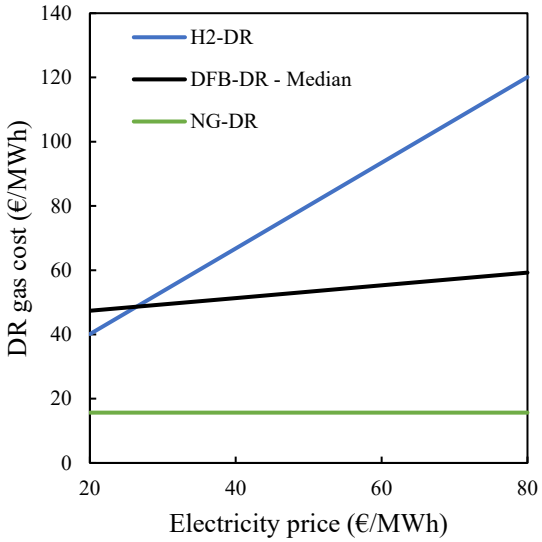

Figure 25. Cost of the reducing gas sent to the DR reactor for the three DR routes, relative to the electricity price. For the DFB-DR route, the biomass price was set at 20 €/MWh.

Figure 26 shows the total production costs for LS for the three DR routes, as well as for the BF-BOF route, as functions of the carbon price, based on an electricity price of 40 €/MWh and biomass price of 20 €/MWh. The carbon price corresponds to both the cost associated with CO_2 emissions and the revenue earned from negative emissions, as described in *Section 8.2.2.1*. The dashed lines in Figure 26 indicate the production costs when there is no accounting for any carbon price.

From Figure 26, it appears that, at the price levels selected for electricity and biomass, the DFB-DR route is more competitive than the H_2-DR route. Even at electricity prices that are low compared with current levels, for instance 20 €/MWh, the DFB-DR route can compete with the H_2-DR route for biomass prices below 10 €/MWh, i.e., if recovered wood is used, which is a likely scenario (not shown in this chapter). In the absence of any carbon price (dashed lines), the DFB-DR route clearly cannot compete with the fossil fuel-based routes. Even when a revenue is associated with negative emissions, the DFB-DR route is not competitive at this biomass price level. It can only compete with the NG-DR route if cheap recovered wood is used (not shown here). As seen in the figure, competing with the fossil fuel routes, in particular the BF-BOF route, requires the introduction of a cost associated with (positive) CO_2 emissions.

The imposition on positive emissions of a carbon price >80 €/tCO_2 enables completion with the BF-BOF route, even without revenue from negative emissions, although carbon prices >100 €/tCO_2 are then required to compete with the NG-DR route. Introducing both a cost and revenue for positive and negative CO_2 emissions (set to be equal here) greatly improves the competitiveness of the DFB-DR route, as shown in Figure 26. At carbon prices >60 €/tCO_2, DFB-DR becomes the most-competitive route. Furthermore, the revenues associated with the biochar and BTX were not included in the production cost of the DFB-DR route. Based on Figure 26, H_2-DR never becomes the most-competitive route. However, more-optimal configurations for the H_2-DR route may exist, such that the differences between the H_2-DR route and the other routes may not be as large as shown here.

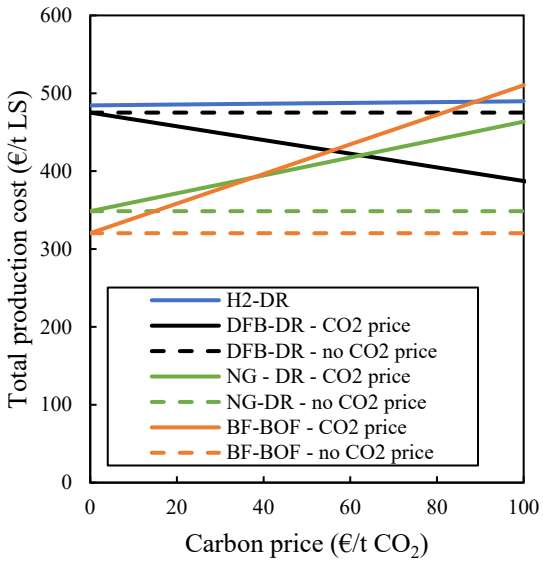

Figure 26. Total production costs of the three DR routes and the BF-BOF route, as a function of the carbon price, assuming that revenues for negative carbon emissions are equal (in €/tCO_2) to the price for emitting CO_2. The assumed prices for biomass and electricity are 20 €/MWh and 40 €/MWh, respectively. For the DFB-DR, NG-DR, and BF-BOF routes, dashed lines represent the total production cost without accounting for a carbon price (revenue or cost).

8.4. A case for the CLG configuration

This analysis presents a case for which the CLG configuration is a natural fit and can offer a competitive and sustainable alternative to well-established technologies. By enabling concentration of the carbon to the gasifier side of the DFB loop, the CLG configuration facilitates the separation of the CO_2, resulting in high negative emissions. As detailed in *Section 2.2.1*, steelmaking slag has been shown to be a suitable oxygen carrier for large-scale chemical-looping and OCAC operations. The use of this material, which is largely a waste that is a challenge to deal with, increases the circularity of the proposed process even further, while overcoming some of the challenges associated with oxygen carriers in CLG. The introduction of the bed reducer in the loop enables the production of a near-pure CO_2 stream, corresponding to 11% of the captured CO_2, while sidestepping the issue of gas oxidation in the fuel reactor.

The proposed system also enables operating under milder conditions than those that are typically envisioned for chemical-looping processes, making for a simpler optimization path. Nevertheless, the choice between separating most of the char and aiming to convert it will be a trade-off between the value of the biochar and that of the steel. It should be noted, however, that achieving complete conversion in the proposed system is challenging and could be counterproductive. Without oxygen transport to the fuel reactor, it is not possible to take advantage of the inhibitor-removal effect of oxygen carriers, which increases the gasification rate (see *Section 1.2.3*). While the circulation rate is decoupled from the oxygen transport thanks to the bed reducer, it remains coupled to the heat transport, so it cannot be readily decreased to increase the fuel residence time. Thus, one can only rely on the temperature and catalytic effects to increase the gasification rate. Increasing the former will increase the heat demand, and thereby the need for top-gas to reduce the bed material. Furthermore, an increase in either temperature or catalytic activity will result in a higher H_2/CO ratio for the raw gas, since both of these factors increase the rate of reforming reactions, which produce more H_2 than CO, and the rate of the WGS, which produces H_2 at the expense of CO. This increase in H_2/CO ratio decreases the

efficiency of the direct reduction step. With this in mind, given that the reduction of the bed material in the bed reducer leads to a bed material with a catalytically active surface, it may be necessary to regulate the overall catalytic activity of the bed to limit the H_2/CO ratio, for instance by diluting the bed with an inert material. As discussed in *Section 7.2*, other factors such as the hydrodynamics of the bed must then be considered.

8.5. Conclusions of the chapter

In this chapter, the DFB gasification technology is shown to have potential to contribute to sustainability in sectors other than the production of carbon-based materials and chemicals. Furthermore, it is shown that, under the appropriate conditions of valorization and penalization of negative and positive CO_2 emissions, respectively, DFB gasification can compete with well-established steelmaking routes, as well as with other emerging routes. This chapter considers many of the aspects permeating this thesis, such as the distribution of the carbon across the different end-products, the use of waste materials, the operation of the DFB process (in this case in the CLG configuration), and the notion of the catalytic activity as an element that may need to be controlled rather than maximized. This chapter also offers a dose of reality to the various aspects of the DFB technology discussed throughout the thesis. By examining the costs associated with the technology and comparing them to existing alternatives, it shows that the aspects discussed are not just intellectually stimulating theoretical considerations, but are actually linked to the real potential of the DFB gasification technology and its various configurations to contribute to the circular economy.

Conclusions

Given that it is a carbon-extraction technology, the potential for carbon recovery of DFB gasification is an essential consideration, the importance of which will only increase in the future. Recovering all the carbon in the regular DFB gasification configuration is challenging, due to the formation of two streams containing diluted CO_2. However, the DFB gasification technology offers a high degree of flexibility in terms of both its design and operation, from which various DFB configurations can be derived. This will enable fine-tuning of the carbon distribution and, thereby, facilitate the complete recovery of carbon. This flexibility makes the DFB gasification technology a valuable technology for the future circular economy, as flexibility will be critical for addressing the complex carbon sources that are biomass and plastic wastes, and for providing a wide range of chemicals, materials, and services.

The flexibility of the DFB gasification technology can be attributed to: (1) separation of the heat production and gasification reactions in two distinct reactors, which create two different atmospheres through which the bed material continuously cycles; and (2) the possibility to use a bed material that has properties that can be leveraged to adjust the carbon distribution. These properties include the direct reaction of the particle with the gas-phase species, which can lead to sorption effects or to oxygen transport, and the indirect catalytic activities towards a wide range of reactions. The catalytic influence of the bed material can be both heterogeneous and homogeneous (through the release of gas-phase ash species), a phenomenon that has been recently supported in the literature. The oxygen transport, the uptake and release of volatile ash species, and, potentially, the formation of catalytic structures are all properties that originate from the cycling of the bed through two distinct atmospheres. Therefore, this is the central factor in the flexibility of the DFB technology.

Design considerations that may affect the carbon distribution include the selection of the two gas atmospheres in the combustor and gasifier, the selection of a bed material with specific properties, and modification of the physical design of the reactors or addition of new elements to the loop. The first aspect can involve the use of pure oxygen as oxidant in the combustor to produce a pure CO_2 stream, thereby greatly facilitating the recovery of CO_2. For the second aspect, catalytic materials can be selected to limit the formation of non-valuable and problematic forms of carbon. A bed that has oxygen transport properties can also be used, to separate inherently the CO_2 from the flue gas and, thereby, concentrate all the carbon in the gasifier. Additional reactors can be installed in the loop to extend the capabilities of the DFB process, for instance to limit the problems caused by oxidation of the gas in the gasifier when an oxygen carrier is used as the bed material. The designs of the combustor and gasifier can also be altered, for instance by adding baffles to control the residence time of the fuel. Finally, the introduction of electrical coils into the loop can partly or entirely cover the heat demand, thereby enabling the concentration of carbon into a single stream.

The operation of the DFB process can also be adjusted to alter the carbon distribution and facilitate complete carbon recovery. Parameters that can be adjusted include the temperature level, the feeding rates of the gases and fuels, and the bed circulation rate. These parameters can be used to alter secondary parameters such as the oxygen transport level, the mixing behavior of the fuel and bed material, and the residence times of solids and gases. However, the interconnectedness of the parameters in a DFB system makes precise control of the carbon distribution by means of parameter adjustment a challenging task. Bed material properties that can be selected for as part of the design of the DFB process can also emerge through interactions with the fuel ash or can be induced using additives. Additives can also be used to alter directly the reactions within the reactors. Predicting and

adjusting the properties of the bed will require a comprehensive understanding of the complex interactions of the bed with the ash and additives, as well as the effects of these interactions on the reactions occurring in the DFB system.

The main goals of this thesis were to gain an understanding of the carbon distribution of the DFB gasification technology and to find ways to adjust this distribution and facilitate the complete recovery of carbon. Several configurations of the DFB gasification process were identified and investigated regarding carbon distribution and potential for carbon recovery. The transport of species by the bed material, in particular of oxygen, and the effects that this transport has on the carbon distribution are central themes of this thesis. The optimization of the operation of DFB gasification processes, *via* the design and selection of operational parameters, is also a major theme. Notably, the operation of the CLG configuration and the associated challenges are extensively discussed. Finally, the possible uses of waste material in DFB gasification are described and analyzed through the lens of their potentials to steer the carbon distribution and facilitate carbon recovery.

The ways in which this thesis contributes to the field of DFB gasification are described below:

- It establishes a formal analysis and comparison of the carbon distributions and possibilities for carbon recovery of some of the DFB gasification configurations. The importance of including the downstream upgrading and synthesis steps in this analysis is shown.

- The recirculation of flue gas coarse ash is demonstrated to be an effective method for enhancing the catalytic activation of the bed. It is recommended that commercial DFB gasifiers should incorporate a flue gas coarse ash storage and be designed to enable continuous ash recirculation, as a means to achieve rapidly the desired activity level during start-up.

- It is demonstrated that, in large-scale DFB gasifiers, oxygen transport properties can emerge in beds that initially lack such properties. The emergence of oxygen transport capabilities can occur through the accumulation of oxygen-carrying ash particles contained in the fuel, as in the case of ASR conversion, or through interactions of the bed particles with biomass ash. The latter is shown for olivine and feldspar, in which cases the oxygen transport develops concurrently with the catalytic activity.

- The conversion of ASR *via* the CLG configuration and using its own ash as oxygen carrier is shown to be possible, provided that a sufficiently high level of oxygen transport can be achieved when full fuel conversion in the gasifier is targeted, or alternatively, provided that the unconverted fraction is separated and valorized. These results provide an indication of how metal-rich rest fractions from intense plastic sorting may behave in a DFB gasifier.

- Oxygen transport is shown to be the main parameter affecting conversion in ASR gasification. The operation of the CLG configuration is extensively discussed based on the results from the conversion of ASR and based on the theoretical carbon distribution of the CLG configuration.

- A potentially viable application for CLG is proposed, whereby the DFB gasification unit provides a reducing gas for the direct reduction of iron ore. This process is shown to be economically viable compared with fossil fuel-based steelmaking routes, but only if carbon prices >60 €/tCO_2 are introduced, with this price corresponding to both the penalty associated

with emitting CO_2 and the revenue obtained from negative emissions. This result shows that the value of DFB gasification is not limited to the production of carbon-based chemicals and materials or biofuels, but that it can also provide negative-emission services to other industries.

Recommendations for future work

Research on the alternative DFB gasification configurations remains limited. While the CLG configuration is attracting growing interest, experimental studies at the pilot and semi-industrial scales remain scarce. The Oxyfuel and Electrical configurations are, for now, only theoretical, and should be investigated, in particular regarding the possibilities to control the process. Similarly, triple-reactor systems warrant in-depth experimental investigations, as they can help overcome challenges with, for instance, the CLG configuration, although they will also likely increase the complexity of controlling the process.

When evaluating applications for the various DFB gasification configurations, their integration into industries other than those typically considered for gasification, i.e., other than systems for the production of chemicals, materials or biofuels, should be explored. This could uncover other areas in which DFB gasification could contribute to circularity and sustainability and drive forward the development of the technology.

The mechanisms through which bed materials develop oxygen transport properties should be investigated, to be able to limit this development when it is not desired, or, conversely, to intensify it if it is deemed beneficial. The role of volatile ash species in the development of oxygen transport capability should be further explored. More generally, the interactions of the ash layer with the gas phase in both reactors need to be elucidated, to control more effectively the balance and impacts of active species in the system. A greater understanding and control of these phenomena would enable more stringent control of the carbon distribution.

Conversion of waste carbon sources through DFB gasification should be further investigated, through experiments both with model compounds to study the mechanisms of decomposition of polymers and with real-world mixed plastic wastes to learn to address the challenges that they engender. Additional ways of using waste in the DFB gasification process should also be investigated, and other waste streams should be considered for the applications discussed in this thesis.

References

1. Masson-Delmotte, V.; Zhai, P.; Pörtner, H.-O.; Roberts, D.; Skea, J.; Shukla, P.R.; Pirani, A.; Moufouma-Okia, W.; Péan, C.; Pidcock, R.; et al. *Global warming of 1.5°C An IPCC Special Report*; 2018; ISBN 9789291691517.

2. Van Buren, N.; Demmers, M.; Van der Heijden, R.; Witlox, F. Towards a Circular Economy: The Role of Dutch Logistics Industries and Governments. *Sustain.* 2016, *8*.

3. Kirchherr, J.; Reike, D.; Hekkert, M. Conceptualizing the circular economy: An analysis of 114 definitions. *Resour. Conserv. Recycl.* 2017.

4. Nuffield Council on Bioethics *Biofuels: ethical issues*; 2011;

5. Jambeck, J.R.; Geyer, R.; Wilcox, C.; Siegler, T.R.; Perryman, M.; Andrady, A.; Narayan, R.; Law, K.L. Plastic waste inputs from land into the ocean. *Science (80-.).* **2015**, doi:10.1126/science.1260352.

6. Ragaert, K.; Delva, L.; Van Geem, K. Mechanical and chemical recycling of solid plastic waste. *Waste Manag.* **2017**, *69*.

7. Ambrogi, V.; Carfagna, C.; Cerruti, P.; Marturano, V. Additives in Polymers. In *Modification of Polymer Properties*; William Andrew Publishing, 2017; pp. 87–108 ISBN 9780323443531.

8. Maric, J.; Berdugo Vilches, T.; Pissot, S.; Cañete Vela, I.; Gyllenhammar, M.; Seemann, M. Emissions of dioxins and furans during steam gasification of Automotive Shredder residue; experiences from the Chalmers 2–4-MW indirect gasifier. *Waste Manag.* **2020**, *102*, 114–121, doi:10.1016/J.WASMAN.2019.10.037.

9. Kirnbauer, F.; Koch, M.; Koch, R.; Aichernig, C.; Hofbauer, H. Behavior of inorganic matter in a dual fluidized steam gasification plant. *Energy and Fuels* **2013**, *27*, 3316–3331, doi:10.1021/ef400598h.

10. Kuba, M.; Kraft, S.; Kirnbauer, F.; Maierhans, F.; Hofbauer, H. Influence of controlled handling of solid inorganic materials and design changes on the product gas quality in dual fluid bed gasification of woody biomass. *Appl. Energy* **2018**, *210*, 230–240, doi:10.1016/j.apenergy.2017.11.028.

11. Thunman, H.; Seemann, M.; Berdugo Vilches, T.; Maric, J.; Pallares, D.; Ström, H.; Berndes, G.; Knutsson, P.; Larsson, A.; Breitholtz, C.; et al. Advanced biofuel production via gasification – lessons learned from 200 man-years of research activity with Chalmers' research gasifier and the GoBiGas demonstration plant. *Energy Sci. Eng.* **2018**, *6*, 6–34, doi:10.1002/ese3.188.

12. Paethanom, A. Twin IHI Gasifier (TIGAR ®)- current status of Indonesian demonstration project and its business plan. In Proceedings of the Gasification and Syngas Technologies Conference; Vancouver, BC, 2016.

13. Maric, J.; Berdugo Vilches, T.; Thunman, H.; Gyllenhammar, M.; Seemann, M. Valorization of Automobile Shredder Residue Using Indirect Gasification. *Energy & Fuels* **2018**, *32*, 12795–12804, doi:10.1021/acs.energyfuels.8b02526.

14. Benedikt, F.; Schmid, J.C.; Fuchs, J.; Mauerhofer, A.M.; Müller, S.; Hofbauer, H. Fuel flexible gasification with an advanced 100 kW dual fluidized bed steam gasification pilot plant. *Energy* **2018**, *164*, 329–343, doi:10.1016/J.ENERGY.2018.08.146.

15. Wilk, V.; Hofbauer, H. Conversion of mixed plastic wastes in a dual fluidized bed steam gasifier. *Fuel* **2013**, *107*, 787–799, doi:https://doi.org/10.1016/j.fuel.2013.01.068.

16. Wilk, V.; Hofbauer, H. Co-gasification of plastics and biomass in a dual fluidized-bed steam gasifier: Possible interactions of fuels. *Energy and Fuels* **2013**, *27*, 3261–3273, doi:10.1021/ef400349k.

17. Berdugo Vilches, T.; Marinkovic, J.; Seemann, M.; Thunman, H. Comparing Active Bed Materials in a Dual Fluidized Bed Biomass Gasifier: Olivine, Bauxite, Quartz-Sand, and Ilmenite. *Energy & Fuels* **2016**, *30*, 4848–4857.

18. Marinkovic, J.; Seemann, M.; Schwebel, G.L.; Thunman, H. Impact of Biomass Ash–Bauxite Bed Interactions on an Indirect Biomass Gasifier. *Energy & Fuels* **2016**, *30*, 4044–4052.

19. Berguerand, N.; Berdugo Vilches, T. Alkali-Feldspar as a Catalyst for Biomass Gasification in a 2-MW Indirect Gasifier. *Energy & Fuels* **2017**, *31*, 1583–1592, doi:10.1021/acs.energyfuels.6b02312.

20. Alamia, A.; Larsson, A.; Breitholtz, C.; Thunman, H. Performance of large-scale biomass gasifiers in a biorefinery,

a state-of-the-art reference. *Int. J. Energy Res.* **2017**, *41*, 2001–2019, doi:10.1002/er.3758.

21. Lind, F. Design and Operation of a Chemical-Looping Reformer for Catalytic Upgrading of Biomass-Derived Gas, Chalmers University of Technology, 2013.

22. Berdugo Vilches, T. Operational strategies to control the gas composition in dual fluidized bed biomass gasifiers, Chalmers University of Technology, 2018.

23. Thunman, H.; Berdugo Vilches, T.; Seemann, M.; Maric, J.; Vela, I.C.; Pissot, S.; Nguyen, H.N.T. Circular use of plastics-transformation of existing petrochemical clusters into thermochemical recycling plants with 100% plastics recovery. *Sustain. Mater. Technol.* **2019**, *22*, e00124, doi:10.1016/j.susmat.2019.e00124.

24. Robert, A.M. UOP/HYDRO MTO PROCESS. In *Handbook of Petrochemicals Production Processes*; McGraw Hill Professional, 2004.

25. Milne, T.A.; Evans, R.J.; Abatzoglou, N. *Biomass Gasifier "Tars": Their Nature, Formation, and Conversion*; Golden, CO, 1998;

26. Baker, E.G.; Brown, M.D.; Elliott, D.C.; Mudge, L.K. CHARACTERIZATION AND TREATMENT OF TARS FROM BIOMASS GASIFIERS. In Proceedings of the AIChE 1988 Summer National Meeting; Denver, Colorado, 1988.

27. Li, C.; Suzuki, K. Tar property, analysis, reforming mechanism and model for biomass gasification—An overview. *Renew. Sustain. Energy Rev.* **2009**, *13*, 594–604, doi:https://doi.org/10.1016/j.rser.2008.01.009.

28. Larsson, A.; Kuba, M.; Berdugo Vilches, T.; Seemann, M.; Hofbauer, H.; Thunman, H. Steam gasification of biomass – Typical gas quality and operational strategies derived from industrial-scale plants. *Fuel Process. Technol.* **2021**, *212*, 106609, doi:10.1016/j.fuproc.2020.106609.

29. Marinkovic, J. Choice of bed material : a critical parameter in the optimization of dual fluidized bed systems, Chalmers University of Technology, 2016.

30. Bramer, E.A. Chapter 2 - Flue Gas Emissions from Fluidized Bed Combustion. In *Atmospheric Fluidized Bed Coal Combustion*; Valk, M.B.T.-C.S. and T., Ed.; Elsevier, 1995; Vol. 22, pp. 51–103 ISBN 0167-9449.

31. Anthony, E.J.; Granatstein, D.L. Sulfation phenomena in fluidized bed combustion systems. *Prog. Energy Combust. Sci.* **2001**, *27*, 215–236, doi:10.1016/S0360-1285(00)00021-6.

32. Kaminsky, W. The Hamburg Fluidized-bed Pyrolysis Process to Recycle Polymer Wastes and Tires. In *Feedstock Recycling and Pyrolysis of Waste Plastics. Converting Waste Plastics into Diesel and Other Fuels.*; Scheirs, J., Kaminsky, W., Eds.; Wiley, 2006; pp. 475–491.

33. Kaminsky, W.; Kim, J.-S. Pyrolysis of mixed plastics into aromatics. *J. Anal. Appl. Pyrolysis* **1999**, *51*, 127–134, doi:https://doi.org/10.1016/S0165-2370(99)00012-1.

34. Delgado, J.; P. Aznar, M.; Corella, J. Biomass Gasification with Steam in Fluidized Bed: Effectiveness of CaO, MgO, and CaO−MgO for Hot Raw Gas Cleaning. *Ind. & Eng. Chem. Res.* **1997**, *36*, 1535–1543, doi:10.1021/ie960273w.

35. Kern, S.; Pfeifer, C.; Hofbauer, H. Reactivity tests of the water–gas shift reaction on fresh and used fluidized bed materials from industrial DFB biomass gasifiers. *Biomass and Bioenergy* **2013**, *55*, 227–233, doi:10.1016/J.BIOMBIOE.2013.02.001.

36. Sutton, D.; Kelleher, B.; Ross, J.R.H. Review of literature on catalysts for biomass gasification. *Fuel Process. Technol.* **2001**, *73*, 155–173, doi:10.1016/S0378-3820(01)00208-9.

37. Devi, L.; Ptasinski, K.J.; Janssen, F.J.J.. A review of the primary measures for tar elimination in biomass gasification processes. *Biomass and Bioenergy* **2003**, *24*, 125–140, doi:10.1016/S0961-9534(02)00102-2.

38. Arnold, R.A.; Hill, J.M. Catalysts for gasification: a review. *Sustain. Energy Fuels* **2019**, *3*, 656–672, doi:10.1039/C8SE00614H.

39. Rapagnà, S.; Jand, N.; Kiennemann, A.; Foscolo, P.U. Steam-gasification of biomass in a fluidised-bed of olivine particles. *Biomass and Bioenergy* **2000**, *19*, 187–197, doi:https://doi.org/10.1016/S0961-9534(00)00031-3.

40. Grimm, A.; Öhman, M.; Lindberg, T.; Fredriksson, A.; Boström, D. Bed Agglomeration Characteristics in

Fluidized-Bed Combustion of Biomass Fuels Using Olivine as Bed Material. *Energy & Fuels* **2012**, *26*, 4550–4559, doi:10.1021/ef300569n.

41. Rauch, R.; Bosch, K.; Hofbauer, H.; Świerczyński, D.; Courson, C. Comparison of different olivines for biomass steam gasification. In Proceedings of the Science in Thermal and Chemical Biomass Conversion; 2004.

42. Devi, L.; Craje, M.; Thüne, P.; Ptasinski, K.J.; Janssen, F.J.J.G. Olivine as tar removal catalyst for biomass gasifiers: Catalyst characterization. *Appl. Catal. A Gen.* **2005**, *294*, 68–79, doi:https://doi.org/10.1016/j.apcata.2005.07.044.

43. Devi, L.; Ptasinski, K.J.; Janssen, F.J.J.G. Pretreated olivine as tar removal catalyst for biomass gasifiers: investigation using naphthalene as model biomass tar. *Fuel Process. Technol.* **2005**, *86*, 707–730, doi:https://doi.org/10.1016/j.fuproc.2004.07.001.

44. Świerczyński, D.; Courson, C.; Bedel, L.; Kiennemann, A.; Vilminot, S. Oxidation Reduction Behavior of Iron-Bearing Olivines (FexMg1-x)2SiO4 Used as Catalysts for Biomass Gasification. *Chem. Mater.* **2006**, *18*, 897–905, doi:10.1021/cm051433+.

45. Fredriksson, H.O.A.; Lancee, R.J.; Thüne, P.C.; Veringa, H.J.; Niemantsverdriet, J.W. (Hans) Olivine as tar removal catalyst in biomass gasification: Catalyst dynamics under model conditions. *Appl. Catal. B Environ.* **2013**, *130–131*, 168–177, doi:https://doi.org/10.1016/j.apcatb.2012.10.017.

46. Kuhn, J.N.; Zhao, Z.; Felix, L.G.; Slimane, R.B.; Choi, C.W.; Ozkan, U.S. Olivine catalysts for methane- and tar-steam reforming. *Appl. Catal. B Environ.* **2008**, *81*, 14–26, doi:https://doi.org/10.1016/j.apcatb.2007.11.040.

47. Constantinou, D.A.; Fierro, J.L.G.; Efstathiou, A.M. A comparative study of the steam reforming of phenol towards H2 production over natural calcite, dolomite and olivine materials. *Appl. Catal. B Environ.* **2010**, *95*, 255–269, doi:https://doi.org/10.1016/j.apcatb.2010.01.003.

48. Koppatz, S.; Pröll, T.; Pfeifer, C.; Hofbauer, H. INVESTIGATION OF REFORMING ACTIVITY AND OXYGEN TRANSFER OF OLIVINE IN A DUAL CIRCULATING FLUIDISED BED SYSTEM WITH REGARD TO BIOMASS GASIFICATION. In Proceedings of the The 13th International Conference on Fluidization - New Paradigm in Fluidization Engineering; 2010.

49. Wen, W.-Y. Mechanisms of Alkali Metal Catalysis in the Gasification of Coal, Char, or Graphite. *Catal. Rev.* **1980**, *22*, 1–28, doi:10.1080/03602458008066528.

50. McKee, D.W. Mechanisms of the alkali metal catalysed gasification of carbon. *Fuel* **1983**, *62*, 170–175, doi:10.1016/0016-2361(83)90192-8.

51. Amenomiya, Y.; Pleizier, G. Alkali-promoted alumina catalysts: II. Water-gas shift reaction. *J. Catal.* **1982**, *76*, 345–353, doi:10.1016/0021-9517(82)90265-2.

52. Abu El-Rub, Z.; Bramer, E.A.; Brem, G. Review of Catalysts for Tar Elimination in Biomass Gasification Processes. *Ind. Eng. Chem. Res.* **2004**, *43*, 6911–6919, doi:10.1021/ie0498403.

53. Öhman, M.; Pommer, L.; Nordin, A. Bed agglomeration characteristics and mechanisms during gasification and combustion of biomass fuels. *Energy and Fuels* **2005**, *19*, 1742–1748, doi:10.1021/ef040093w.

54. Niu, Y.; Tan, H.; Hui, S. Ash-related issues during biomass combustion: Alkali-induced slagging, silicate melt-induced slagging (ash fusion), agglomeration, corrosion, ash utilization, and related countermeasures. *Prog. Energy Combust. Sci.* **2016**, *52*, 1–61, doi:10.1016/j.pecs.2015.09.003.

55. Gatternig, B.; Karl, J. Investigations on the mechanisms of ash-induced agglomeration in fluidized-bed combustion of biomass. *Energy and Fuels* **2015**, *29*, 931–941, doi:10.1021/ef502658b.

56. He, H.; Boström, D.; Öhman, M. Time Dependence of Bed Particle Layer Formation in Fluidized Quartz Bed Combustion of Wood-Derived Fuels. *Energy & Fuels* **2014**, *28*, 3841–3848, doi:10.1021/ef500386k.

57. He, H.; Ji, X.; Boström, D.; Backman, R.; Öhman, M. Mechanism of Quartz Bed Particle Layer Formation in Fluidized Bed Combustion of Wood-Derived Fuels. *Energy & Fuels* **2016**, *30*, 2227–2232, doi:10.1021/acs.energyfuels.5b02891.

58. Faust, R.; Berdugo Vilches, T.; Malmberg, P.; Seemann, M.; Knutsson, P. Comparison of Ash Layer Formation Mechanisms on Si-Containing Bed Material during Dual Fluidized Bed Gasification of Woody Biomass. *Energy & Fuels* **2020**, *34*, 8340–8352, doi:10.1021/acs.energyfuels.0c00509.

59. Kirnbauer, F.; Hofbauer, H. The mechanism of bed material coating in dual fluidized bed biomass steam gasification plants and its impact on plant optimization. *Powder Technol.* **2013**, *245*, 94–104, doi:10.1016/j.powtec.2013.04.022.

60. Kuba, M.; He, H.; Kirnbauer, F.; Skoglund, N.; Boström, D.; Öhman, M.; Hofbauer, H. Mechanism of Layer Formation on Olivine Bed Particles in Industrial-Scale Dual Fluid Bed Gasification of Wood. *Energy & Fuels* **2016**, *30*, 7410–7418, doi:10.1021/acs.energyfuels.6b01522.

61. Marinkovic, J.; Thunman, H.; Knutsson, P.; Seemann, M. Characteristics of olivine as a bed material in an indirect biomass gasifier. *Chem. Eng. J.* **2015**, *279*, 555–566, doi:10.1016/j.cej.2015.05.061.

62. Faust, R.; Sattari, M.; Maric, J.; Seemann, M.; Knutsson, P. Microscopic investigation of layer growth during olivine bed material aging during indirect gasification of biomass. *Fuel* **2020**, *266*, 117076, doi:https://doi.org/10.1016/j.fuel.2020.117076.

63. He, H.; Skoglund, N.; Öhman, M. Time-Dependent Layer Formation on K-Feldspar Bed Particles during Fluidized Bed Combustion of Woody Fuels. *Energy & Fuels* **2017**, *31*, 12848–12856, doi:10.1021/acs.energyfuels.7b02386.

64. Wagner, K.; Häggström, G.; Skoglund, N.; Priscak, J.; Kuba, M.; Öhman, M.; Hofbauer, H. Layer formation mechanism of K-feldspar in bubbling fluidized bed combustion of phosphorus-lean and phosphorus-rich residual biomass. *Appl. Energy* **2019**, *248*, 545–554, doi:10.1016/J.APENERGY.2019.04.112.

65. Faust, R.; Hannl, T.K.; Vilches, T.B.; Kuba, M.; Öhman, M.; Seemann, M.; Knutsson, P. Layer Formation on Feldspar Bed Particles during Indirect Gasification of Wood. 1. K-Feldspar. *Energy & Fuels* **2019**, *33*, 7321–7332, doi:10.1021/acs.energyfuels.9b01291.

66. Hannl, T.K.; Faust, R.; Kuba, M.; Knutsson, P.; Berdugo Vilches, T.; Seemann, M.; Öhman, M. Layer Formation on Feldspar Bed Particles during Indirect Gasification of Wood. 2. Na-Feldspar. *Energy & Fuels* **2019**, *33*, 7333–7346, doi:10.1021/acs.energyfuels.9b01292.

67. Kuba, M.; Havlik, F.; Kirnbauer, F.; Hofbauer, H. Influence of bed material coatings on the water-gas-shift reaction and steam reforming of toluene as tar model compound of biomass gasification. *Biomass and Bioenergy* **2016**, *89*, 40–49, doi:10.1016/J.BIOMBIOE.2015.11.029.

68. Kuba, M.; Kirnbauer, F.; Hofbauer, H. Influence of coated olivine on the conversion of intermediate products from decomposition of biomass tars during gasification. *Biomass Convers. Biorefinery* **2017**, *7*, 11–21, doi:10.1007/s13399-016-0204-z.

69. Berdugo Vilches, T.; Seemann, M.; Thunman, H. Influence of In-Bed Catalysis by Ash-Coated Olivine on Tar Formation in Steam Gasification of Biomass. *Energy & Fuels* **2018**, *32*, 9592–9604, doi:10.1021/acs.energyfuels.8b02153.

70. Umeki, K.; Häggström, G.; Bach-Oller, A.; Kirtania, K.; Furusjö, E. Reduction of Tar and Soot Formation from Entrained-Flow Gasification of Woody Biomass by Alkali Impregnation. *Energy & Fuels* **2017**, *31*, 5104–5110, doi:10.1021/acs.energyfuels.6b03480.

71. Bach-Oller, A.; Furusjö, E.; Umeki, K. On the role of potassium as a tar and soot inhibitor in biomass gasification. *Appl. Energy* **2019**, *254*, 113488, doi:https://doi.org/10.1016/j.apenergy.2019.113488.

72. Berdugo Vilches, T.; Maric, J.; Knutsson, P.; Rosenfeld, D.C.; Thunman, H.; Seemann, M. Bed material as a catalyst for char gasification: The case of ash-coated olivine activated by K and S addition. *Fuel* **2018**, *224*, 85–93, doi:10.1016/J.FUEL.2018.03.079.

73. Knutsson, P.; Cantatore, V.; Seemann, M.; Tam, P.L.; Panas, I. Role of potassium in the enhancement of the catalytic activity of calcium oxide towards tar reduction. *Appl. Catal. B Environ.* **2018**, *229*, 88–95, doi:10.1016/J.APCATB.2018.02.002.

74. Cho, P. Development and Characterisation of Oxygen-Carrier Materials for Chemical-Looping Combustion, Chalmers University of Technology, 2005.

75. Larsson, A.; Israelsson, M.; Lind, F.; Seemann, M.; Thunman, H. Using ilmenite to reduce the tar yield in a dual fluidized bed gasification system. *Energy and Fuels* **2014**, *28*, 2632–2644, doi:10.1021/ef500132p.

76. Berdugo Vilches, T.; Thunman, H. Experimental Investigation of Volatiles–Bed Contact in a 2–4 MWth Bubbling Bed Reactor of a Dual Fluidized Bed Gasifier. *Energy & Fuels* **2015**, *29*, 6456–6464,

doi:10.1021/acs.energyfuels.5b01303.

77. Mattisson, T.; Lyngfelt, A.; Leion, H. Chemical-looping with oxygen uncoupling for combustion of solid fuels. *Int. J. Greenh. Gas Control* **2009**, *3*, 11–19, doi:10.1016/J.IJGGC.2008.06.002.

78. Keller, M.; Leion, H.; Mattisson, T.; Lyngfelt, A. Gasification inhibition in chemical-looping combustion with solid fuels. *Combust. Flame* **2011**, *158*, 393–400, doi:10.1016/j.combustflame.2010.09.009.

79. Leion, H.; Mattisson, T.; Lyngfelt, A. Solid fuels in chemical-looping combustion. *Int. J. Greenh. Gas Control* **2008**, *2*, 180–193, doi:10.1016/S1750-5836(07)00117-X.

80. Bayarsaikhan, B.; Sonoyama, N.; Hosokai, S.; Shimada, T.; Hayashi, J.I.; Li, C.Z.; Chiba, T. Inhibition of steam gasification of char by volatiles in a fluidized bed under continuous feeding of a brown coal. *Fuel* **2006**, *85*, 340–349, doi:10.1016/j.fuel.2005.06.001.

81. Fushimi, C.; Wada, T.; Tsutsumi, A. Inhibition of steam gasification of biomass char by hydrogen and tar. *Biomass and Bioenergy* **2011**, *35*, 179–185, doi:10.1016/j.biombioe.2010.08.017.

82. Lundberg, L. Solid Fuel Conversion in Dual Fluidized Bed Gasification - Modelling and Experiments, Chalmers University of Technology, 2018.

83. Fuchs, J.; Schmid, J.C.; Müller, S.; Hofbauer, H. Dual fluidized bed gasification of biomass with selective carbon dioxide removal and limestone as bed material: A review. *Renew. Sustain. Energy Rev.* **2019**, *107*, 212–231, doi:10.1016/j.rser.2019.03.013.

84. Mattisson, T.; Keller, M.; Linderholm, C.; Moldenhauer, P.; Rydén, M.; Leion, H.; Lyngfelt, A. Chemical-looping technologies using circulating fluidized bed systems: Status of development. *Fuel Process. Technol.* **2018**, *172*, 1–12, doi:10.1016/j.fuproc.2017.11.016.

85. Fan, L.-S.; Zeng, L.; Wang, W.; Luo, S. Chemical looping processes for CO2 capture and carbonaceous fuel conversion – prospect and opportunity. *Energy Environ. Sci.* **2012**, *5*, 7254–7280, doi:10.1039/C2EE03198A.

86. Kramp, M.; Thon, A.; Hartge, E.U.; Heinrich, S.; Werther, J. Carbon Stripping - A Critical Process Step in Chemical Looping Combustion of Solid Fuels. *Chem. Eng. Technol.* **2012**, *35*, 497–507, doi:10.1002/ceat.201100438.

87. Bruni, G.; Solimene, R.; Marzocchella, A.; Salatino, P.; Yates, J.G.; Lettieri, P.; Fiorentino, M. Self-segregation of high-volatile fuel particles during devolatilization in a fluidized bed reactor. *Powder Technol.* **2002**, *128*, 11–21, doi:10.1016/S0032-5910(02)00149-3.

88. Cuadrat, A.; Abad, A.; Adánez, J.; de Diego, L.F.; García-Labiano, F.; Gayán, P. Behavior of ilmenite as oxygen carrier in chemical-looping combustion. *Fuel Process. Technol.* **2012**, *94*, 101–112, doi:https://doi.org/10.1016/j.fuproc.2011.10.020.

89. Abad, A.; Adánez, J.; Cuadrat, A.; García-Labiano, F.; Gayán, P.; de Diego, L.F. Kinetics of redox reactions of ilmenite for chemical-looping combustion. *Chem. Eng. Sci.* **2011**, *66*, 689–702, doi:https://doi.org/10.1016/j.ces.2010.11.010.

90. Mei, D.; Mendiara, T.; Abad, A.; de Diego, L.F.; García-Labiano, F.; Gayán, P.; Adánez, J.; Zhao, H. Evaluation of Manganese Minerals for Chemical Looping Combustion. *Energy & Fuels* **2015**, *29*, 6605–6615, doi:10.1021/acs.energyfuels.5b01293.

91. Adánez, J.; Abad, A.; Mendiara, T.; Gayán, P.; de Diego, L.F.; García-Labiano, F. Chemical looping combustion of solid fuels. *Prog. Energy Combust. Sci.* **2018**, *65*, 6–66, doi:10.1016/J.PECS.2017.07.005.

92. Di Blasi, C.; Branca, C.; Santoro, A.; Gonzalez Hernandez, E. Pyrolytic behavior and products of some wood varieties. *Combust. Flame* **2001**, *124*, 165–177, doi:https://doi.org/10.1016/S0010-2180(00)00191-7.

93. Di Blasi, C. Combustion and gasification rates of lignocellulosic chars. *Prog. Energy Combust. Sci.* **2009**, *35*, 121–140, doi:https://doi.org/10.1016/j.pecs.2008.08.001.

94. Vermeulen, I.; Van Caneghem, J.; Block, C.; Baeyens, J.; Vandecasteele, C. Automotive shredder residue (ASR): Reviewing its production from end-of-life vehicles (ELVs) and its recycling, energy or chemicals' valorisation. *J. Hazard. Mater.* **2011**, *190*, 8–27, doi:10.1016/J.JHAZMAT.2011.02.088.

95. Buekens, A.; Zhou, X. Recycling plastics from automotive shredder residues: A review. *J. Mater. Cycles Waste*

Manag. **2014**, *16*, 398–414, doi:10.1007/s10163-014-0244-z.

96. Zevenhoven, R.; Saeed, L. *Automotive shredder residue (ASR) and compact disc (CD) waste : options for recovery of materials and energy*; 2003;

97. Harder, M.K.; Forton, O.T. A critical review of developments in the pyrolysis of automotive shredder residue. *J. Anal. Appl. Pyrolysis* **2007**, *79*, 387–394, doi:10.1016/J.JAAP.2006.12.015.

98. Directive 2000/53/EC of the European Parliament and of the Council of 18 September 2000 on end-of life vehicles Available online: http://data.europa.eu/eli/dir/2000/53/oj.

99. *Implementing Plastic and Polymer Composite Lightweighting Solutions to Meet 2025 Corporate Average Fuel Economy Standards*; 2015;

100. Morselli, L.; Santini, A.; Passarini, F.; Vassura, I. Automotive shredder residue (ASR) characterization for a valuable management. *Waste Manag.* **2010**, *30*, 2228–2234, doi:10.1016/J.WASMAN.2010.05.017.

101. Pasel, C.; Wanzl, W. Experimental investigations on reactor scale-up and optimisation of product quality in pyrolysis of shredder waste. *Fuel Process. Technol.* **2003**, *80*, 47–67, doi:10.1016/S0378-3820(02)00187-X.

102. Lanoir, D.; Trouvé, G.; Delfosse, L.; Froelich, D.; Kassamaly, A. PHYSICAL AND CHEMICAL CHARACTERIZATION OF AUTOMOTIVE SHREDDER RESIDUES. *Waste Manag. Res.* **1997**, *15*, 267–276, doi:10.1006/WMRE.1996.0083.

103. Sakai, S.; Noma, Y.; Kida, A. End-of-life vehicle recycling and automobile shredder residue management in Japan. *J. Mater. Cycles Waste Manag.* **2007**, *9*, 151–158, doi:10.1007/s10163-007-0180-2.

104. Brand, A.S.; Fanijo, E.O. A review of the influence of steel furnace slag type on the properties of cementitious composites. *Appl. Sci.* **2020**, *10*, 1–27, doi:10.3390/app10228210.

105. Remus, R.; Roudier, S.; Aguado-Monsonet, M.A.; Delgado Sancho, L. *Best available techniques - iron and steel production*; 2013; ISBN 9789279264757.

106. Yildirim, I.Z.; Prezzi, M. Chemical, mineralogical, and morphological properties of steel slag. *Adv. Civ. Eng.* **2011**, *2011*, doi:10.1155/2011/463638.

107. Tossavainen, M.; Engstrom, F.; Yang, Q.; Menad, N.; Lidstrom Larsson, M.; Bjorkman, B. Characteristics of steel slag under different cooling conditions. *Waste Manag.* **2007**, *27*, 1335–1344, doi:10.1016/J.WASMAN.2006.08.002.

108. Chand, S.; Paul, B.; Kumar, M. Sustainable Approaches For Ld Slag Waste Management In Steel Industries : A Review. **2016**, *60*, 116–128, doi:10.1007/s11015-016-0261-3.

109. Das, B.; Prakash, S.; Reddy, P.S.R.; Misra, V.N. An overview of utilization of slag and sludge from steel industries. *Resour. Conserv. Recycl.* **2007**, *50*, 40–57, doi:10.1016/j.resconrec.2006.05.008.

110. Rydén, M.; Hanning, M.; Lind, F. Oxygen Carrier Aided Combustion (OCAC) of Wood Chips in a 12 MWth Circulating Fluidized Bed Boiler Using Steel Converter Slag as Bed Material. *Appl. Sci.* 2018, *8*.

111. Keller, M.; Leion, H.; Mattisson, T.; Thunman, H. Investigation of Natural and Synthetic Bed Materials for Their Utilization in Chemical Looping Reforming for Tar Elimination in Biomass-Derived Gasification Gas. *Energy & Fuels* **2014**, *28*, 3833–3840, doi:10.1021/ef500369c.

112. Mattison, T.; Hildor, F.; Li, Y.; Linderholm, C. Negative emissions of carbon dioxide through chemical-looping combustion (CLC) and gasification (CLG) using oxygen carriers based on manganese and iron. *Mitig. Adapt. Strateg. Glob. Chang.* **2019**, doi:10.1007/s11027-019-09860-x.

113. Xu, L.; Schwebel, G.L.; Knutsson, P.; Leion, H.; Li, Z.; Cai, N. Performance of Industrial Residues as Low Cost Oxygen Carriers. *Energy Procedia* **2017**, *114*, 361–370, doi:10.1016/J.EGYPRO.2017.03.1178.

114. Thunman, H.; Lind, F.; Breitholtz, C.; Berguerand, N.; Seemann, M. Using an oxygen-carrier as bed material for combustion of biomass in a 12-MWth circulating fluidized-bed boiler. *Fuel* **2013**, *113*, 300–309, doi:10.1016/J.FUEL.2013.05.073.

115. Hildor, F.; Mattisson, T.; Leion, H.; Linderholm, C.; Rydén, M. Steel converter slag as an oxygen carrier in a 12 MWth CFB boiler – Ash interaction and material evolution. *Int. J. Greenh. Gas Control* **2019**, *88*, 321–331,

doi:10.1016/J.IJGGC.2019.06.019.

116. Hildor, F.; Leion, H.; Linderholm, C.J.; Mattisson, T. Steel converter slag as an oxygen carrier for chemical-looping gasification. *Fuel Process. Technol.* **2020**, *210*, 106576, doi:https://doi.org/10.1016/j.fuproc.2020.106576.

117. Pissot, S.; Berdugo Vilches, T.; Maric, J.; Seemann, M. Chemical looping gasification in a 2-4 MWth dual fluidized bed gasifier. In Proceedings of the 23rd International Conference on Fluidized Bed Conversion; Seoul, Korea, 2018.

118. Gómez-Barea, A.; Vilches, L.F.; Leiva, C.; Campoy, M.; Fernández-Pereira, C. Plant optimisation and ash recycling in fluidised bed waste gasification. *Chem. Eng. J.* **2009**, *146*, 227–236, doi:10.1016/j.cej.2008.05.039.

119. Pels, J.R.; Nie, D.S. De Utilization of ashes from biomass combustion and gasification. In Proceedings of the 14th European Biomass Conference and Exhibition; 2005; pp. 17–21.

120. Nieminen, M.; Hiltunen, M.; Pels, J.; Barea, A.G.; Isotalo, J.; Vesanto, P.; Spanjers, M.; Barnes, I.; Oy, W.E.; Box, P.O. GASASH – The improvement of the economics of biomass / waste gasification by higher carbon conversion and advanced ash management.

121. James, A.K.; Thring, R.W.; Helle, S.; Ghuman, H.S. Ash management review-applications of biomass bottom ash. *Energies* **2012**, *5*, 3856–3873, doi:10.3390/en5103856.

122. Larsson, A.; Seemann, M.; Neves, D.; Thunman, H. Evaluation of Performance of Industrial-Scale Dual Fluidized Bed Gasifiers Using the Chalmers 2–4-MWth Gasifier. *Energy & Fuels* **2013**, *27*, 6665–6680, doi:10.1021/ef400981j.

123. Israelsson, M.; Seemann, M.; Thunman, H. Assessment of the solid-phase adsorption method for sampling biomass-derived tar in industrial environments. *Energy and Fuels* **2013**, *27*, 7569–7578, doi:10.1021/ef401893j.

124. Israelsson, M.; Larsson, A.; Thunman, H. Online Measurement of Elemental Yields, Oxygen Transport, Condensable Compounds, and Heating Values in Gasification Systems. *Energy & Fuels* **2014**, *28*, 5892–5901, doi:10.1021/ef501433n.

125. Alamia, A.; Thunman, H.; Seemann, M. Process Simulation of Dual Fluidized Bed Gasifiers Using Experimental Data. *Energy & Fuels* **2016**, *30*, 4017–4033, doi:10.1021/acs.energyfuels.6b00122.

126. Lundberg, L.; Tchoffor, P.A.; Pallarès, D.; Johansson, R.; Thunman, H.; Davidsson, K. Influence of surrounding conditions and fuel size on the gasification rate of biomass char in a fluidized bed. *Fuel Process. Technol.* **2016**, *144*, 323–333, doi:https://doi.org/10.1016/j.fuproc.2016.01.002.

127. Bui, M.; Adjiman, C.S.; Bardow, A.; Anthony, E.J.; Boston, A.; Brown, S.; Fennell, P.S.; Fuss, S.; Galindo, A.; Hackett, L.A.; et al. Carbon capture and storage (CCS): The way forward. *Energy Environ. Sci.* 2018.

128. Garðarsdóttir, S.Ó.; Normann, F.; Andersson, K.; Johnsson, F. Postcombustion CO2 Capture Using Monoethanolamine and Ammonia Solvents: The Influence of CO2 Concentration on Technical Performance. *Ind. Eng. Chem. Res.* **2015**, *54*, 681–690, doi:10.1021/ie503852m.

129. Lancee, R.J.; Dugulan, A.I.; Thüne, P.C.; Veringa, H.J.; Niemantsverdriet, J.W.; Fredriksson, H.O.A. Chemical looping capabilities of olivine, used as a catalyst in indirect biomass gasification. *Appl. Catal. B Environ.* **2014**, *145*, 216–222, doi:10.1016/J.APCATB.2013.01.041.

130. Kirnbauer, F.; Wilk, V.; Kitzler, H.; Kern, S.; Hofbauer, H. The positive effects of bed material coating on tar reduction in a dual fluidized bed gasifier. *Fuel* **2012**, *95*, 553–562, doi:https://doi.org/10.1016/j.fuel.2011.10.066.

131. Fürsatz, K.; Kuba, M.; Janisch, D.; Aziaba, K.; Hammerl, C.; Chlebda, D.; Łojewska, J.; Hofbauer, H. Impact of residual fuel ash layers on the catalytic activation of K-feldspar regarding the water–gas shift reaction. *Biomass Convers. Biorefinery* **2020**, doi:10.1007/s13399-020-00645-w.

132. Leion, H.; Frick, V.; Hildor, F. Experimental Method and Setup for Laboratory Fluidized Bed Reactor Testing. *Energies* **2018**, *11*, 2505, doi:10.3390/en11102505.

133. Dieringer, P.; Marx, F.; Alobaid, F.; Ströhle, J.; Epple, B. Process Control Strategies in Chemical Looping Gasification—A Novel Process for the Production of Biofuels Allowing for Net Negative CO2 Emissions. *Appl. Sci.* **2020**, *10*, 4271, doi:10.3390/app10124271.

134. Morgan, A.B. A Review of Transition Metal-Based Flame Retardants: Transition Metal Oxide/Salts, and

Complexes. In *Fire and Polymers V - Materials and Concepts for Fire Retardancy*; Wilkie, C.A., Morgan, A.B., Nelson, G.L., Eds.; American Chemical Society, 2009.

135. Ōya, A.; Marsh, H. Phenomena of catalytic graphitization. *J. Mater. Sci.* **1982**, *17*, 309–322, doi:10.1007/BF00591464.

136. IEA Global crude steel production by process route and scenario, 2019-2050 Available online: https://www.iea.org/data-and-statistics/charts/global-crude-steel-production-by-process-route-and-scenario-2019-2050 (accessed on May 20, 2021).

137. Toktarova, A.; Karlsson, I.; Rootzén, J.; Göransson, L.; Odenberger, M.; Johnsson, F. Pathways for Low-Carbon Transition of the Steel Industry—A Swedish Case Study. *Energies* **2020**, *13*, doi:10.3390/en13153840.

138. European Commission - SETIS - Energy Efficiency in the Iron and Steel Industry Available online: https://setis.ec.europa.eu/technologies/energy-intensive-industries/energy-efficiency-and-co2-reduction-iron-steel-industry/info (accessed on Feb 23, 2021).

139. *Direct From MIDREX - 1st quarter 2020*; 2020;

140. *HYBRIT - Summary of findings from HYBRIT Pre-Feasibility Study 2016–2017*;

141. Fuss, S.; Canadell, J.G.; Peters, G.P.; Tavoni, M.; Andrew, R.M.; Ciais, P.; Jackson, R.B.; Jones, C.D.; Kraxner, F.; Nakicenovic, N.; et al. Betting on negative emissions. *Nat. Clim. Chang.* **2014**, *4*, 850–853, doi:10.1038/nclimate2392.

142. *Direct from MIDREX - Third quarter 2017*; 2017;

143. Tanaka, H. *Potential for CO2 emissions reduction in MIDREX direct reduction process*; 2013;

144. Parisi, D.R.; Laborde, M.A. Modeling of counter current moving bed gas-solid reactor used in direct reduction of iron ore. *Chem. Eng. J.* **2004**, *104*, 35–43, doi:https://doi.org/10.1016/j.cej.2004.08.001.

145. Béchara, R.; Hamadeh, H.; Mirgaux, O.; Patisson, F. Optimization of the Iron Ore Direct Reduction Process through Multiscale Process Modeling. *Mater.* 2018, *11*.

146. Hammerschmid, M.; Müller, S.; Fuchs, J.; Hofbauer, H. Evaluation of biomass-based production of below zero emission reducing gas for the iron and steel industry. *Biomass Convers. Biorefinery* **2021**, *11*, 169–187, doi:10.1007/s13399-020-00939-z.

147. Miller, D.D.; Siriwardane, R. Mechanism of Methane Chemical Looping Combustion with Hematite Promoted with CeO2. *Energy & Fuels* **2013**, *27*, 4087–4096, doi:10.1021/ef302132e.

148. Iaquaniello, G.; Antonetti, E.; Cucchiella, B.; Palo, E.; Salladini, A.; Guarinoni, A.; Lainati, A.; Basini, L. Natural Gas Catalytic Partial Oxidation: A Way to Syngas and Bulk Chemicals Production. In *Natural Gas Extraction to End Use*; Gupta, S., Ed.; IntechOpen, 2012 ISBN 978-953-51-0820-7.

149. Wörtler, M.; Schuler, F.; Voigt, N.; Schmidt, T.; Dahlmann, P.; Bodo Lüngen, H.; Ghenda, J.-T. *Steel's Contribution to a Low-Carbon Europe 2050 Technical and Economic Analysis of the Sector's CO2 Abatement Potential*; 2013;